An *in vitro* model to study the role of IOL: Lens Capsule Interactions in Posterior Capsule Opacification

By Arjun Jaitli

A Dissertation Submitted to the Graduate School of the University of Texas at Arlington in Partial Fulfillment of the Requirements for the Degree of Doctor of Philosophy

Arlington, Texas

May 2021

The University of Texas at Arlington

DISSERTATION DEFENSE REPORT (DDR)

This report must be submitted to the Office of the Registrar, via email to gradteam@uta.edu, after the examination is administered regardless of the outcome of the defense. Students & advisors should consult the current Graduate Catalog for deadline dates applicable to the administration & report of the exam. The student must be enrolled in the term in which he/ she takes the Dissertation Defense. An unconditional pass is required before degree can be conferred. In order to update a student from "passed with conditions" the Milestone Conditions Update form will need to be submitted.

Student: Arjun (Last Name:) Jaitli (First Name:) Date of Examination: 04/16/2021

UTA ID: 1475653 Program: Biomedical Engineering College/ School: College of Engineering Dept: BE

Title of Dissertation: An in vitro model to study the role of IOL:Lens capsule interactions in posterior capsule opacification

This is to report that the above-named student, under the direction of their committee, completed the Dissertation Defense with the following results

- [x] Passed Unconditionally, the dissertation document and defense fully satisfy requirements for the doctoral degree.
- [ ] Passed, with following conditions that must be satisfied
- [ ] Failed, with permission to retake with these stipulations
- [ ] Failed, dismissed from the program

Name (typed)	Signature	Date (mm/dd/yyyy)
Liping Tang Select Title	Liping Tang Digitally signed by Liping Tang Date: 2021.04.19 15:33:55 -05'00'	4/16/2021
Ali Akinay Select Title	Akinay, Ali Digitally signed by Akinay, Ali Date: 2021.04.20 13:43:01 -05'00'	4/16/2021
Brett Thomes Select Title	04.21.21	4/16/2021
Jun Liao Select Title	Digitally signed by Jun Liao Date: 2021.04.19 18:26:14 -05'00'	4/16/2021
Yi Hong Committee Member	Yi Hong Digitally signed by Yi Hong Date: 2021.04.19 18:45:10 -05'00'	4/16/2021
Select Title		
Student		

DEDICATION

This dissertation is dedicated to my family, friends and every individual who has motivated and supported me during my years at UTA as a PhD student.

ACKNOWLEDGEMENTS

First, I would like to thank my mentor and advisor, Dr. Liping Tang whose guidance and support made my journey as a PhD student exciting and enlightening. I will forever be grateful for the great discussions I had with him over the years, both professional and personal. His key insights, deep understanding of tissue engineering concepts and most importantly, empowerment of his students including myself to lead their research work and experiments were instrumental in helping me accomplish my goals. I would also like to acknowledge Dr. Jun Liao for his advice and support during the early years of my research. His guidance during the initial stages of my model development were extremely vital and laid the foundation for my research. Additionally, I would like to extend my sincere thanks and appreciation to the other members of my committee – Dr. Yi Hong, Dr. Brett Thomes, and Dr. Ali Akinay who have provided knowledge, guidance, and resources that were essential to completing my dissertation.

Next, I would like to acknowledge and express my appreciation for my lab mates and project team. I would like to thank Joyita for her help and support in conducting numerous experiments and tasks during the course of my research. I will always be grateful for her willingness to help and her dedication to the work we did as a group in Dr Tang's laboratory. I would also like to thank Amjad and Sara for their support in helping me set up various testing benches and imaging systems to complete my research work.

Last, I would like to acknowledge the support of my wife, Palak who has always inspired me to be a better person and has encouraged me to strive for more. She was the source of my strength and I will be forever be grateful for the sacrifices she made for us so I could finish my research.

TABLE OF CONTENTS

DEDICATION iv
ACKNOWLEDGEMENTS v
LIST OF FIGURES AND TABLES ix
ABSTRACT 1
CHAPTER 1 4
Introduction and Rationales for Dissertation Research 4
1.1. Cataracts and PCO 5
1.2. Clinical PCO Performance of various IOLs 5
1.3. Role of IOL Material Properties and Design in pathogenesis of PCO 7
1.4. Role of LECs 8
1.5. Role of ECM Proteins in mediating PCO 9
1.6. Potential role of IOL surface coatings in PCO prevention 10
1.7. Rationale and Scientific Premise for Dissertation Research 12
CHAPTER 2 15
An In Vitro system to investigate IOL: Lens Capsule Interaction 15
2.1. Introduction 16
2.2. Materials and Methods 17
2.2.1. Intraocular Lenses 17
2.2.2. Fabrication of Simulated Lens Capsule 18
2.2.3. Mechanical Adhesion Force Apparatus 21
2.2.4. Gelatin Weight and Concentration Optimization 24
2.2.5. Statistical analyses 24
2.3. Results 25
2.4. Discussion 31
2.5. Conclusions 36
Supplemental Figure(s) 38
CHAPTER 3 39
Effect of Time and Temperature-Dependent Changes of IOL Material Properties on IOL: Lens Capsule Interactions 39
3.1. Introduction 40
3.2. Materials and Methods 42
3.2.1. Intraocular Lenses 42

3.2.2. Fabrication of simulated lens capsule 42
3.2.3. Characterization of simulated lens capsule 43
3.2.4. Adhesion force measurements 45
3.2.5. Surface hydrophilicity and roughness measurements 46
3.2.6. Visualize “cell” infiltration at the space between IOL and LC....47
3.2.7. Statistical analyses 49
3.3. Results 49
3.3.1. Effect of temperature and incubation time on IOL: LC Adhesion Force....49
3.3.2. Effect of temperature and hydration time on surface hydrophobicity 53
3.3.3. Effect of temperature and hydration time on surface roughness....54
3.3.4. Examination of “no space no cell” hypothesis in vitro 55
3.4. Discussion....57
3.5. Conclusions....63
Supplemental Materials 65
3.S.1. Crosslinking of simulated gelatin capsules 65
3.S.2. Dye Infusion Results after incubation of IOL: LC for 4 hours at 37 °C....66
CHAPTER 4....67
Role of Fibronectin and IOL surface modification in IOL: Lens Capsule Interactions 67
4.1. Introduction....68
4.2. Materials and Methods 71
4.2.1. Intraocular Lenses 71
4.2.2. Surface modification of acrylic foldable IOLs 72
4.2.3. Preparation of Simulated Capsules....73
4.2.4. Surface Coating and Fibronectin Adsorption on IOL: LC force and cell penetration 73
4.2.6. Surface characterization of various treated IOLs....74
4.2.7. Statistical analyses 74
4.3. Results 74
4.3.1. Effect of Fibronectin on IOL: LC adhesion force for acrylic foldable IOLs 74
4.3.2. Effect of Fibronectin on IOL: LC adhesion for different materials....75
4.3.3. Dye infusion for different IOL materials in presence of Fibronectin 77
4.3.4. Influence of surface coatings and fibronectin on surface hydrophilicity....78
4.3.5. Effect of Surface Coatings on IOL: LC adhesion force 79
4.3.6. Dye Infusion for Acrylic foldable-PEG and acrylic foldable-DG IOLs 82
4.4. Discussion....83

4.5. Conclusions....86
CHAPTER 5....88
Conclusions and Future Direction....88
5.1. Conclusions....89
5.2. Future Direction....90
REFERENCES....92
BIOGRAPHICAL INFORMATION....102

LIST OF FIGURES AND TABLES

Figure 1. 1. A schematic showing the role of LECs in PCO formation (Kappelholf et al., 1992) 9

Figure 2.1. Simulated lens capsule fabrication process flow (A-C) with a top-down view photograph of IOL placement with weights (B, bottom) prior to refrigeration and photograph of a cross-section of simulated capsule depicted by blue dye after IOL removal.....20

Table 2.1. Comparison of material properties of the simulated lens Capsules and the human lens capsule 21

Figure 2.2. Mechanical apparatus system schematic (A) and test process schematic (B & C) with photographs.....22

Figure 2.3. Adhesion force calculation process flowchart. A process flow diagram highlighting position tracking and force calculations (A) accompanied with graphical representation of change in position over time and consequential force data calculated as a function of change in position of the bending bar (B).....23

Figure 2.4. Adhesion force of PMMA and acrylic foldable IOLs with lens capsules for high and low molecular weight gelatin at 1% and 10% w/v concentration. Adhesion force measured using bending bar mechanical apparatus (n = 5, NS $p > 0.05$, **$p < 0.01$).....26

Figure 2.5. Adhesion force of PMMA and acrylic foldable IOLs with lens capsules as a function of high molecular weight concentration. Adhesion force measured using bending bar mechanical apparatus (n = 4, NS $p > 0.05$, *$p < 0.05$). 28

Figure 2.6. Adhesion force of PMMA (n=5), silicone (n=4) and acrylic foldable (n=5) IOLs with lens capsules at 10% w/v high mol wt condition (A) and clinical PCO performance of IOLs made from same materials (B). Adhesion force measured using bending bar mechanical apparatus (A:

*p<0.05, **p < 0.01, ***p<0.001) is inversely related to clinical PCO rates of acrylic foldable, PMMA and silicone material IOLs (B : NS p>0.05, **p<0.01, ***p<0.001) (Ursell et al, 1998) 30

Supplementary Figure 2.1. Mechanical property characterization of various simulated lens capsule formulations. (A) Elastic modulus and (B) Ultimate stress of lens capsules made of high (5%, 10%, 15% w/v) and low molecular weight gelatin (10% w/v).....38

Table 3.1. Comparison of material properties of the simulated lens capsule and the human lens capsule 44

Figure 3.1. Mechanical Apparatus System Schematic (A) and Test Process Schematic (B).....45

Figure 3.2. Frontview (A) and sideview (B) photographs of the imaging System.....48

Figure 3.3. Imaging Test Process Schematic (A) of blue dextran dye occupying posterior side of IOL and on the periphery of the IOL: LC interface (B). The collected image(s) was analyzed to calculate the % of dye penetration in ImageJ software as shown below (C).....49

Figure 3.4. IOL:LC adhesion force for PMMA, silicone and acrylic foldable IOLs at different incubation time (0, 4 and 24 hours) and temperatures (21 °C and 37°C) (n = 10, significance vs 0 hour of the same group, NS: p > 0.05, *p < 0.05, **p < 0.01).....50

Table 3.2. Summary of two-sample t-tests (95% CI) for observed IOL: LC adhesion forces for PMMA, silicone and acrylic foldable IOLs at 21 °C and 37 °C. Significance, *p<0.05, **p<0.01. 51

Table 3.3. Summary of paired t-test (95% CI, $\alpha = 0.05$) between different time points (0, 4 and 24 hours) for IOL: LC adhesion forces for PMMA, silicone and acrylic foldable IOLs at 21 and 37 °C. Significance, NS: p > 0.05, **p<0.01 52

Figure 3.5. Change in surface contact angle as a function of incubation time and temperature. Contact angle measurements for PMMA, silicone and acrylic foldable test IOLs were carried out at 0 and 24 hours post hydration in BSS at different temperatures (21 °C and 37 °C) (n=10, significance vs 0 h of the same group, *p < 0.05, **p<0.01).....53

Table 3.4. Summary of paired t-test (95% CI, α = 0.05) between different time points (0 vs 24 hours) for average contact angle (in degrees) (@ 21 °C and 37 °C), average surface roughness (nm) (@ 21 °C and 37 °C), and average dye penetration (%) (@ 37 °C) for all materials. Significance, NS p > 0.05, *p<0.05, **p<0.01.....54

Figure 3.6. Change in surface roughness as a function of incubation time and temperature in BSS. Surface Roughness measurement on PMMA, silicone and acrylic foldable test IOLs was carried out at 0 and 24 h post hydration in BSS at 21 and 37 °C (n=10, significance vs 0 hour of the same group, NS: p > 0.05). 55

Figure 3.7. Photographs collected using the IOL: LC imaging system depicting visualization of dye penetration at IOL: LC interface at 37°C. (A) Representative images and (B) percentages of dye coverage at IOL: LC interface for for acrylic foldable, PMMA and silicone IOLs (n = 10, significance: **p<0.01).....56

Figure 3.8. Percentage change in average IOL: LC adhesion force, contact angle, surface roughness and dye penetration for PMMA, silicone and acrylic foldable IOLs at 37°C.....62

Supplementary Figure 3.1. Dye penetration results before and after incubation for 4 hours @ 37°C for PMMA, silicone and acrylic foldable IOLs.....66

Figure 4. 1. IOL: LC adhesion force as a function of fibronectin concentration after incubation @ 37°C for 24 hours (n=5, Significance vs Control group, NS: p > 0.05, **p<0.01).....75

Figure 4. 2. IOL: LC adhesion force after injecting 2 uL of 1 mg/mL FN solution at IOL: LC interface for different IOL materials – Acrylic foldable, PMMA and Silicone (n=5, significance vs Control of same group, NS: p > 0.05, ***p<0.001) 76

Figure 4. 3. Photographs collected using the IOL: LC imaging system depicting visualization of dye penetration at IOL: LC interface at 37°C. (A) Representative images and (B) percentages of dye coverage at IOL: LC interface for for acrylic foldable, PMMA and silicone IOLs (n=3, significance vs control of same group, NS: p>0.05, ***p<0.001) 77

Figure 4. 4. Surface contact angle of acrylic foldable, acrylic foldable-DG and acrylic foldable-PEG) with and without Fibronectin. All test samples were coated with either 0 (labeled as "BSS") or 1 mg/mL FN injection for 24 hours @ 37°C. (n=5, NS: p > 0.05, ***p<0.001).....79

Figure 4. 5. IOL:LC adhesion force for acrylic foldable control, acrylic foldable – DG and acrylic foldable-PEG lenses at different incubation time (0 and 24 hours) @ 37 °C (n=5, Significance vs acrylic foldable control, NS: p>0.05, **p<0.01, ***p < 0.001).....80

Figure 4. 6. IOL:LC adhesion force for coated acrylic foldable lenses after injecting 2 uL of 1 mg/mL FN solution for acrylic foldable – PEG and acrylic foldable – DG lenses (n=3, significance vs control of same group, ***p < 0.001).....82

Figure 4. 7. Photographs collected using the IOL: LC imaging system depicting visualization of dye penetration at IOL: LC interface at 37°C. (A) Representative images and (B) percentages of dye coverage at IOL: LC interface for for acrylic foldable-control, acrylic foldable-PEG and acrylic foldable-DG IOLs (n=3, Significance vs control group (without FN), NS: p > 0.05, **p<0.01, ***p<0.001).....83

ABSTRACT

Posterior capsule opacification (PCO) is the most common complication associated with intraocular lens (IOL) implantation. Unfortunately, current *in vitro* models cannot be used to assess the potential of PCO due to their failure to simulate posterior curvature of the lens capsule (LC), contradicting observations, different testing conditions and inherent challenges associated with use of human capsular bag models, cells and other tissue substrates. To overcome such a challenge, a new system to study IOL: LC interaction and potentially predict PCO was developed in this effort. It is believed that the interactions between an IOL and the lens capsule (LC) may influence the extent of PCO formation. Specifically, strong adhesion force between an IOL and the LC may impede lens epithelial cell migration and proliferation and thus reduce PCO formation.

For Aim 1, to measure the adhesion force between an IOL and LC, a new *in vitro* model was established with simulated LCs and a custom-designed micro-force tester. A method to fabricate simulated LCs was developed by imprinting IOLs onto molten gelatin to create simulated three dimensional (3D) LCs with curvature resembling the bag-like structure that collapses on the IOL post implantation. An *in vitro* system that can measure the adhesion force reproducibly between an IOL and LC with a resolution of ~ 1 μN was established in this study. During system optimization, the 10% high molecular weight gelatin produced the best LC with the highest IOL-LC adhesion force with all test lenses that were fabricated from acrylic foldable, polymethylmethacrylate (PMMA) and silicone materials. Test IOLs exerted different adhesion force with the 3D simulated LCs in the following sequence: acrylic foldable IOL > silicone IOL > PMMA IOL. These results were in good agreement with the clinical observations associated with PCO performance of IOLs made of the same materials.

In Aim 2, using the aforementioned custom designed micro force tester, the influence of

temperature and incubation time on the adhesion force between IOLs and LCs was investigated. Using this system, we examined the influence of temperature (room temperature vs. body temperature) and incubation time (0 vs. 24 hours) on the adhesion force between IOLs and LCs. The results show that, in line with clinical observations of PCO incidence, the adhesion force increased at body temperature and with increase in incubation time in the following order, Acrylic foldable IOLs > Silicone IOLs > PMMA IOLs. By examining the changes of surface properties as a function of temperature and incubation time, we found that acrylic foldable IOLs showed the largest increase in their hydrophilicity and reported the lowest surface roughness in comparison to other IOL groups. Coincidentally, using a newly established macromolecular dye imaging system to simulate cell migration between IOLs and LC, we observed that the amount of macromolecular dye infiltration between IOLs and LCs was in the following order: PMMA IOLs > Silicone IOLs > Acrylic foldable IOLs. These results support a new potential mechanism that both the surface hydrophilicity and smoothness of IOLs greatly contribute to their tight binding to LCs and such tight binding may lead to reduced IOL: LC space, cell infiltration, and thus PCO formation.

In Aim 3, the role of fibronectin in mediating the adhesion between different IOL materials and the simulated lens capsule was examined. Briefly, a range of fibronectin concentrations were first studied using an acrylic foldable IOL that is believed to interact with fibronectin *in vivo* to create a strong bond between the lens capsule and the IOL surface. Our results indicated that the adhesion of the acrylic foldable IOLs increased significantly in the presence of Fibronectin. Using surface contact angle measurements, we observed that the adsorption of fibronectin on acrylic foldable groups creates a hydrophilic layer on their surface that may increase its adhesion with the lens capsule. Our dye infusion study further confirmed this tight binding by showing reduced dye penetration in acrylic foldable IOLs in the presence of fibronectin. However, the presence of

fibronectin in lens capsules did not affect the adhesion for silicone and PMMA materials. Next, the influence of surface modification of the acrylic foldable IOLs on its adhesion characteristics was also assessed by modifying them with Poly(ethyleneglycol) (PEG) and Di(ethyleneglycol) dimethyl ether (Digylme). Our results indicated that surface modification of acrylic foldable IOLs with PEG did not affect their adhesive forces and interaction with fibronectin, which are both well known material properties of the Acrysof lens that contribute to its excellent PCO performance in the clinic. However, surface modification of the acrylic lenses with Digylme showed drastically reduced adhesion forces with the capsule, and high rate of dye penetration making it an undesirable candidate as a potential hydrophilic coating for IOL materials.

Keywords: Intraocular lens, lens capsule, adhesion force, posterior capsule opacification, in vitro model, gelatin, 3D model.

CHAPTER 1

Introduction and Rationales for Dissertation Research

1.1. Cataracts and PCO

Cataract is the second most common cause of blindness in the world after age-related macular degeneration affecting ~ 27 million people in the United States alone (Pérez-Vives, 2018). At present, cataract induced visual impairment is treated by surgical removal of the cataractous lens and implantation of an artificial Intraocular Lens (IOL) (Eldred et al., 2019). While surgical intervention followed by IOL implantation initially restores vision in patients, some patients develop Posterior Capsule Opacification (PCO) leading to secondary vision loss. It is generally believed that the interaction of an implanted IOL with the lens capsule plays a pivotal role in affecting the path of PCO progression (Jaitli et al., 2021; Katayama et al., 2007; Linnola, 1997; Linnola et al., 2003, 2000a; Nibourg et al., 2015; Oshika et al., 1998a; Pérez-Vives, 2018; Versura et al., 1997; Wormstone, 2020). Despite numerous research efforts aimed at studying the pathogenesis of PCO formation, its development and mechanisms are still not clearly understood which makes it increasing difficult for leading eye care companies such as Abbot Medical Optics, Allergan, Alcon Research LLC, Zeiss, AT-Lisa etc. to develop IOLs with improved safety and biocompatibility. Thus, it is imperative to improve the understanding of PCO pathogenesis so that an improved IOL can be developed for reducing IOL-induced PCO formation.

1.2. Clinical PCO Performance of various IOLs

PCO performance of IOLs has been assessed in numerous clinical studies (Oshika et al., 1996; Rønbeck and Kugelberg, 2014a; Rönbeck et al., 2009a; Ursell et al., 1998; Wejde et al., 2003). Some studies conducted in the early nineties have focused on the incidence rate of PCO for various IOL materials such as plate-haptic silicone (Artaria et al., 1994a), PMMA and sulcus-fixated silicone (Shepherd, 1989), three-piece prolene (Cumming, 1994), soft acrylics (Oshika et al., 1996) and hydrogels (Noble et al., 1990). These clinical studies collected data that showed lowest incidence of PCO in plate-haptic silicone IOLs (~ 1.1 % at 23 months) followed by PMMA (7.9%

at 24 months), hydrogels (8% at 20 months) and then soft acrylics (11.1 % @ 24 months) (Chehade and Elder, 1997). With the development of small incision cataract surgery, there was an increasing need to develop foldable IOL materials leading to the launch of hydrophobic acrylic materials in the mid-nineties (Ursell et al., 1998). Acrylics, along with silicone and PMMA materials became the most widely used IOLs at that time and have been studied extensively since for PCO performance in the clinic. In 1998, Ursell et al. conducted a randomized clinical trial on 90 eyes by implanting PMMA (Alcon MC60BM), silicone (Iolab L141U) and acrylic (Alcon MA60BM) IOLs and calculated the percentage area of opacified capsule to determine the extent of PCO in patients at 2 years postoperatively. Percentage of PCO observed was significantly reduced for acrylic IOLs (~11.75%) followed by silicone (~33.50%) and PMMA (43.65%) (Ursell et al., 1998). In 2003, Wejde et al. performed a PCO comparison study on 180 patients that were randomly implanted with heparin-surface-modified (HSM) PMMA IOLs (809C, Pharmacia & Upjohn), silicone IOLs (SI-40NB, Allergan) and acrylic IOLs (Acrysof MA60BM, Alcon) (Wejde et al., 2003). Wejde et al.'s study results further strengthened results from Ursell et al.'s study showing significantly higher PCO for HSM PMMA than the silicone and acrylic IOL group @ 2 years postoperatively. Furthermore, silicone had significantly more PCO than the acrylic group. There have also been extended follow-ups of randomized clinical trials to assess PCO development on a long-term basis. Ronbeck et al. compared PCO performance of HSM PMMA, silicone and acrylic IOLs at 12 year post-operatively (Rønbeck and Kugelberg, 2014b). Interestingly, after 12 years, there was no significant difference in PCO formation of silicone and acrylic IOLs (Rønbeck and Kugelberg, 2014b). PMMA IOL groups had a significantly higher rate of PCO than the silicone groups but not acrylics. Furthermore, PCO evaluation using the retro illumination photograph technique described in Wejde et al. showed that differences between the IOLs became

increasingly lower (Wejde et al., 2003). The authors attributed the ability of silicone to inhibit PCO growth in the long run to its adhesiveness to vitronection and Collagen IV which was significantly higher than the adhesiveness of acrylic groups to these proteins (Vasavada and Praveen, 2014) .Thus, different IOL materials have been associated with different rates of clinical PCO performance. Clinical data summarized in this section indicates that PCO performance of hydrophobic acrylics like Acrysof is significantly better than silicone and PMMA lenses at 2 years post-op but have similar PCO rates on a long term basis (>5 years) in comparison to silicone materials IOLs. PMMA, has the worst short-term and long-term PCO performance when compared to acrylics and silicone IOLs (Oshika et al., 1996; Rønbeck and Kugelberg, 2014a; Rönbeck et al., 2009a; Ursell et al., 1998; Wejde et al., 2003).

1.3. Role of IOL Material Properties and Design in pathogenesis of PCO

An IOL's adhesiveness to the lens capsule, its surface hydrophobicity, surface roughness and posterior optic edge geometry have been linked to PCO formation (Boulton and Saxby, 1998; Katayama et al., 2007; Kim et al., 2001; Linnola et al., 2003, 2000a; Oshika et al., 1998b; Ursell et al., 1998; Versura, 1999; Xu et al., 2016a, 2016b). It is believed that the strong adhesion of the IOL to capsule leaves less or no space for cells to grow into i.e. 'No space, No cell', a theory which has been used to describe the different rates of PCO for various older IOLs (Pearlstein et al., 1988a). Interestingly, a study demonstrated that the adhesiveness of different acrylic materials showed a correlation with PCO incidence in rabbits and concluded that the more adhesive acrylic IOLs were associated with a lower rate of PCO (Katayama et al., 2007). It is also possible that as the lens becomes adherent to the capsule, the physical pressure may squeeze out the LECs present in the capsule space and cause their atrophy. Within hours of cataract surgery, the implanted IOL adsorbs a complex protein biofilm that determines the cellular and tissue reactions to the IOL

(Pearlstein et al., 1988a). Various ECM proteins like fibronectin, vitronectin, fibrinogen, and transferrin have been identified in these biofilms in various animal studies (Kochounian et al., 1994). LECs produce collagen types I, IV, V and VI post-cataract surgery (Nishi et al., 1995) and IOLs coated with Collagen IV have been associated with lower PCO growth (Miyak et al., 1991) indicating that the surface adhesion properties of IOLs play a critical role in the pathogenesis of PCO. The adhesiveness of an IOL material to the lens capsule is also believed to be associated with its surface characteristics such as hydrophobicity, water uptake characteristics and surface roughness (Bertrand et al., 2014; Katayama et al., 2007; Miyata and Yaguchi, 2004; Mukherjee et al., 2012; Tanaka et al., 2005). Several studies have indicated a relationship between an IOL's surface hydrophilicity and its adhesion force to ECM (Bertrand et al., 2014; Miyata and Yaguchi, 2004). Further, many studies have also concluded that higher surface roughness of an IOL biomaterial leads to higher PCO growth as surface irregularities could increase the number of inflammatory cells adhering to the IOL optic surface and result in tissue formation (Katayama et al., 2007; Tanaka et al., 2005). Thus, an IOL's material properties determined by its surface properties such as hydrophobicity, in vivo water uptake characteristics, and surface roughness all play a critical in mediating IOL-induced PCO rates.

1.4. Role of LECs

Histological evidence from donor eyes implanted with an artificial IOL has shown that LECs are typically left behind in the capsular bag after this procedure (Meacock et al., 2000). These remaining LECs after the removal of the cataractous lens and intraocular lens (IOL) implantation are considered the primary source of PCO (Ohmi and Uenoyama, 1993). Residual LECs left in the capsule interact with growth factors and other molecules present in the lens capsule (Boulton and Saxby, 1998; Garg et al., 2005). They migrate from the equatorial region of the capsule and

proliferate onto the posterior capsule eventually leading to PCO formation (Apple et al., 1992; Linnola 1997; Kappelhof et al., 1992; Mansfield et al., 2004). Furthermore, the release of inflammatory mediators post-cataract surgery complement activation of cytokines such as interleukin-1 and -6 and further stimulate LEC growth (Linnola 1997; Meacock et al., 2000). Additionally, in response to a variety of stimuli, LECs may undergo phenotypic changes to form epithelial pearls and smooth muscle like cells (α-SMA) with contractile properties that initiate fibrotic tissue formation over the posterior capsule as depicted in Figure 1.1 (Kappelholf et al., 1992)

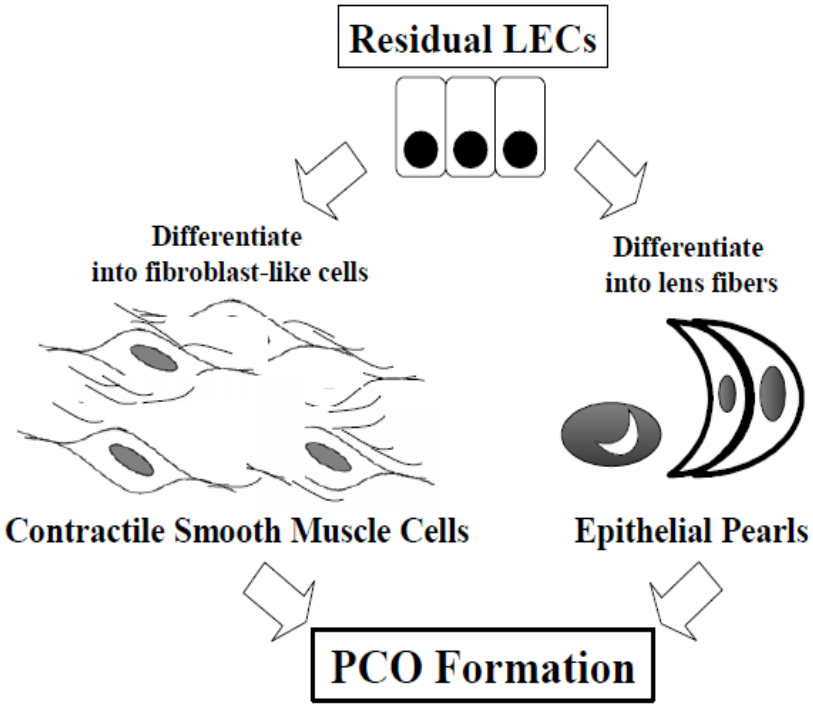

Figure 1. 1. A schematic showing the role of LECs in PCO formation (Kappelholf et al., 1992)

1.5. Role of ECM Proteins in mediating PCO

ECM proteins play an important role in PCO formation, can act as mediators of IOL adhesion and have been observed in the connective tissue that accumulates between the capsule and IOL (S.

Saika, 1997; Saika et al., 1998, 1993; Shizuya Saika, 1997) . Better and faster adhesion of the IOL to the lens capsule post-implantation is believed to decrease the number of LECs between the IOL surface and the capsular bag (Ursell et al., 1998). Fibronectin, a major glycoprotein of the extracellular matrix found in soluble form in plasma is believed to impact the degree of PCO formation owing to its affinity for Collagen, an essential material constituent of the lens capsule (Linnola, 1997). Soluble fibronectin is available in the aqueous humor after surgery as a result of the breakdown of the blood–aqueous barrier and is also produced by LECs that have transformed into fibroblasts (Linnola et al., 2000b). Fibronectin's several functional domains promote its binding to collagen and the cell surface enabling it to be a mediator between an IOL and the capsule (Shimizu et al., 1997; Sottile et al., 2007). Furthermore, various autopsy-eye studies have concluded that fibronectin appeared to act as a biological clue between the IOL material and the capsular bag for lens materials that are associated with less PCO (Apple et al., 2001). Thus, differences in fibronectin adhesion to the IOL surface could explain differences in the development of PCO with different IOL materials. The next ECM protein that is assumed to play a role in affecting the degree of PCO is vitronectin and has been seen inside the fibrotic tissue (Linnola et al., 2000b, 2000a) . However, its role is believed to be less significant than that of fibronectin since it is not present in the tissue between the IOL surface and the capsular bag. Lastly, Collagen Type IV, a basic ECM protein, is observed in the fibrotic tissue forming PCO with all IOL materials (Linnola et al., 2000b, 2000a).

1.6. Potential role of IOL surface coatings in PCO prevention

Hydrophilic surface coatings such as Heparin, Poly(ethylene glycol) (PEG) and Poly (ethylene) glycol) methyl acrylate have been studied extensively to improve the biocompatibility of many IOL materials (Arthur et al., 2001; Bozukova et al., 2007; Hyeon et al., 2007; Kang et al., 2008;

Kim et al., 2001; Lee et al., 2007; Tognetto et al., 2003; Xu et al., 2016b, 2016a). Within hours of cataract surgery, the IOL surface adsorbs a complex protein biofilm and the interaction of the IOL surface with this biofilm can determine the extent of inflammatory response (Tognetto et al., 2003). PEG polymers are nontoxic, nonimmunogenic and nonantigenic which is believed to reduce attractive forces to proteins due to their high mobility and steric repulsion (Bozukova et al., 2007). Thus, these protein repellent properties of PEG could potentially prevent extracellular matrix formation on implanted IOLs and can reduce cell attachment, and may reduce the extent of PCO formation. For instance, various clinical and *in vitro* investigations have shown the efficacy of heparin surface modified PMMA and PEG modified PMMA lenses in reducing the extent of inflammatory reactions on the lens surface post-implantation i.e. reduced cell attachment and consequently lower PCO rates in clinic when compared to traditional PMMA lenses (Bozukova et al., 2007; Kang et al., 2008; Kim et al., 2001; Tognetto et al., 2003; Versura et al., 1997; Xu et al., 2016b, 2016a) . Alcon's Acrysof lens has excellent biocompatibility and is clinically known to have the lowest PCO rates. Some studies have also modified Acrysof lenses with both PEG and PEGMA and reported reduced cell attachment in *in vitro* and *in vivo* rabbit studies (Hyeon et al., 2007; Xu et al., 2016b). While the first few weeks post-implantation in rabbits, the PEG/PEGMA groups showed reduced PCO rates (~ 6 weeks), over time, both Acrysof control and PEG/PEGMA modified Acrysof lenses showed insignificant differences in rate of PCO formation in rabbits. Thus, surface modification of hydrophobic acrylates with hydrophilic coatings such as PEG/PEGMA may be instrumental in retarding the rate of PCO development, initial inflammatory responses and reduce cell attachment leading to better uveal biocompatibility. However, the effect of these coatings on long-term capsular biocompatibility of the Acrysof lens in the clinic is still unknown and requires further studies.

1.7. Rationale and Scientific Premise for Dissertation Research

While a lot of efforts have been made in recent years to uncover the mechanism governing PCO formation, the progress has been slow due to various limitations. The *in vivo* rabbit model has been used extensively to assess the PCO performance of IOL materials (Aliancy et al., 2018; Wormstone and Eldred, 2016). Although rabbit models have the ability to detect the PCO signal (Aliancy et al., 2018), simulate protein adsorption (S. Saika, 1997) and assess the clinical performance of various IOL design and materials, the rabbit model is time consuming, expensive and cannot always predict the human response due to the following drawbacks. First, the rabbit model may not be used to decipher the mechanism of PCO formation (Wormstone and Eldred, 2016a). Second, due to inherent variability associated with surgical technique and post-op care, the observed PCO rate & bag shrinking/wrinkling may differ leading to confounding results (Raj et al., 2007). Third, it is well established that rabbit models are often associated with significantly stronger inflammatory response than observed with humans (Davidson et al., 1998). Last, rabbits often trigger significantly stronger proliferation of residual LECs and foreign body reactions to IOL implantation than human patients (Aliancy et al., 2018), which makes the model less suitable for simulating differential PCO responses to different lens materials. These drawbacks significantly limit the potential of using the rabbit *in vivo* model to predict PCO responses in human.

Several *ex vivo* models have been utilized for assessing PCO responses to IOLs. In fact, *ex vivo* studies and/or clinical investigations have been performed on human patients post-operatively at different time points or post-mortem to assess the rate of PCO performance. These studies measured the PCO density scores on reteroillumination photographs collected with a slit lamp setup for different IOL materials (Meacock et al., 2000; Oshika et al., 1996; Zehetmayer et al., 1994). *Ex vivo* studies have also been conducted by examining collagenous tissue formation

between the IOL and the LCs in pseudophakic human autopsy eyes (Linnola et al., 2000a, 2000b). While these models can produce results by analyzing the PCO outcome of existing IOLs in human specimens, these *ex vivo* models cannot be used to assess PCO potential of new IOLs prior to implantation.

Several *in vitro models* have also been established to study the mechanisms responsible for IOL induced PCO formation. Cell culture models have been used to access the extent of LEC proliferation, collagenous tissue growth and ECM components on both the IOL and the capsule (Linnola et al., 2000a, 2003; Oshika et al., 1996). While these studies have produced a lot of useful information, these models cannot be used to simulate the 3D interactions between the lens capsule and IOLs. While these *in vitro* studies have been able to study the influence of IOL material chemical, physical, and adhesion properties on their PCO performance, such models and predications are often unreliable. For instance, Oshika et al.'s study to measure adhesion forces of PMMA, silicone and acrylic foldable IOLs with flat bovine collagen sheets *in vitro* provided useful information about the adhesion characteristics of these biomaterials (Oshika et al., 1998a). However, the absence of a LC (or a simulated mold) that mimics the mechanical geometry of the capsule questions the validity of the data to draw clinically relevant conclusions. Further, there is sufficient evidence in literature that supports the theory that more adhesive IOL materials are associated with lower clinical PCO rates (Ursell et al., 1998; Wejde et al., 2003). However, adhesive forces of 0 mg for silicone and 583 mg for PMMA reported by Oshika (Oshika et al., 1998) is counterintuitive to that theory as clinical observations demonstrate that silicone materials IOLs have better PCO performance in comparison to PMMA material IOLs (Ursell et al., 1998; Wejde et al., 2003). To address some of these limitations, a human capsular bag model, which uses lens capsule isolated from human cadaver eyes, has been used to study the interactions

between IOLs and lens capsule during the shrink wrapping process (Dawes et al., 2012; Eldred et al., 2019, 2014; Wormstone, 2020; Wormstone et al., 2021; Wormstone and Eldred, 2016b). While the human capsular bag model can simulate the microenvironment similar to that found inside the human patients, this model has several drawbacks that limit their use for large scale testing. First, the lens capsule bag tissue is isolated from patients with different physical characteristics (size, diameter, thickness, etc.), different ages and disease conditions. The influence of these variables on the experimental results has not been systematically evaluated. Second, the results reported in studies using the human capsular bag model show that the model can only be used to provide qualitative comparison of cell distribution on different IOLs without statistical analysis (Dawes et al., 2012; Eldred et al., 2019, 2014; Wormstone, 2020; Wormstone and Eldred, 2016b). Last, based on literature search, this model has not been used or modified to quantitatively assess the adhesive force/interactions between IOLs and lens capsule

Thus, there is a need for an *in vitro* system that is capable of measuring adhesion forces of different materials with a simulated lens capsule fabricated utilizing the ECM components of the human capsule that simulates the true clinical PCO performance of different IOL materials to allow industry professionals to screen materials in an inexpensive and quick fashion. Taking advantage of these observations i.e. limitations of existing *in vivo*, *ex vivo and in vitro* models and unclear mechanisms that contribute to IOL induced PCO, the following research aims were proposed:

Aim 1: Develop an *in vitro* model to study IOL: LC interactions.

Aim 2: Study the influence of temperature and time dependent changes in IOL material properties on IOL: LC interactions.

Aim 3: Role of Fibronectin and hydrophilic surface coatings in mediating IOL: LC interactions.

CHAPTER 2

An In Vitro system to investigate IOL: Lens Capsule Interaction

2.1 Introduction

Stronger and faster adhesion of the IOL to the lens capsule (LC) post-implantation is believed to passively prevent the ingrowth of LECs between the IOL surface and the capsular bag (Linnola, 1997) and thereby prevent fibrotic tissue formation i.e. PCO (Pearlstein et al., 1988b). While many efforts have been made in recent years to uncover the mechanism governing PCO formation, the progress has been slow due to limitations in existing *ex vivo* and *in vivo* models that do not accurately capture the mechanism and pathogenesis of PCO formation in humans. It is well established that posterior edge/surface geometry of the IOL and how the surface of an IOL interacts with inner surface of the capsule post-implantation plays a vital role in determining cell growth and IOL-capsule adhesion (Katayama et al., 2007, Linnola et al., 2000a, 2003; Oshika et al., 1998; Versura, 1999). In light of the above observations and the identified gaps with the existing *in vivo, ex vivo,* and *in vitro* models described in section 1.5, there is a need for the development of an *in vitro* system to study IOL: LC interactions and, perhaps, to predict PCO formation. Most importantly to this work, there is a need to develop an *in vitro* model to assess the adhesion force between an IOL and the lens capsule based on the following evidence. First, it is believed that the strong adhesion of the IOL to capsule leaves less or no space for cells to grow into i.e. 'No space, No cell', a theory which has been used to describe different rates of PCO for various older IOLs (Pearlstein et al., 1988b). Second, among lenses made of different materials, a hydrophobic acrylic foldable IOL is well recognized to stick tightly to the capsular bag and has a low PCO incidence rate (Katayama et al., 2007; Oshika et al., 1996, 1998). On the other hand, PMMA, a rigid polymer composed of methylmethacrylate (MMA) may have a higher rate of PCO due its minimal capsule adhesion and low rate of ECM protein adsorption as shown in *in vitro* studies (Linnola et al., 2003; Oshika et al., 1998b). Coincidentally, both silicone and PMMA IOLs are found to have higher degree of PCO than acrylic foldable IOLs as reported in many clinical examinations (Artaria et al.,

1994; Chehade and Elder, 1997; Chehade and Elder, 1997; Shepherd, 1989; Zehetmayer et al., 1994). These above results support the hypothesis that by measuring the adhesion force between an IOL and lens capsule, an *in vitro* system may be developed to predict PCO potential which was the primary objective of the work described here.

To achieve this goal, an *in vitro* system was established to simulate IOL: LC interactions and to measure the adhesion force between them. The system is composed of a capsule mold to mimic 3D lens capsule geometry and a micro-adhesion force measurement apparatus. The capsule molds were made of gelatin (denatured collagen) with matched curvature of IOLs. After IOLs were placed in the capsule mold, they were connected to the bending bar inside the measurement apparatus. By gently moving the mold downward, attached IOLs pull the bending bar to a certain angle before they detach from the mold. By recording the change in position of the bending bar during the measurement, the adhesion force between the IOL and the LC was then calculated. Studies were carried out to examine the influence of capsule mold formulation on IOL: LC adhesion force for three commonly used IOLs made of acrylic foldable, PMMA and silicone materials. The results were then compared with clinical PCO incidence rates of these IOLs.

2.2. Materials and Methods

2.2.1. Intraocular Lenses

IOLs fabricated from three types of materials – Acrylic foldable, PMMA and silicone were utilized in this study. The single piece acrylic foldable IOLs had a 6.0 mm biconvex optic and planar haptics with an overall length of 13.0 mm (Alcon's SN60WF, Alcon Research, Fort Worth, Texas). The PMMA group were three-piece IOLs with a 6.0 mm biconvex PMMA optic and 10-degree monoflex haptics with an overall length of 13.5 mm (Alcon's MC60BM, Alcon Research, Fort Worth, Texas). The silicone group comprised of three-piece IOLs with a 6.0 mm biconvex silicone

optic and PMMA mod C haptics with an overall length of 13.0 mm. 'Mod C Haptics' is the term that describes the haptic configuration of the IOL which is listed as 'Modified-C' in the technical specifications of this IOL. This information can be found on the package document and its directions for use (DFU) of this commercially available IOL product. The term 'Mod C' is an acronym used by the manufacturer to describe the configuration of the haptic portion of this IOL that the authors assume refers to the shape of the haptic loop which looks similar to the alphabet 'C'. These haptics were fabricated from blue polypropylene monofilament or blue core polymethylmethacrylate (PMMA) monofilament material. All test IOLs utilized in this *in vitro* study had dioptric powers of 25.0D ± 1.0 D and weighed ~15 – 20 mg.

2.2.2. Fabrication of Simulated Lens Capsule

Simulated LCs were created to possess a spherical cup shaped structure that closely mimics the morphology, structure and mechanical integrity of the human capsular bag. Simulated LCs were fabricated using two different types of gelatin – high gel strength gelatin (Product # 48724, 240-270 g Bloom gel strength) and low gel strength gelatin (Product # 48720, 50-80 g Bloom gel strength) from Porcine Skin (Millipore Sigma, St. Louis, Missouri, USA).

The primary objective of this research effort is to develop and optimize an inexpensive and safe system that can be used to predict the potential PCO performance of various IOL materials during the early design/ideation phase. Gelatin was used to fabricate the simulated lens capsule due to various reasons. First, gelatin is denatured collagen and collagen is the most abundant ECM protein in the lens capsule (Danysh and Duncan, 2009; Xing et al., 2014). Second, gelatin's low cost, easy availability and its widespread use in tissue engineering applications made it an ideal candidate for this study. Third, gelatin can be molded into different shapes without affecting its biological properties and has been used in many biomedical engineering applications (Byju et al., 2013; Su

and Wang, 2015). Fourth, gelatin is one of the most promising biopolymers for formation of scaffolds and can improve infiltration, adhesion, spreading and proliferation of cells on scaffolds (Wang et al., 2012). Finally, gelatin is commonly used as tissue phantom (Farrer et al., 2015; Leibinger et al., 2016; Pogue and Patterson, 2006) and has excellent biomechanical properties. Gelatin from porcine skin was used in this study instead of bovine collagen from cow skin for the following reasons. First, while bovine collagen is commercially available for use, it is not commonly used to simulate lens capsule properties. Second, there is a concern about the safety of the bovine collagen due to the potential transmission of the mad cow disease.

Simulated LCs with different physical properties were generated using high and low molecular weight porcine skin gelatin with 1-15% weight/volume concentration in de-ionized water. Water was first heated to 40°C, added with pre-determined amounts of gelatin, and then stirred using a magnetic stirrer for 20 minutes until the gelatin was completely dissolved (Fig 2.1, A) . The prepared solution was poured into acrylic petri-dishes immediately prior to the placement of IOLs. Next, IOLs with haptics intact were taped onto small thin circular lightweight support materials to ensure the IOL stayed afloat through the solidification process accelerated by the placement of this assembly in a 4°C refrigerator (Fig 2.1, B). By gently peeling the IOLs from the gelatin surfaces with the help of thin forceps, a simulated lens capsule mold with a geometry identical to the posterior surface of the lens was created (Fig 2.1, C). To minimize variability potentially resulting from different IOL geometries, every capsule was custom built using the test IOL itself. The posterior IOL surface of the lens was then cleaned by gently rubbing a fine Q-tip dipped in distilled water on the surface followed by a 24h soak in distilled water and a 48h air dry in a laminar flow hood to remove any gelatin remnants prior to testing.

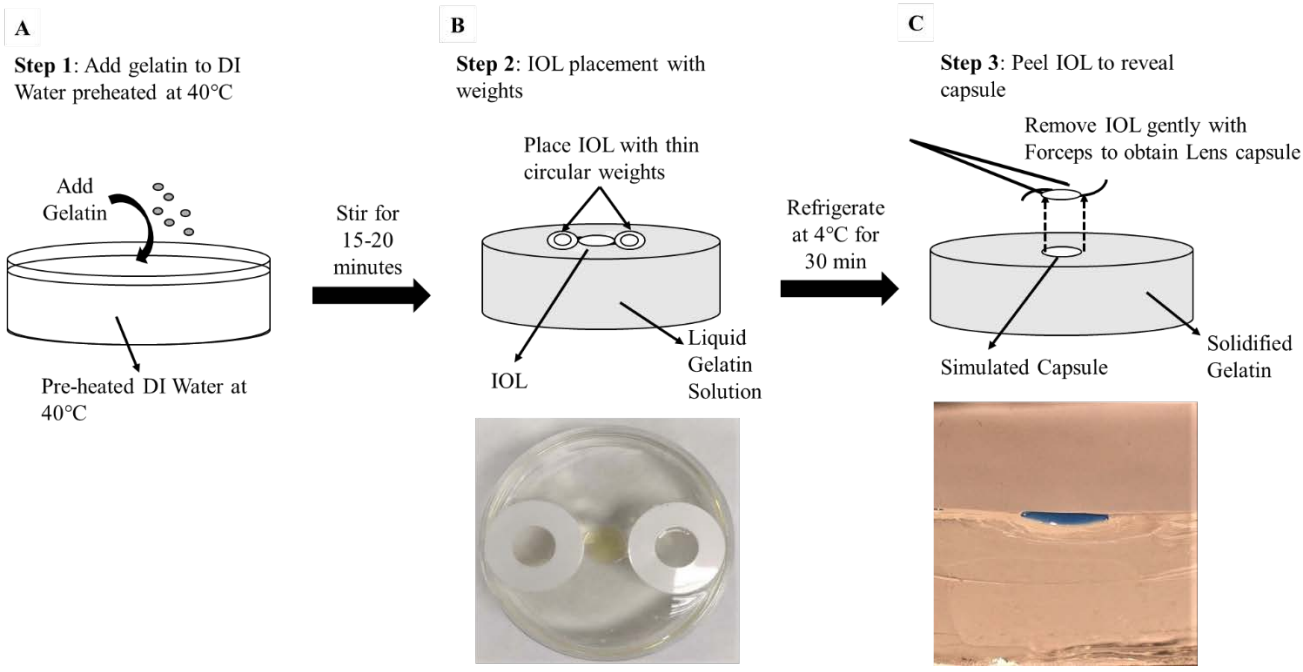

Figure 2.1. Simulated lens capsule fabrication process flow (A-C) with a top-down view photograph of IOL placement with weights (B, bottom) prior to refrigeration and photograph of a cross-section of simulated capsule depicted by blue dye after IOL removal.

Furthermore, to verify that the simulated lens capsules possessed material properties similar to the human capsule, the gelatin capsule's material properties were characterized and compared to the properties of the human capsule (Danysh and Duncan, 2009; Zieberth et al., 2011) as shown in Table 2.1

Properties	Human Lens capsule	Simulated Lens Capsule(s)
Protein composition	Collegen (type IV), Laminin, Nidogen/Entactin, Heparan Sulfate Proteoglycans, Perlecan, Collagen XVIII, Fibronectin, SPARC (osteonectin)	Collagen (type I)
Surface hydrophobicity	Hydrophilic	Hydrophilic
Physical property	Thin membrane around the natural lens	Curved soft gel around IOLs
Elastic Modulus	~ 0.02 N/mm^2	0.0121 N/mm^2
Ultimate Stress	~ 1.5 N/mm^2	0.0061 N/mm^2
Interaction with IOL	Shrink wrap around IOL	Custom made to fit IOL

Table 2.1. Comparison of material properties of the simulated lens Capsules and the human lens capsule

2.2.3. Mechanical Adhesion Force Apparatus

The adhesion force between the IOLs and LCs was determined using a custom made adhesion force apparatus as shown in Figure 2.2. The system's operational procedure is briefly described as follows. First, the fabricated LC molds were mounted onto a motor driven stage of the custom bending machine (Fig 2.2, A). A bending bar, made of titanium wire with a length of 15 cm and a diameter of 0.58 mm (grade 23, Small Parts, Inc., Seattle, WA), was horizontally aligned and fixed on a post at one end. A small hook was made on the free end for attaching the pinhole structure glued to the IOL, and a marker was affixed at the free end of the bending bar for position tracking (Fig 2.2, A). A 3-D printed pinhole structure with a flat circular disk head (diameter = 3 mm) was glued to the anterior surface of the IOL. To start the testing, the free end of the horizontally aligned bending bar was inserted into the pinhole structure glued on each IOL (Fig 2.2, B). The IOL was then attached to the gelatin capsule that was fixed on a motor-driven stage. By controlling the step

motor (Velmex, Inc., Bloomfield, NY), the gelatin capsule was moved vertically downward, and the pinhole structure attached to the bending bar was dragged down by the adhesive force between the IOL: LC assembly. The bending bar was moved downwards until reaching the maximum deflection, at which point the upward bending force was equal to the maximum adhesive force (Fig 2.2, C). With further downward movement of the stage, the bending bar-pinhole-IOL complex detached from the gelatin capsule. A 30V DC ImagingSource camera (Model # DMK 21AF04, The Imaging Source, Charlotte, NC) was used to capture the movement of the bending bar during this process. A custom LabVIEW program was used to threshold the moving marker and track the real time marker coordinates.

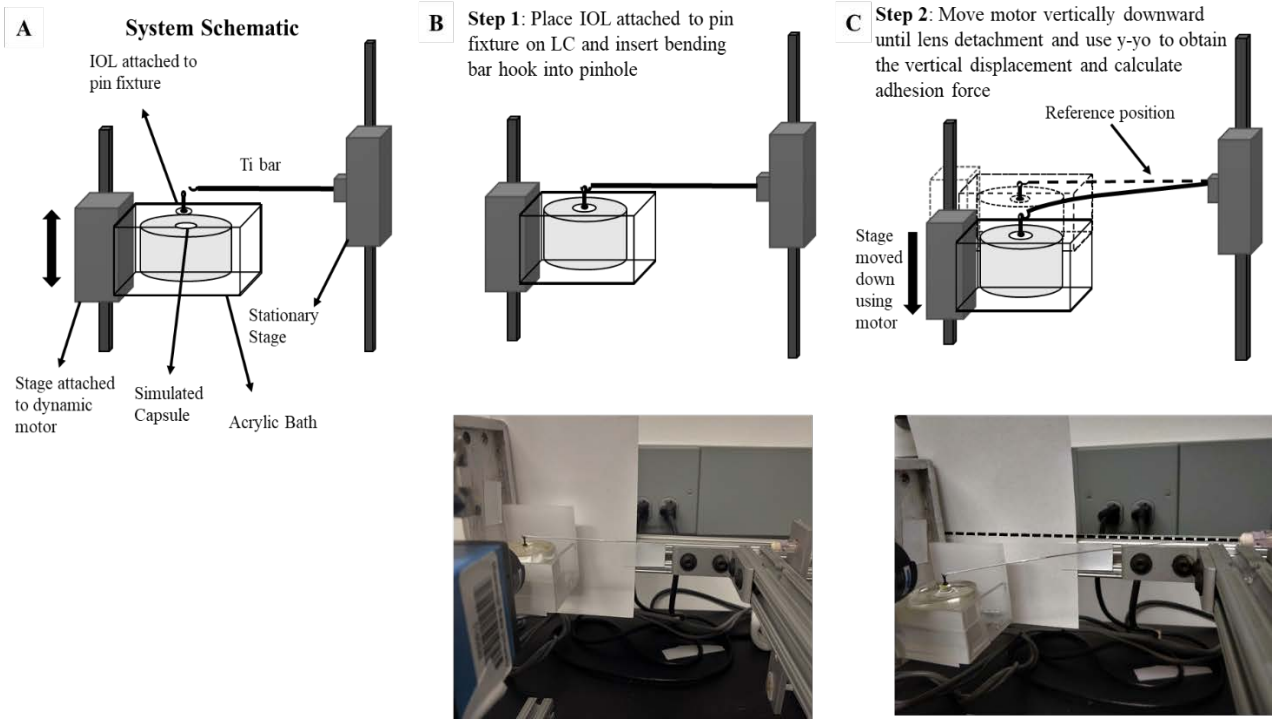

Figure 2.2. Mechanical apparatus system schematic (A) and test process schematic (B & C) with photographs

The coordinates of the marker were recorded for the entire procedure (Fig 2.3, A), and the program was stopped after the IOL detached from the gelatin capsule so that the position at the maximum bending angle could be recorded. The LabVIEW program exported the coordinate data into a spreadsheet and was then analyzed using a custom adhesion force calculation program (R Studio). This program took into consideration variables such as bending bar parameters and free end deflection and estimated the maximum adhesion force experienced by each lens.

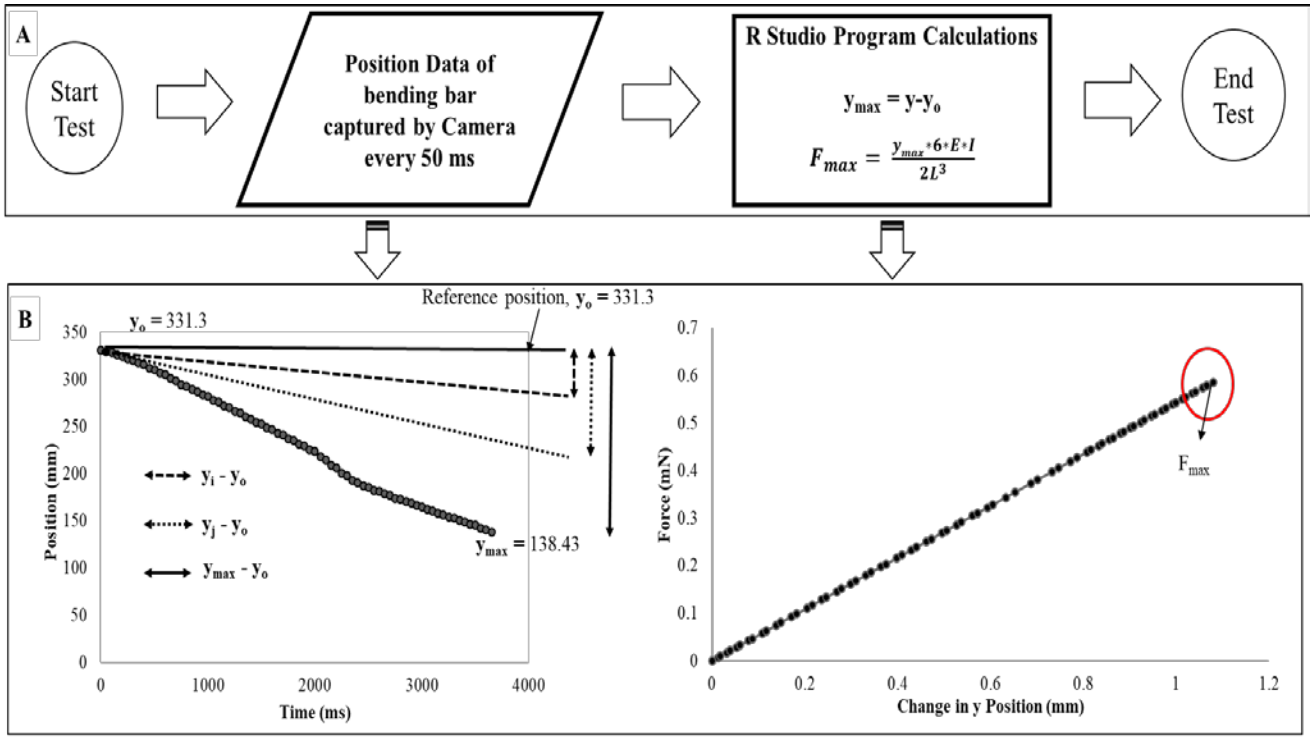

Figure 2.3. Adhesion force calculation process flowchart. A process flow diagram highlighting position tracking and force calculations (A) accompanied with graphical representation of change in position over time and consequential force data calculated as a function of change in position of the bending bar (B)

The maximum adhesion force was determined utilizing a cantilever beam deflection model, where the beam (bending bar) is fixed on one end and undergoes deflection from a vertical load at the free end. Using the marker coordinates acquired by the LabVIEW program, the R program

calculated the y displacement using $y-y_o$, where y_o is original y coordinate of the marker, and y is the final vertical coordinate of the marker (Fig 2.3, B). The maximum adhesive force was then estimated utilizing an equation specific to the cantilever beam model utilized in this system (Beer et al., 2005):

$$F_{max} = \frac{y * 6 * E * I}{2L^3}$$

where F_{max} is maximum adhesion force, E is the Young's modulus of titanium (1.11×10^{11} N/m^2), I is the moment of inertia of the bar (5.55×10^{-15} m^4) , L represents the length of the bending bar.

2.2.4. Gelatin Weight and Concentration Optimization

The influence of LC material properties on IOL adhesion force was assessed by fabricating simulated LCs with different gelatin molecular weight (high vs. low) and concentrations (@ 1%, 5%, 10% and 15% w/v). Two IOL materials with extreme clinical PCO rates- acrylic foldable (low clinical PCO rate) and PMMA (high clincal PCO rate) were used as test subjects. The adhesion forces of these IOLs to various simulated LCs were quantified at room temperature (19-21°C) and used to determine the most optimal condition that would show the largest difference in mean adhesion force between the two groups.

2.2.5. Statistical analyses

All statistical data analysis was conducted utilizing the Minitab 19 Statistical Software Package. Two sample t-tests @ 95% Confidence Interval were conducted to determine if there was a statistically significant difference between the observed adhesion force for acrylic foldable and PMMA group IOLs at different concentrations for both high molecular weight and low molecular weight gelatin molds. Lastly, two sample t-tests combined with a one-way ANOVA analysis was performed with Tukey and Fisher pairwise comparisons to determine if there was a statistically significant difference between force data obtained for all three test materials – PMMA, silicone

and acrylic foldable at the optimized gelatin weight and concentration condition.

2.3. Results

The gelatin weight/concentration was optimized by measuring the adhesion force of two materials with known clinical PCO performance –acrylic foldable (~ 11.75 % PCO incidence rates) and PMMA (~ 43.65% PCO incidence rates) with simulated LCs of different gelatin weight and concentrations. A total of four conditions were studied to optimize the gelatin molecular weight using different combinations of different gel strength (high vs. low) and concentrations (1% vs 10%) hereafter referred to as 1% Low, 10% Low, 1% High and 10% High. The mean adhesion force for the Acrylic foldable group was observed to be 0.306 ± 0.010 mN and the PMMA group was 0.302 ± 0.023 mN at 1% Low condition with no statistically significant difference between the two groups ($p = 0.686$). When the concentration of the low molecular weight gelatin was increased to 10%, mean adhesion forces for both materials increased significantly. However, there was no statistically significant intergroup difference ($p = 0.846$) between the acrylic foldable (0.759 ± 0.090 mN) and the PMMA (0.748 ± 0.078 mN) group. In line with clinically relevant observations and the material characteristics of these two materials, the system started to detect a difference in the mean adhesion force of the two materials with the simulated 3D lens capsule at the high molecular weight conditions. Mean adhesion force for the acrylic foldable (0.647 ± 0.068 mN) was slightly higher than PMMA (0.599 ± 0.059 mN) at the 1% High condition. However, there was no statistically significant difference reported between the two groups ($p = 0.264$). The 10% High condition showed the maximum difference between the two materials with mean adhesion forces for the acrylic foldable (0.747 ± 0.035 mN) ~ 1.3X PMMA (0.558 ± 0.062 mN) with a reported statistically significant intergroup difference ($p = 0.001$). These results indicate that the observed adhesion forces of each material can differ depending on the gelatin type and

concentration. The minimal difference in weights (~ 2-5 mg) of the various tested IOLs is believed to cause minimal contribution to the adhesion force results and was not considered to be significant factor. Fig 2.4. shows a plot of the mean adhesion forces observed for each material as a function of the gelatin type and concentration. From the tested conditions, only high molecular weight gelatin was able to detect a significant difference in the adhesion forces for the two test materials at the 10% w/v concentrations.

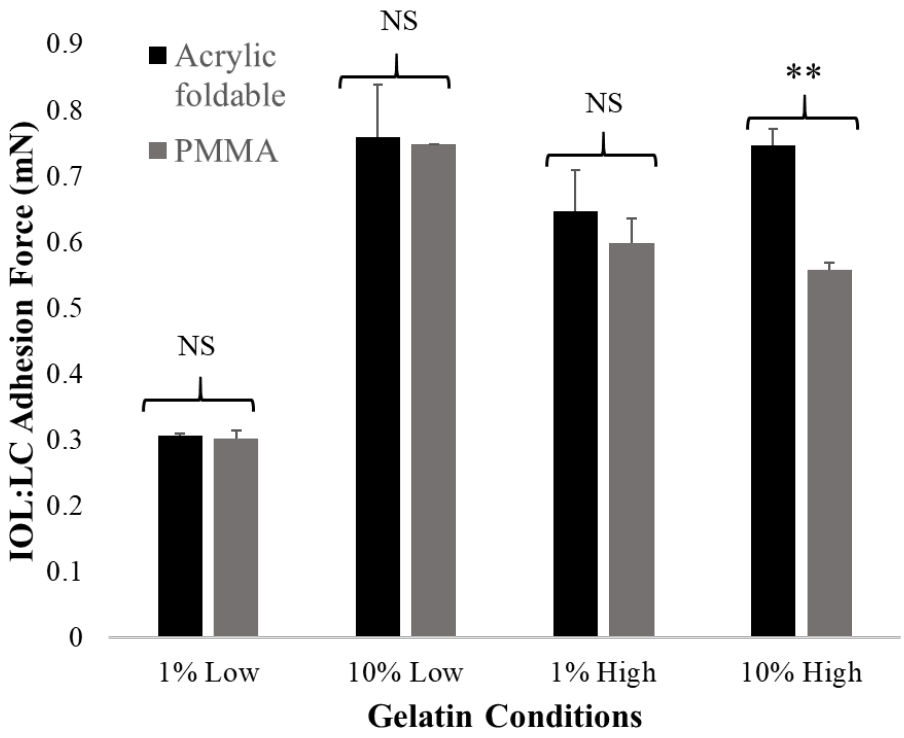

Figure 2.4. Adhesion force of PMMA and acrylic foldable IOLs with lens capsules for high and low molecular weight gelatin at 1% and 10% w/v concentration. Adhesion force measured using bending bar mechanical apparatus (n = 5, NS $p > 0.05$, **$p < 0.01$).

Thus, to further evaluate this phenomena, adhesion force testing was conducted at different concentrations of high molecular gelatin. Simulated 3D Lens capsules were fabricated with high molecular weight gelatin at 5%, 10% and 15% w/v concentrations to study the effect of concentration on adhesion force of acrylic foldable and PMMA IOLs. At the 5% high condition, there was no statistically significant difference in the mean adhesion force of the acrylic foldable (0.570 ± 0.030 mN) and the PMMA (0.548 ± 0.037 mN) group ($p = 0.613$). At the 10% high condition, the mean adhesion force for the acrylic foldable group (0.648 ± 0.113 mN) was ~ 1.3X the PMMA (0.500 ± 0.039 mN) group with a statistically significant intergroup difference ($p = 0.047$) which agreed with the results reported above affirming the reliability of this system. Interestingly, an increase in concentration from 10% to 15% showed a significant decrease in the mean adhesion force for both groups with no statistically significant intergroup differences ($p = 0.996$). The mean adhesion forces for the acrylic foldable (0.466 ± 0.092 mN) and PMMA (0.466 ± 0.057 mN) were identical. Figure 2.5 depicts a graphical representation of these results.

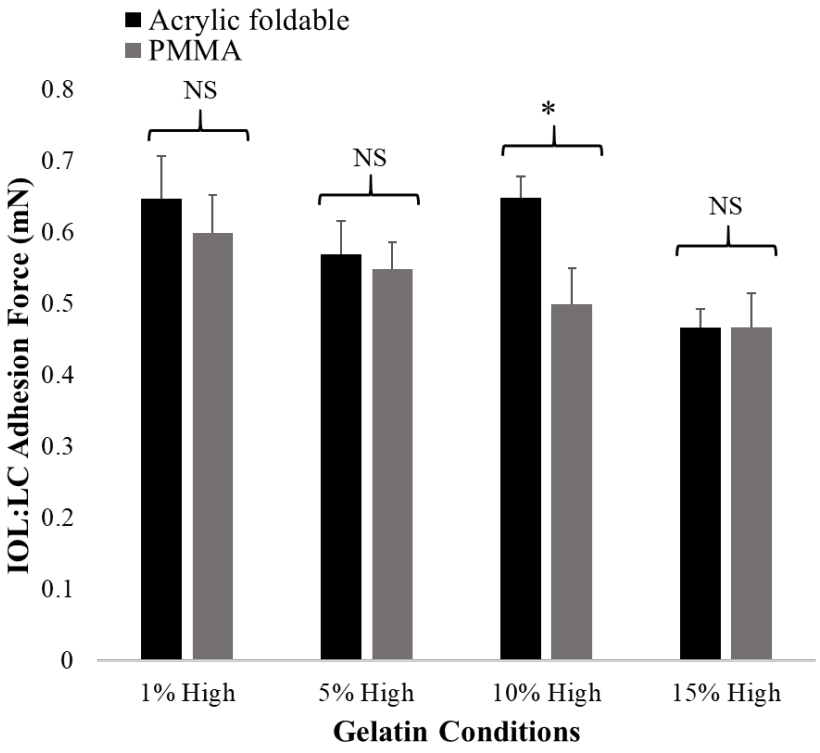

Figure 2.5. Adhesion force of PMMA and acrylic foldable IOLs with lens capsules as a function of high molecular weight concentration. Adhesion force measured using bending bar mechanical apparatus (n = 4, NS $p > 0.05$, *$p < 0.05$).

The physiological properties of any gelatin solution is influenced by its concentration, temperature and viscoelasticity. At a temperature higher than 40°C, an aqueous solution of gelatin is more viscous and its viscosity gradually decreases as the temperature comes down. The formation of gel takes place in the form of a three-dimensional helical structure with crosslinking of hydrophobic, electrostatic and hydrogen bonds. The rigidity of the gel is also directly proportional to the concentration of the gelatin solution. The strength of a gelatin gel can be evaluated by measuring its Bloom value. As the concentration of gelatin increases, the bloom value also increases. According to published literature (GMIA, 2012) , a gelatin solution with concentration less than 5% w/v has a bloom value of less than 50, which is considered low. At a lower concentration, the cross-bonds in the gel are weaker which may not allow the IOL to bind well with the gelatin

capsule. On the other hand, an aqueous solution of 15% w/v has a bloom value higher than 350. Such a high bloom strength makes the gelatin extremely rigid, which decreases its adhesiveness at the surface. However, a gelatin solution with concentration of 10% w/v has a medium bloom strength of 190, which showed the correct amount of adhesiveness at the surface as indicated by results presented in this study. Furthermore, in line with clinical observations and our expectations, the adhesiveness of the acrylic foldable group was more sensitive to changes in gelatin concentration than PMMA material IOLs that are reported to have minimal capsule adhesion owing to their glassy/brittle nature and rigid structure (Linnola et al., 2003; Oshika et al., 1998b) as depicted in Fig. 2.6. Thus, 10% w/v high molecular weight gelatin was able to show the maximum difference in the adhesion force between the two test materials and this optimized LC condition was then used to collect data for all our test materials in subsequent studies.

In line with hypothesis presented in this effort and predicate clinical PCO data on the adhesiveness of these materials, mean adhesion forces of 0.684 ± 0.028 mN, 0.546 ± 0.027 mN, 0.445 ± 0.043 mN were observed for acrylic foldable, silicone and PMMA groups respectively (Fig. 2.6, A). Two sample t-tests showed a statistically significant intergroup difference between each group i.e. silicone vs PMMA ($p = 0.024$), Acrylic foldable vs Silcone ($p=0.001$) and acrylic foldable vs PMMA ($p=0.000$). Tukey and Fisher pairwise comparisons grouped each material into a different category further confirming a statistically significant difference between each group.

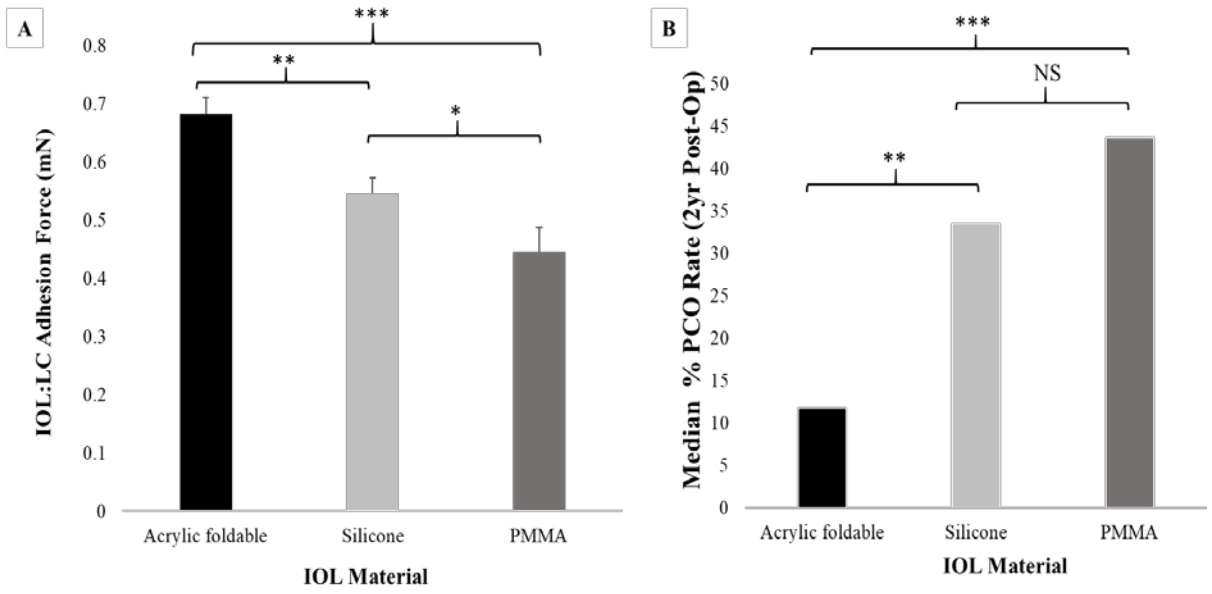

Figure 2.6. Adhesion force of PMMA (n=5), silicone (n=4) and acrylic foldable (n=5) IOLs with lens capsules at 10% w/v high mol wt condition (A) and clinical PCO performance of IOLs made from same materials (B). Adhesion force measured using bending bar mechanical apparatus (A: *p<0.05, **p < 0.01, ***p<0.001) is inversely related to clinical PCO rates of acrylic foldable, PMMA and silicone material IOLs (B : NS p>0.05, **p<0.01, ***p<0.001) (Ursell et al, 1998)

Thus, these results confirmed the inverse relationship between IOL material adhesiveness and its clinical PCO rates validating the hypothesis presented in this study that higher the adhesiveness of an IOL material, the lower its clinical PCO rate (Ursell et al, 1998) (Fig 2.6, B). While Ursell's article used all three-piece IOLs to report their clinical outcomes, our study was focused on the adhesion of the optic material to the simulated capsule as the haptics of each test IOL were cut prior to testing adhesion force. Thus, we believe that for our study, haptics would be irrelevant and adhesion force should be no different between a three piece and a single-piece IOL fabricated from the same material. While the mechanical design of an IOL, specifically, the geometry of posterior optic edge has been reported to affect clinical PCO outcomes (Findl et al., 2005; Katayama et al., 2007; Mester et al., 2004; Nishi et al., 2004), we account for that variation by designing capsules from the IOL itself to ensure that the capsule geometry is identical to posterior IOL geometry. The

potential influence of IOL design on the adhesion force may be investigated in a future study.

2.4. Discussion

In this study, a procedure to fabricate simulated lens capsules from gelatin was established and utilized to measure their adhesion force with various IOL materials. This is a significant improvement over the existing *in vitro* models that have not studied this interaction when assessing the adhesion force and/or tackiness of different IOL materials. A novel, yet simple mechanical force system was utilized to measure the adhesion force between the IOLs and the simulated lens capsules. Interestingly, this study indicated that there is a good relationship between the adhesion force and clinical PCO incidence rate. These results support the hypothesis that the measurement of adhesion force may be used to assess the PCO potential of new IOLs.

Using the custom-made bending bar-based adhesive force measurement apparatus, a maximal adhesive force between the IOL and gelatin capsule was determined. This model used a common cantilever beam model and predetermined parameters, such as bar dimensions and titanium material properties, to determine the exact adhesion force before the IOL is released from the gelatin capsule. Although, this system was able to show a correlation between adhesion characteristics of the tested materials, it has some limitations. First, current system does not allow the measurement to be done at 37 °C to better mimic physiological phenomena. Next, since the system's data collection is completely image based, large adhesion forces might deflect the bar out of the view of camera and stop further data acquisition which is likely to happen at elevated temperatures and with incubation of lenses with the capsules over time. However, the use of a bending bar with a larger diameter to keep the deflection of bar in the view of camera can provide a solution to this perceived issue. Any changes made to the bending bar (dimensions, material properties, etc.) could be accounted for in the equation, giving this system the opportunity to

present accurate results for a wide range of adhesion measurements. Thus, this bending bar measurement scheme offers a feasible, accurate, and highly adaptable method to quantitatively assess the interaction between an IOL and capsule at various conditions.

Various gelatin formulations were studied to optimize this *in vitro* system. Lens capsules fabricated from low and high molecular weight gelatin at different w/v concentration (1-15%) were studied and utilized to assess the efficacy of this system in detecting adhesion force differences between acrylic foldable and PMMA IOLs. In line with published literature (GMIA, 2012), the 10% w/v high molecular weight gelatin condition was ideal in detecting adhesion force differences given its optimum adhesiveness and ability to differentiate between the test materials. The main motivation of this work was to create human capsule mimetics. The major component of this capsule mimetics is porcine skin gelatin. Gelatin is denatured collagen which consists of a mixture of collagen fibril fragments of different lengths, structural integrity, and aggregation configuration (Báez et al., 2005; Liu et al., 2015). The overall lengths of collagen fibril fragments and the degree of entanglement of those fibrils are larger in the higher molecular weight gelatin when compared with the lower molecular weight gelatin (Báez et al., 2005; Liu et al., 2015). Those constitutive variations affect the physical, rheological, and mechanical properties of the gelatin greatly (Chien and Chang, 1972; Davidenko et al., 2016). It has been documented that the concentration of gelatin also affects its gelling and physical, rheological, and mechanical properties (Liu et al., 2015). Although the mechanism governing the differential adhesive force for the 10% w/v high molecular weight gelatin, but not other formulae, has yet to be determined, the results from several earlier studies suggest that molecular weight, mechanical strength and tissue porosity may determine the tissue adhesive property. First, it is well established that high molecular weight gelatin has better mechanical properties and offers higher elasticity in comparison to low molecular weight gelatin

(Eysturskard et al., 2009). These observations are in agreement with our finding that higher strength gelatin formulations were associated with a higher elasticity and ultimate strength (Supplemental figure 2). Second, the mechanical strength of gelatin is also directly proportional to its concentration (Usta et al, 2003). While 15% gelatin shows significantly higher ultimate stress and elastic modules than 5 and 10% gelatin formulations (Supplemental figure 2), 10% gelatin has been shown to possess the best stability among various gelatin concentrations (5, 10, 15, 20, and 50%) with a true equilibrium (Jordan-Lloyd 1931). Such true equilibrium would minimize the effect of dehydration and over-saturation on the adhesive force. The equilibrium condition may explain why 10% gelatin mold is able to show differential adhesion force to different IOLs. Finally, coincidentally, studies have shown that a high bloom value (>300) is associated with decreased biocompatibility, reduced cell proliferation and higher inflammation whereas low bloom strength gelatin (<200) does not show such undesired behavior (Lai 2009; Lai et al., 2009). A 10% gelatin yields a bloom value of ~ 190 whereas a 15% gelatin yields a high bloom value of 350 (GMIA, 2012). Using this capsule mimetic model, our experimental results showed that the *in vitro* capsule mimetic model (10% high molecular weight) was able to capture the different adhesive interactions when attached with the acrylic foldable and the PMMA IOL, which was consistent with the clinical observations of how the human capsule interacts with the acrylic foldable and the PMMA IOLs. This model is thus promising and valuable to predict PCO of various IOLs. Quantitative biomechanical comparison of various gelation formulations using tensile testing (Table 1 and Supplemental figure 2.1) was performed and their microstructure and composition were compared with the human capsule material. Even though, the reported Young's modulus of the selected 10% high formulation (~0.012 N/mm^2) used was slightly lower than the 15% high formulation (~0.062 N/mm^2), it was close to the Young's Modulus for primate (~ 0.013

N/mm^2) and human lens capsules (~ 0.020 N/mm^2) reported in other studies (Danysh and Duncan, 2009; Ziebarth et al., 2011). While we understand that the mechanical strength of these simulated capsules was lower than the human capsule, studies aimed at improving the mechanical strength of these gelatin capsules while maintaining its adhesiveness will be conducted in the future. Due to the low strength of the 1% Low and 1% High formulations, we were unable to perform tensile testing for those formulations due to issues with specimen handling.

This optimized *in vitro* model was able to successfully capture the differential adhesion force of acrylic foldable, PMMA and silicone material IOLs with simulated LCs. The forces observed in this study were highest for the acrylic foldable group, followed by silicone and PMMA that proved the hypothesis that high adhesiveness is associated with lower clinical PCO rates. These results are clinically more relevant than Oshika's adhesion study that was unable to detect any adhesion force of silicone materials to the collagen substrate (Oshika et al., 1998). By utilizing lens capsules that were fabricated from the test IOLs themselves, simulated LCs with structure and mechanical dimensions (radius and curvature) similar to the test IOLs were utilized in this study as opposed to predicate study conducted by Oshika that utilized flat collagen sheets as their test substrate (Oshika et al., 1998). The human capsule is a membranous structure that completely encloses the lens (Danysh and Duncan, 2009). Thus, both the posterior and the anterior interior surfaces of the lens capsule have a curvature that can play a role in the way the LECs proliferate and migrate on the capsule and the IOL surface post-implantation. The *in vitro* model established in this effort is more in line with clinical phenomena where the lens capsule collapses and shrinks wrap on the IOL post-implantation (Raj et al., 2007). Clinical evidence from predicate studies have shown that the tissue response to Alcon's acrysof IOLs, a hydrophobic acrylic foldable IOL is different from other biomaterials such as PMMA and silicone. The adhesive properties of the Acrysof lens are

believed to play a pivotal role in preventing PCO formation. When the biological substrate is the posterior LC, its rapid and strong adhesion to the Acrysof surface (Linnola et al., 2000a) may seal off the interfacial space preventing the proliferation and migration of residual LECs in the capsule space thereby preventing PCO as supported by many previous observations (Katayama et al., 2007; Ursell et al., 1998).

Clinical anecdotal evidence from surgeons who have attempted to explant Acrysof IOLs have suggested that the capsular bag actually sticks to this IOL over time, making it increasingly difficult for them to explant, unless the procedure is carried within few weeks of surgery (Ursell et al., 1998). Acrylic foldable IOLs such as the Acrysof IOLs are associated with a decreased surface hydrophobicity and an increased amount of water uptake in an aqueous medium (Bertrand et al., 2014; Miyata and Yaguchi, 2004). At physiological temperatures and under incubation with the simulated capsules, it is possible that over time, the acrylic foldable IOLs will undergo surface functionalization and/or modification resulting from absorption of water from the gelatin capsule leading to an increase in the adhesion force, a phenomenon that will be studied in future efforts. Furthermore, It has also been proven that the formation of cross-bonds is a slow process and the strength of gelatin gel increases with time as the cross-bonds are formed (Slade and Levine, 1987). This phenomenon can also takes place on the surface of the fabricated gelatin capsules and may contribute to an increase in adhesion force as a function of time, similar to clinically observed phenomenon. Therefore, the high adhesion force between the simulated lens capsules and the acrylic foldable IOLs may be attributed to its functional surface changes and water uptake characteristics. On the other hand, the relatively higher adhesive forces for the silicone material IOLs in comparison to PMMA may be attributed to the presence of functional moieties on its surface that possess a high affinity for collagen (a major constituent of the gelatin capsule)

(Rønbeck and Kugelberg, 2014a; Vasavada and Praveen, 2014) leading to tight binding between the two substrates. Lastly, the PMMA IOLs reported to have minimal capsule adhesion (Linnola et al., 2003; Oshika et al., 1998b), possibly do not experience any noticeable surface modification unlike the silicone and acrylic foldable materials given their rigid structure.

The results presented in this study demonstrate the capability of this system to simulate IOL: LC interactions in an *in vitro* setting laying the foundation for future studies aimed at predicting PCO. This system has the potential to be utilized to investigate the role of different IOL physical/chemical properties, ECM proteins, and lens epithelial cells on IOL: LC interactions and may be instrumental in reducing the number of *in vivo* and clinical studies to assess the safety and efficacy of novel IOL platforms at physiological conditions. Furthermore, given the demographics of the cataract population with >90% patient population at least 45 years of age or over (Thylefors et al., 1995), there is a medical need for presbyopia correcting accommodative IOLs. Technological advancements in the field of IOL fabrication have led to the development IOLs that utilize curvature changing viscoelastic optic materials (Alió et al., 2018; Sheppard et al., 2010; Wolffsohn et al., 2006) to facilitate accommodation and this system may be instrumental in screening these IOLs by simulating force responses necessary to generate the desired accommodation. The ease of manufacturability and the low expenditure associated with the proposed simulated lens-capsule adhesion model will be instrumental in facilitating its adoption to study PCO, test the efficacy of accommodative IOLs and address current limitations in existing models.

2.5. Conclusions

Here we report the creation of a new *in vitro* 3D system which can be used to assess the interaction (adhesion force) between an IOL and a simulated LC. This *in vitro* model was established with

simulated LCs and a custom-designed micro-force tester. A method to fabricate simulated LCs was developed to create simulated 3D LCs with curvature resembling the human capsule bag-like structure that collapses on the IOL post implantation. By pushing the LC mold vertically downward and measuring the change in position of the bending bar with respect to its start position, the adhesion force between the IOLs and LCs was measured. This effort has led to the determination of the optimal simulated LC formulation and testing apparatus to differentiate the adhesion force of simulate LCs with various biomaterials. There is also a good relationship between adhesion force measured by this system and PCO incident rates reported based on clinical observations. This new system has the potential to address current gaps in existing PCO models by providing researchers and IOL manufacturers with an *in vitro* system that allows rapid collection of data and enables simulation of clinical PCO phenomena.

Supplemental Figure(s)

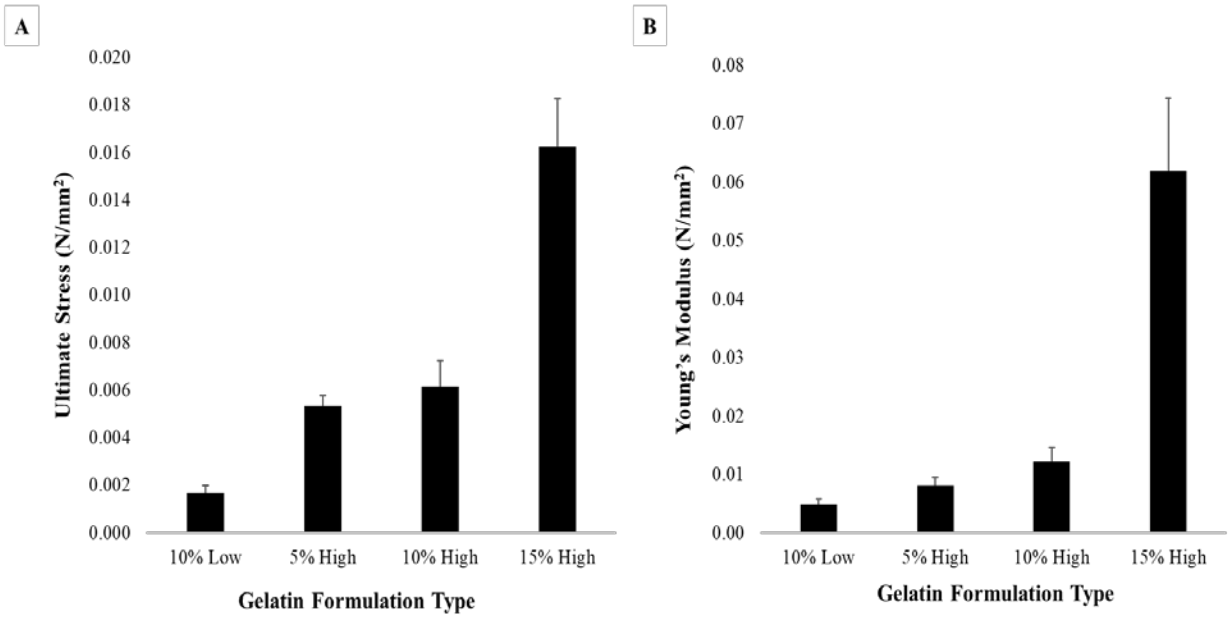

Supplementary Figure 2.1. Mechanical property characterization of various simulated lens capsule formulations. (A) Elastic modulus and (B) Ultimate stress of lens capsules made of high (5%, 10%, 15% w/v) and low molecular weight gelatin (10% w/v)

CHAPTER 3

Effect of Time and Temperature-Dependent Changes of IOL Material Properties on IOL: Lens Capsule Interactions

3.1. Introduction

The interaction of an implanted IOL with the lens capsule plays a pivotal role in affecting the path of PCO progression (Jaitli et al., 2021; Katayama et al., 2007; Linnola, 1997; Linnola et al., 2003, 2000a; Nibourg et al., 2015; Oshika et al., 1998a; Pérez-Vives, 2018; Versura et al., 1997; Wormstone, 2020). While the adherence and then proliferation of residual lens epithelial cells (LECs) onto the implanted IOL may proliferate at the IOL: Lens capsule (LC) interface and eventually lead to PCO formation (Eldred et al., 2019; Huang et al., 2010; Linnola, 1997; Nibourg et al., 2015; Nishi et al., 2004a; Oshika et al., 1998b; Pérez-Vives, 2018; Vasavada and Praveen, 2014; Versura, 1999; Wormstone, 2020; Wormstone and Eldred, 2016a), the factors that influence IOL: LC interactions are still not clearly understood due to the multifactorial pathogenesis of PCO (Cheng et al., 2007; Findl et al., 2010; Hyeon et al., 2007; Pérez-Vives, 2018)

Current established *in vitro* models have several limitations as described in section 1.7. To overcome such limitations, a new *in vitro* 3D system to assess the adhesion force between an IOL and a simulated LC was established (Jaitli et al., 2021). This *in vitro* model utilized simulated LCs that were fabricated by imprinting IOLs onto molten gelatin to create simulated three dimensional (3D) LCs with curvature resembling the bag-like structure that collapses on the IOL post implantation (Jaitli et al., 2021). This model may serve as a new and alternative system to evaluate the interactions between IOLs and LCs.

Several physical and chemical properties of IOLs, such as surface hydrophobicity, adhesiveness and posterior edge geometry, have been known to influence the rate of PCO formation (Boulton and Saxby, 1998; Katayama et al., 2007; Kim et al., 2001; Linnola et al., 2003, 2000a, 2000b; Oshika et al., 1998; Ursell et al., 1998; Versura, 1999; Xu et al., 2016a, 2016b). PCO rate of different acrylic IOL materials was found to be inversely proportional to their adhesiveness (Katayama et al., 2007). Studies have also shown that a sharp posterior optic edge may create a

barrier effect to suppress the migration of LECs and thus the pathogenesis of IOL induced PCO (Buehl et al., 2005; Haripriya et al., 2017; Nishi, 1999a, 1999b; Nishi et al., 2000; Nishi et al., 2004; Wormstone, 2020; Wormstone and Eldred, 2016b). Furthermore, the adhesiveness or "tackiness" of IOL materials has also been shown to influence the rate of PCO formation. Results have found that IOLs with high adhesiveness may bind tightly to lens capsule and indirectly suppress the migration of lens epithelial cells and thus reduce the rate of PCO formation (Oshika et al., 1998b). In an attempt to answer some of the above questions, intensive research efforts have been placed in this field. Unfortunately, many of these results are contradicting with each other. Coincidentally, many of these studies were carried out at different conditions, such as study temperature and incubation time. For example, Nagata conducted a study to measure the adhesive force of both Acrysof and PMMA IOLs at 37 °C but only tested adhesion of these IOLs after 1 minute incubation with a collagen film (Nagata et al., 1998). Further, Oshika's *in vitro* study to assess adhesion of different IOL materials with collagen was conducted at 22 °C with adhesion force measured after 30 seconds of incubation (Oshika et al., 1998). To assess the influence of experimental condition on the interaction between IOLs and LCs, this study was carried out to examine the influence of incubation time (0 vs 24 hours) and temperature (21 °C vs. 37 °C) on the adhesion force between LCs and three commonly used IOLs (hydrophobic acrylic foldable, PMMA and Silicone IOLs). We also examined whether and how body temperature may affect the surface properties of different IOL materials by conducting hydrophilicity and surface roughness measurements of these IOLs. Last, to indirectly test the "No space, No cell" hypothesis (Ursell et al., 1998), a novel imaging technique was developed to determine whether the high adhesion force would lead to reduced macromolecule dye infiltration between the LC and IOLs.

3.2. Materials and Methods

3.2.1. Intraocular Lenses

IOLs fabricated from three types of materials – Hydrophobic acrylic foldable (hereafter referred to as 'acrylic foldable'), PMMA and Silicone were utilized in this study. The single piece acrylic foldable IOLs had a 6.0 mm biconvex optic, a sharp rectangular posterior edge and planar haptics with an overall length of 13.0 mm (Alcon's SN60WF, Alcon Research, Fort Worth, Texas) with a dioptric power of 21.0D. The PMMA group were single piece IOLs with a 5.5 mm PMMA optic, round posterior edge and multiflex haptics with an overall length of 13.0 mm (Alcon's MTA4U0, Alcon Research, Fort Worth, Texas) with a dioptric power of 23.5D. The Silicone group comprised of three-piece posterior chamber biconvex silicone 6.0 mm optics that had a round edged profile and blue PMMA mod C haptics with an overall length of 13.0 mm (Allergan's AMO Array SA40N, Allergan Inc, Irvine, California) with dioptric powers between 10.0 D and 26.0 D. 'Mod C Haptics' is the term that describes the haptic configuration of the IOL which is listed as 'Modified-C' in the technical specifications of this IOL. This information can be found on the package document and its directions for use (DFU) of this commercially available IOL product. The term 'Mod C' is an acronym used by the manufacturer to describe the configuration of the haptic portion of this IOL that the authors assume refers to the shape of the haptic loop which looks similar to the alphabet 'C'. These haptics were fabricated from blue polypropylene monofilament or blue core polymethylmethacrylate (PMMA) monofilament material.

3.2.2. Fabrication of simulated lens capsule

Simulated LCs were created to possess a spherical cup shaped structure that closely mimics the morphology, structure and mechanical integrity of the human capsular bag (Jaitli et al., 2021). To better mimic the mechanical strength of the LCs, simulated LCs were gently crosslinked with

glutaraldehyde using previously published crosslinking method (Dardelle et al., 2011). The modified procedure is described as follows. Briefly, simulated LCs were fabricated using high strength gelatin from porcine skin (Sigma-Aldrich, #48724, 240-270 g Bloom gel strength). A 10% gelatin solution was dissolved and stirred in de-ionized water at 40 °C for 10 minutes. To simulate real LCs which possess high mechanical strength and withstand high temperature, the solution was then crosslinked with 0.25% w/v glutaraldehyde solution (Sigma Aldrich, #G6257, grade II, 25% in water) as established earlier (Dardelle et al., 2011). The prepared solution was poured into acrylic petri-dishes immediately prior to the placement of IOLs. Next, IOLs with haptics intact were taped onto small thin circular lightweight support materials to ensure the IOL stayed afloat through the solidification process at 4 °C for 1 hour. By gently peeling the IOLs from the gelatin surfaces with the help of thin forceps, a simulated lens capsule mold with a geometry identical to the posterior surface of the lens was created. To minimize variability potentially resulting from different IOL geometries, every capsule was custom built using the test IOL itself. Further, the concentration of cross-linker was optimized by assessing the potential influence of different concentrations on the surface adhesiveness and the stability of the simulated capsules at body temperatures. This analysis has been included in the supplemental materials of this chapter (section 3.S.1.).

3.2.3. Characterization of simulated lens capsule

Uniaxial testing was performed on the crosslinked gelatin mold specimens that were dissected into 10 thin rectangular strips with Length: 35mm, Width: 6mm, and Thickness: 5.15-6.37 mm. All uniaxial tensile testing was performed using a universal mechanical testing system (TestResources, MN) as described earlier (Weed et al., 2012). Briefly, uniaxial testing was performed at a ramping speed of 25 mm/min until fracture was observed. The stress-strain curve showed an overall linear

trend and the elastic modulus was estimated using linear regression. For all samples, engineering stress was calculated by normalizing the applied force to the original cross-sectional area, and engineering strain was calculated by normalizing the amount of specimen deformation to the initial gauge length. To verify that the simulated lens capsules possessed material properties similar to the human capsule, the gelatin capsule's material properties were characterized and compared to the properties of the human capsule (Danysh and Duncan, 2009; Ziebarth et al., 2011).

Properties	Human Lens capsule	Simulated Lens Capsule(s)
Protein composition	Collegen (type IV), Laminin, Nidogen/Entactin, Heparan Sulfate Proteoglycans, Perlecan, Collagen XVIII, Fibronectin, SPARC (osteonectin)	Collagen (type I)
Surface hydrophobicity	Hydrophilic	Hydrophilic
Physical property	Thin membrane around the natural lens	Curved soft gel around IOLs
Elastic Modulus	~ 0.02 N/mm^2	0.0121 N/mm^2
Ultimate Stress	~ 1.5 N/mm^2	0.0061 N/mm^2
Interaction with IOL	Shrink wrap around IOL	Custom made to fit IOL

Table 3.1. Comparison of material properties of the simulated lens capsule and the human lens capsule

The average elastic modulus of the specimens was observed to be 0.023±0.005 N/mm^2 and their average Ultimate Strength was observed to be 0.021±0.002 N/mm^2. A comparison of the material and mechanical properties of the simulated capsules and the human lens capsule has been summarized in Table 3.1.

3.2.4. Adhesion force measurements

All test samples (Acrylic foldable, PMMA and Silicone) and LC assemblies were incubated in a temperature controlled chamber at 21 ± 1 °C and 37±1 °C for 4 hours and 24 hours to assess the influence of incubation time and temperature on IOL: LC adhesion force for all materials. A 3-D printed pinhole structure with a flat circular 3-mm disk head was attached to the anterior surface of the IOL optic and placed carefully at the gelatin capsule. The IOL: LC assemblies were then placed in an airtight container to minimize the change in concentration of the 3D LC molds resulting from evaporation of water at elevated temperatures and placed inside the incubation chamber for predefined time points. Adhesion force was measured at the predefined time points and analyzed to calculate the differences in the forces observed at the different time points.

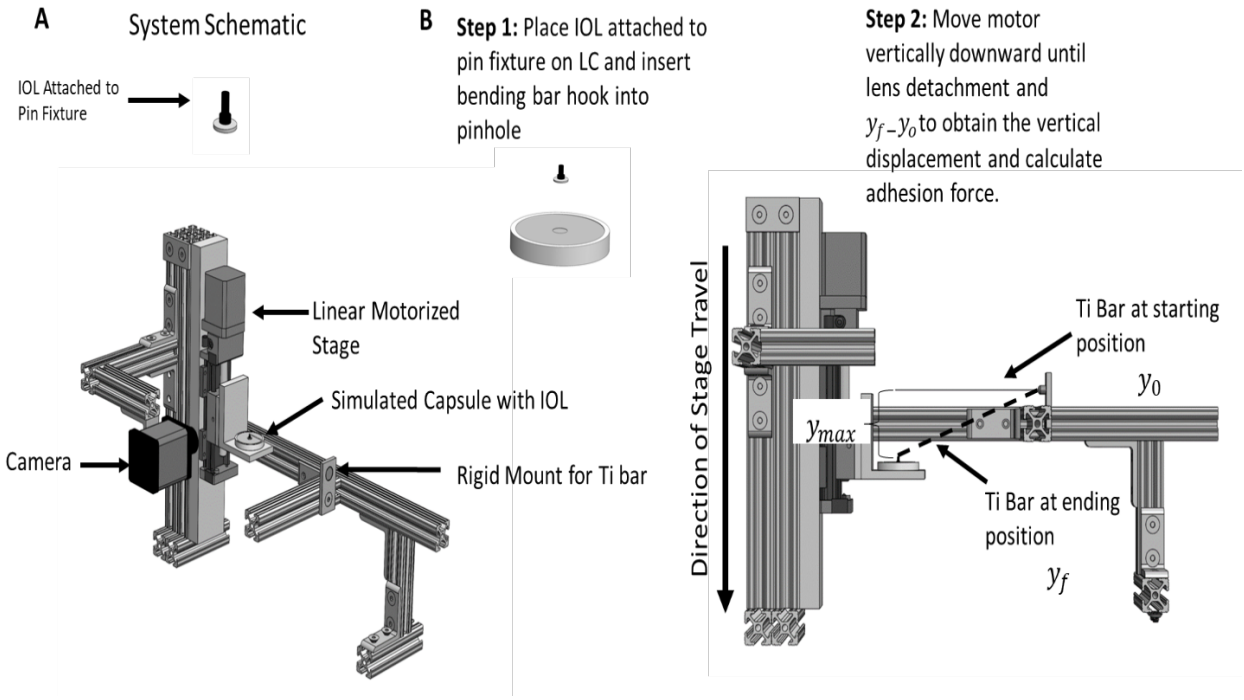

Figure 3.1. Mechanical Apparatus System Schematic (A) and Test Process Schematic (B).

After incubation at 4 and 24 hours, the adhesion force between the IOLs and LCs was determined using previously established custom made adhesion force apparatus (Jaitli et al, 2021). Figure 3.1 shows a 3-D model of the system apparatus (Fig. 3.1, A) and the test process (Fig. 3.1, B).

3.2.5. Surface hydrophilicity and roughness measurements

Material surface properties play a critical role in its adhesion to a biological substrate such as the lens capsule and influence biological responses post implantation (Jung et al., 2017). To assess the influence of temperature and hydration, surface properties of the test IOL materials before and after incubation in Balanced Salt Solution (BSS) at 21 °C and 37 °C for 24 hours were characterized by contact angle measurements to determine the surface hydrophobicity and by white light interferometry (WLI) to measure their surface roughness. Both measurements were made on acrylic foldable, PMMA, and silicone IOLs. Contact Angle measurements of all IOLs were made using the Video Contact Angle (VCA) Optima system (AST Product Inc., Billerica, MA) by following manufacturer's instruction. The contact angle was calculated using the Sessile Drop method with an accuracy of ± 0.5° as described earlier (Cunanan et al., 1998; Jung et al., 2017). The surface roughness, morphology and topology of test IOL materials were characterized using a Taylor Hobson Coherence Correlation Interferometry (CCI) instrument (Model # CCI MPHS, Taylor Hobson, Leicester, United Kingdom). All data was acquired using a TalySurf CCI software and post processed in TalyMap Platinum. To avoid discrepancies in surface roughness results caused by debris/particulate on the test samples, the lens surface was cleaned with a fine Q-tip soaked in DI water. The "Sloped or Curved" measurement mode was utilized for all scans in the study for surface roughness characterization. Raw data comprised of 2D maps and 3D surface morphology and topology information and was processed using a 4^{th} degree polynomial function to remove the general form of the test surface i.e. the curvature of the lens. Resulting data

consisted of peaks and valleys that were utilized to collect surface roughness of the test surface. The surface roughness parameters examined in this study was *Sa* (mean surface roughness or arithmetic mean of the absolute value of the height within a sampling area) as shown in the equation provided below.

$$Sa = \frac{1}{A}\int_{A} |z(x,y)|\, dxdy$$

where *A* refers to the sampling area and *z(x, y)* is the surface departure.

3.2.6. Visualize "cell" infiltration at the space between IOL and LC

To test the "No space, No cell" hypothesis (Pearlstein et al., 1988; Ursell et al., 1998), a novel imaging system was established to assess the available space between IOLs and LC using a macromolecule dye solution to simulate cell infiltration. Briefly, the imaging set-up consisted of a 3.2 MP color camera with a 2048 x 1536 resolution (GS3-U3-32S4C-C, Wilsonville, OR) paired with an Edmund Optics telecentric lens (54-798, Tucson, AZ) mounted vertically utilizing Edmund Optics mounting clamp (56-024, Tucson, AZ) to maximize the field of view capturing the lens and LC. A diffused white light (LND2-200SW, Japan) was used to fully illuminate the mold and lens. The imaging assembly was mounted on the following opto-mechanical hardware: Newport optical rail carrier (PRC-3, Irvine, CA), Newport precision optical rail (PRL-12, Irvine, California), with a 3D printed part to interface with mounting clamp and carrier. The rail was mounted to an optical bread board (MB612F, Newton, NJ) held by two right angle brackets (VB01, Newton, NJ) mounted to another optical breadboard (MB12, Newton, NJ). Figure 3.2 shows photographs of the imaging bench in frontview (Fig. 3.2, A) and sideview (Fig 3.2, B) orientations.

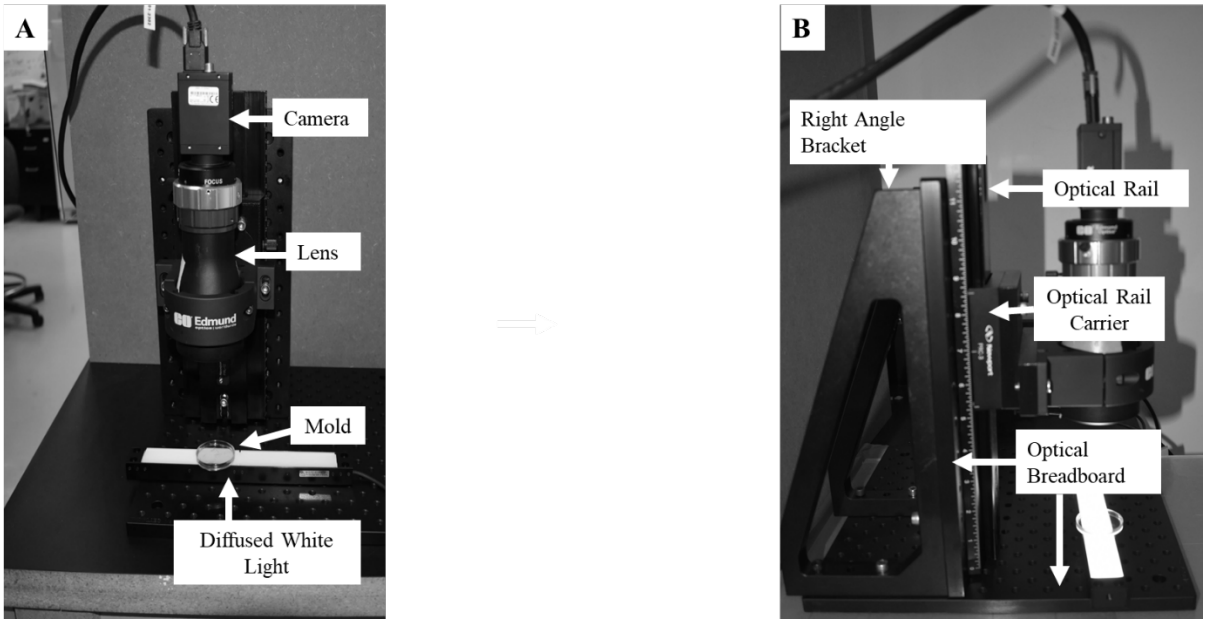

Figure 3.2. Frontview (A) and sideview (B) photographs of the imaging System

Blue Dextran dye (Sigma-Aldrich D575) at 5 mg/mL concentration was used to simulate cell infiltration and provide a visual cue on the space between IOLs and LCs. The studies were carried out as follows. IOLs were placed inside the gelatin molds which were then placed in 37 ± 1°C incubator for 24 hours (Fig. 3.3, A). The dye solution (10µL) was then injected at the edge of IOL-filled molds (Fig. 3.3, A) and the molds were then imaged (Fig. 3.3, A). The extent of dye penetration in the space between IOL and LC was then calculated by analyzing the images (Fig. 3.3, B) using NIH ImageJ software (Fig. 3.3, C).

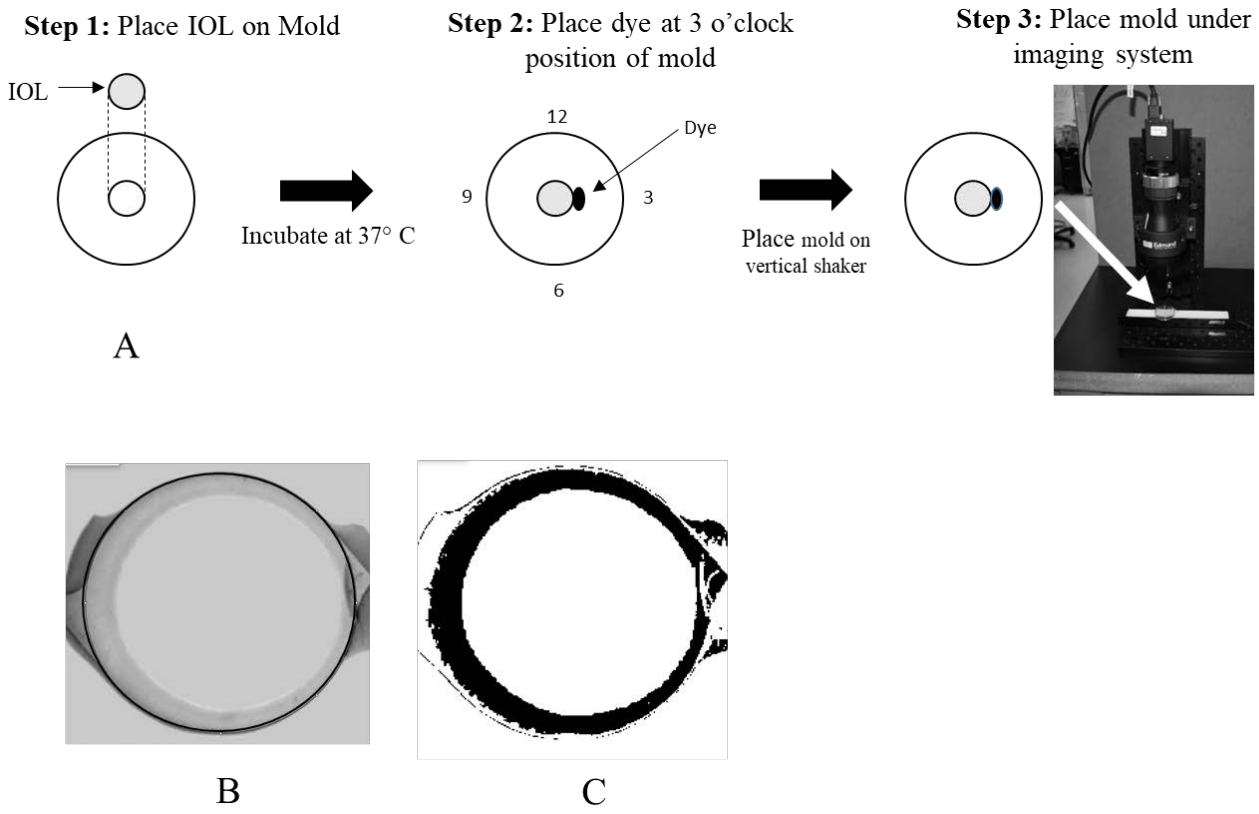

Figure 3.3. Imaging Test Process Schematic (A) of blue dextran dye occupying posterior side of IOL and on the periphery of the IOL: LC interface (B). The collected image(s) was analyzed to calculate the % of dye penetration in ImageJ software as shown below (C).

3.2.7. Statistical analyses

All statistical data analysis was conducted utilizing the Minitab 19 Statistical Software Package. Two sample t-tests @ 95% Confidence Interval (CI) were conducted to determine statistically significant differences between the IOL materials at specific time and temperature conditions. Intragroup differences for each material resulting as a function of time and/or temperature were determined by paired t-tests @ 95% CI.

3.3. Results

3.3.1. Effect of temperature and incubation time on IOL: LC Adhesion Force

To study the effect of temperature and incubation time on IOL: LC interaction and also simulate

true clinical phenomena, it was imperative to study the IOL: LC adhesion forces at different temperatures (ambient temperature ~ 21°C and body temperature ~ 37°C) and incubation time (0 , 4, and 24 hours). At 0 hour, the adhesion forces of 0.757 ± 0.111 mN, 0.473 ± 0.075 mN, 0.377 ± 0.111 mN were observed for acrylic foldable, silicone and PMMA IOLs, respectively (Fig. 3.4).

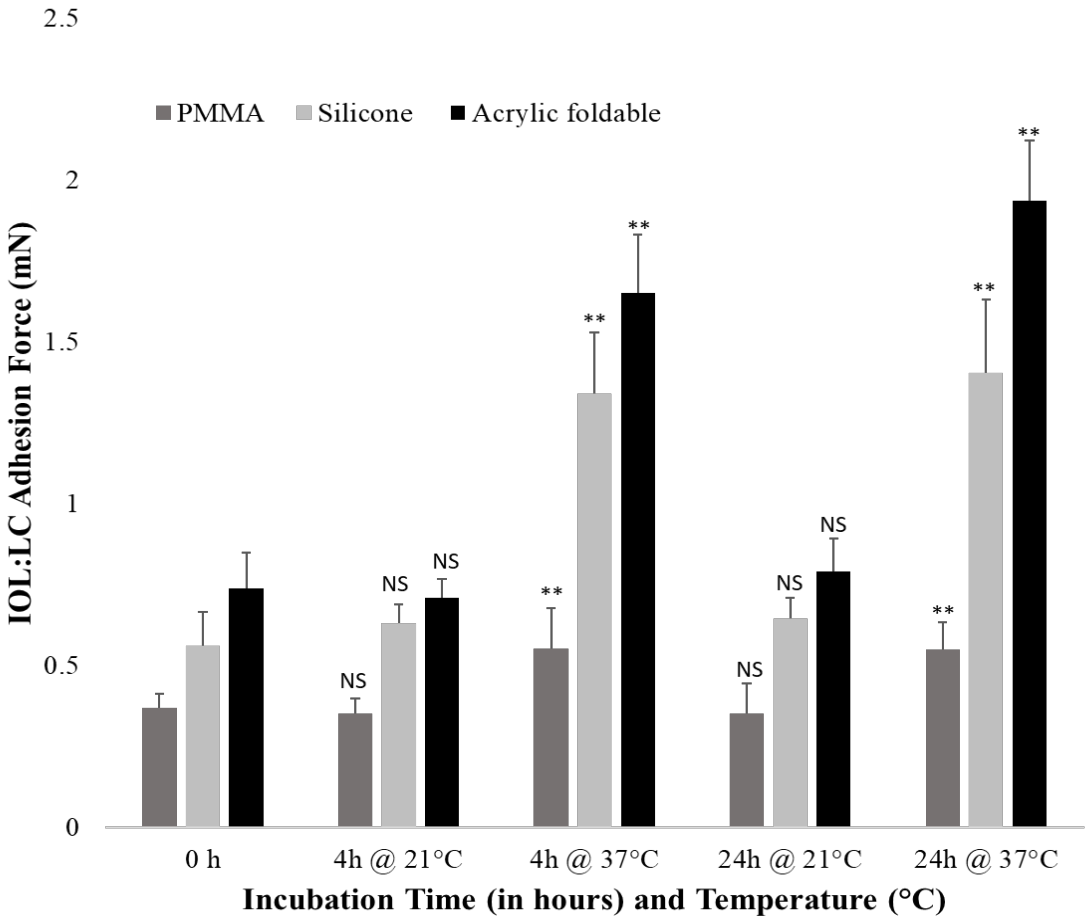

Figure 3.4. IOL:LC adhesion force for PMMA, silicone and acrylic foldable IOLs at different incubation time (0, 4 and 24 hours) and temperatures (21 °C and 37°C) (n = 10, significance vs 0 hour of the same group, NS: $p > 0.05$, *$p < 0.05$, **$p < 0.01$).

A two-sample t-test showed that the average force observed for each group was statistically different from each other (Table 3.2).

Comparison Group	Incubation Time	p-value (α = 0.05)	
		21 °C	37 °C
PMMA vs Silicone	T = 0 h	0.000**	0.000**
PMMA vs Acrylic foldable		0.000**	0.000**
Silicone vs Acrylic foldable		0.003**	0.003**
PMMA vs Silicone	T= 4 h	0.000**	0.000**
PMMA vs Acrylic foldable		0.000**	0.000**
Silicone vs Acrylic foldable		0.013*	0.002**
PMMA vs Silicone	T = 24h	0.000**	0.000**
PMMA vs Acrylic foldable		0.000**	0.000**
Silicone vs Acrylic foldable		0.002**	0.000**

Table 3.2. Summary of two-sample t-tests (95% CI) for observed IOL: LC adhesion forces for PMMA, silicone and acrylic foldable IOLs at 21 °C and 37 °C. Significance, *p<0.05, **p<0.01.

After incubation for 4 and 24 hours, we found that the change in adhesion force for all groups over time at 21°C was insignificant with a paired t-test at 95% CI (Table 3.3). The adhesion forces among all IOLs were in the following order: acrylic foldable > silicone > PMMA. On the other hand, at 37 °C, there was substantial increase of adhesion forces with increasing incubation time among all three IOLs in the following order: acrylic foldable > silicone > PMMA (Fig. 3.4). Further, paired t-tests at a 95% CI showed statistically significant difference in average forces between T0, T4, and T24 time points for each group (Table 3.3). It should be noted that the difference between average forces reported for T4 and T24 time points was statistically

insignificant for PMMA and silicone groups at 37°C (Table 3.3). These results suggest that the adhesion force between IOL and LCs achieve plateau at or before 4 hours for these groups. The acrylic foldable group, however, reported further increase in adhesion force after 4 hours (Fig 3.4 and Table 3.3). These results show that there is a much stronger interaction between the IOL and LC at 37 °C in comparison to 21 °C.

Comparison Group		p-value (α = 0.05)	
		21 °C	37 °C
PMMA	**0 vs 4 hours**	0.447 ^{NS}	0.003**
	4 vs 24 hours	0.985^{NS}	0.934^{NS}
	0 vs 24 hours	0.620^{NS}	0.001**
Silicone	**0 vs 4 hours**	0.198^{NS}	0.000**
	4 vs 24 hours	0.395^{NS}	0.508^{NS}
	0 vs 24 hours	0.117^{NS}	0.000**
Acrylic foldable	**0 vs 4 hours**	0.526^{NS}	0.000**
	4 vs 24 hours	0.081^{NS}	0.002**
	0 vs 24 hours	0.286^{NS}	0.000**

Table 3.3. Summary of paired t-test (95% CI, α = 0.05) between different time points (0, 4 and 24 hours) for IOL: LC adhesion forces for PMMA, silicone and acrylic foldable IOLs at 21 and 37 °C. Significance, NS: $p > 0.05$, **$p<0.01$

3.3.2. Effect of temperature and hydration time on surface hydrophobicity

Since hydration time and temperature have been shown to influence hydrophobicity of some materials (Bertrand et al., 2014; Miyata and Yaguchi, 2004) and IOL surface hydrophobicity has been found to influence IOL:LC interactions (Li et al., 2013; Zhao et al., 2017), subsequent studies were carried out to investigate the potential role of IOLs' surface hydrophobicity in temperature and hydration time-dependent IOL: LC adhesion force. To find the answer, contact angle measurements were collected for acrylic foldable, silicone and PMMA IOLs before and after 24-hour incubation at both 21 °C and 37 °C (Figure 3.5).

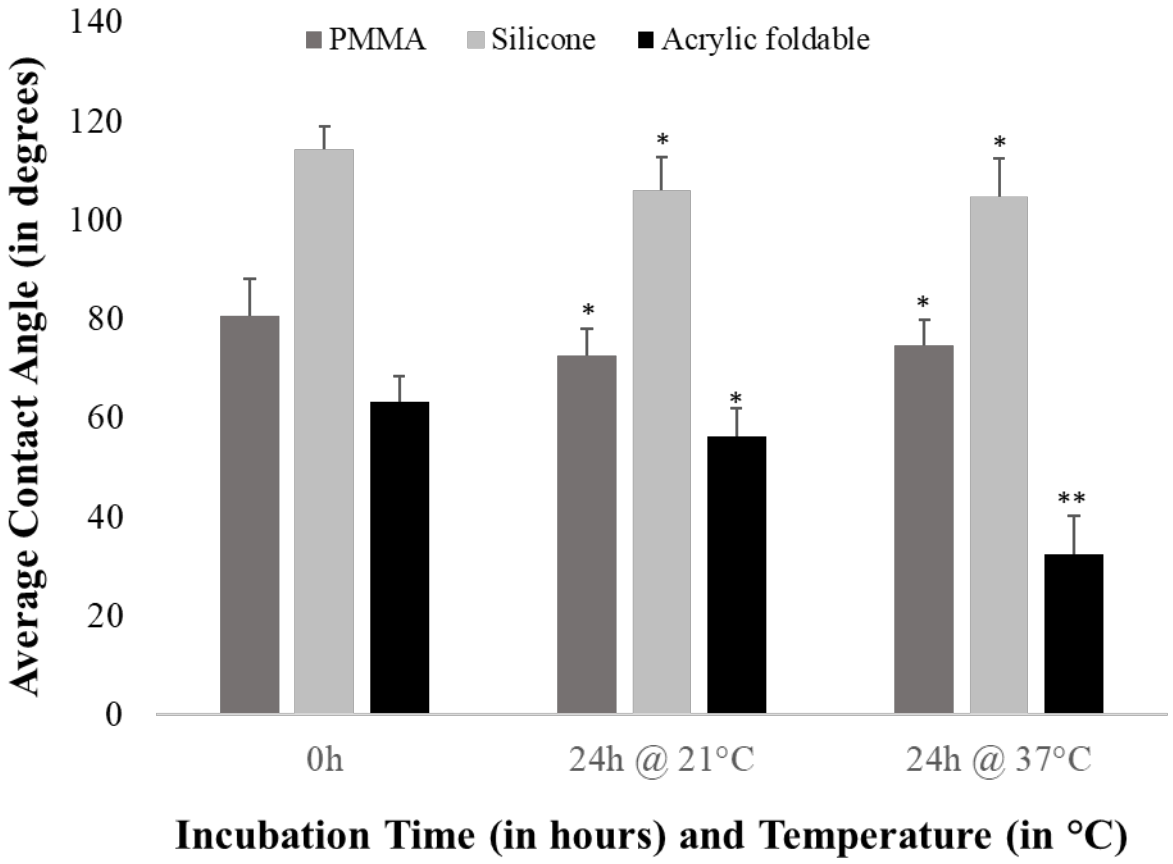

Figure 3.5. Change in surface contact angle as a function of incubation time and temperature. Contact angle measurements for PMMA, silicone and acrylic foldable test IOLs were carried out at 0 and 24 hours post hydration in BSS at different temperatures (21 °C and 37 °C) (n=10, significance vs 0 h of the same group, *$p < 0.05$, **$p<0.01$).

First, at T=0 prior to incubation, the hydrophobicity of all test IOLs was in the following order: silicone > PMMA > acrylic foldable. At T=24 hours, there was slightly reduction (~7-8%) of surface hydrophobicity in all three IOLs at 21 °C. Similar slight reduction of surface hydrophobicity were also observed in PMMA and silicone IOLs at 37 °C. Rather surprisingly, we observed a drastic and significant reduction (~ 49%) in surface hydrophobicity in acrylic foldable IOLs at 37 °C (Fig. 3.5, Table 3.4). These results show that body temperature has significant influence on the surface hydrophilicity of acrylic foldable IOLs, but not PMMA and silicone IOLs.

IOL Material	Contact Angle		Surface Roughness		% Dye Penetration
	21°C	37°C	21°C	37°C	37°C
PMMA	0.033^{*}	0.047^{*}	0.307^{NS}	0.293^{NS}	0.000^{**}
Silicone	0.014^{*}	0.014^{*}	0.555^{NS}	0.195^{NS}	0.001^{**}
Acrylic foldable	0.010^{**}	0.000^{**}	0.601^{NS}	0.780^{NS}	0.000^{**}

Table 3.4. Summary of paired t-test (95% CI, $\alpha = 0.05$) between different time points (0 vs 24 hours) for average contact angle (in degrees) (@ 21 °C and 37 °C), average surface roughness (nm) (@ 21 °C and 37 °C), and average dye penetration (%) (@ 37 °C) for all materials. Significance, NS $p > 0.05$, *$p<0.05$, **$p<0.01$

3.3.3. Effect of temperature and hydration time on surface roughness

Subsequent studies were carried out to determine the influence of incubation time and temperature on the surface roughness of IOLs. At T=0, we observed that there were large differences in surface roughness between different IOLs in the following order: PMMA > silicone > acrylic foldable

IOLs. There were slight, but not statistically significant, changes in surface roughness with time (Figure 3.6, Table 3.4). Furthermore, similar surface roughnesses were found in all groups at 21 °C and 37 °C. In other words, temperature changes and incubation time do not seem to affect the surface roughness of these IOL groups.

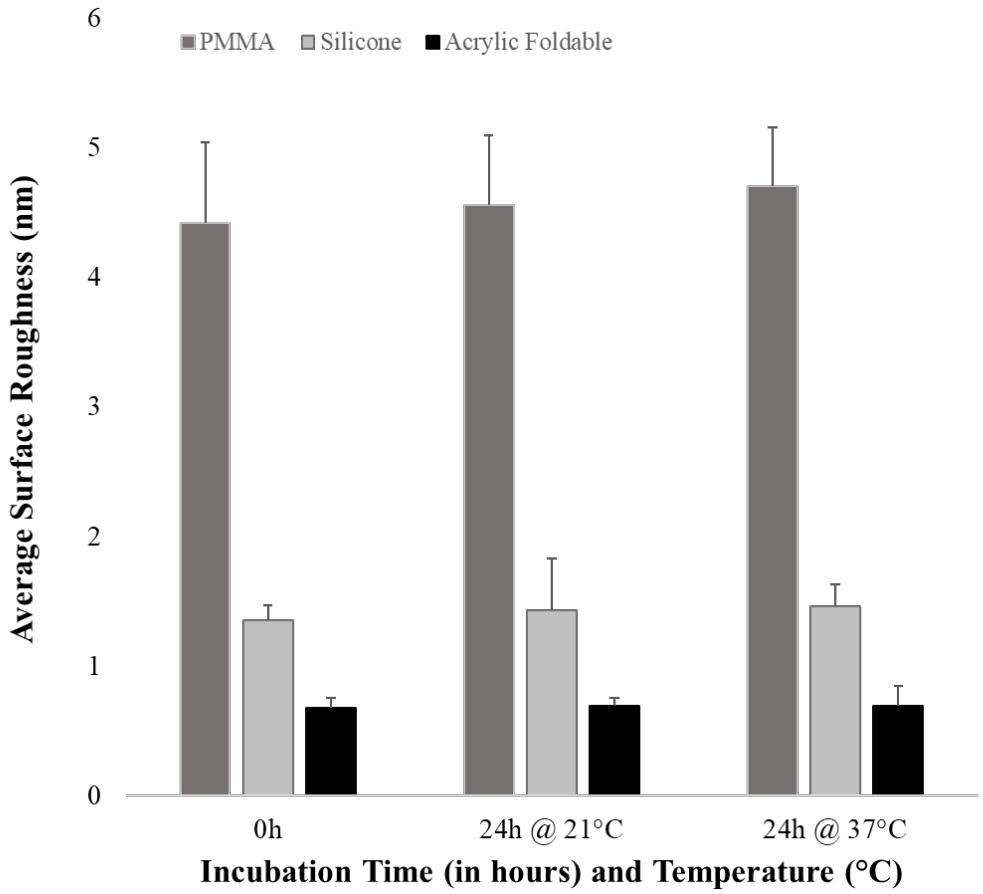

Figure 3.6. Change in surface roughness as a function of incubation time and temperature in BSS. Surface Roughness measurement on PMMA, silicone and acrylic foldable test IOLs was carried out at 0 and 24 h post hydration in BSS at 21 and 37 °C (n=10, significance vs 0 hour of the same group, NS: $p > 0.05$).

3.3.4. Examination of "no space no cell" hypothesis in vitro

To examine the "No space, No cell" hypothesis at a physiological condition, IOLs were placed inside the gelatin mold and placed in a 37 °C incubator for 24 hours with dye added after

incubation. Baseline images for each IOL were collected and compared to images of samples after incubation (Fig. 3.7, A).

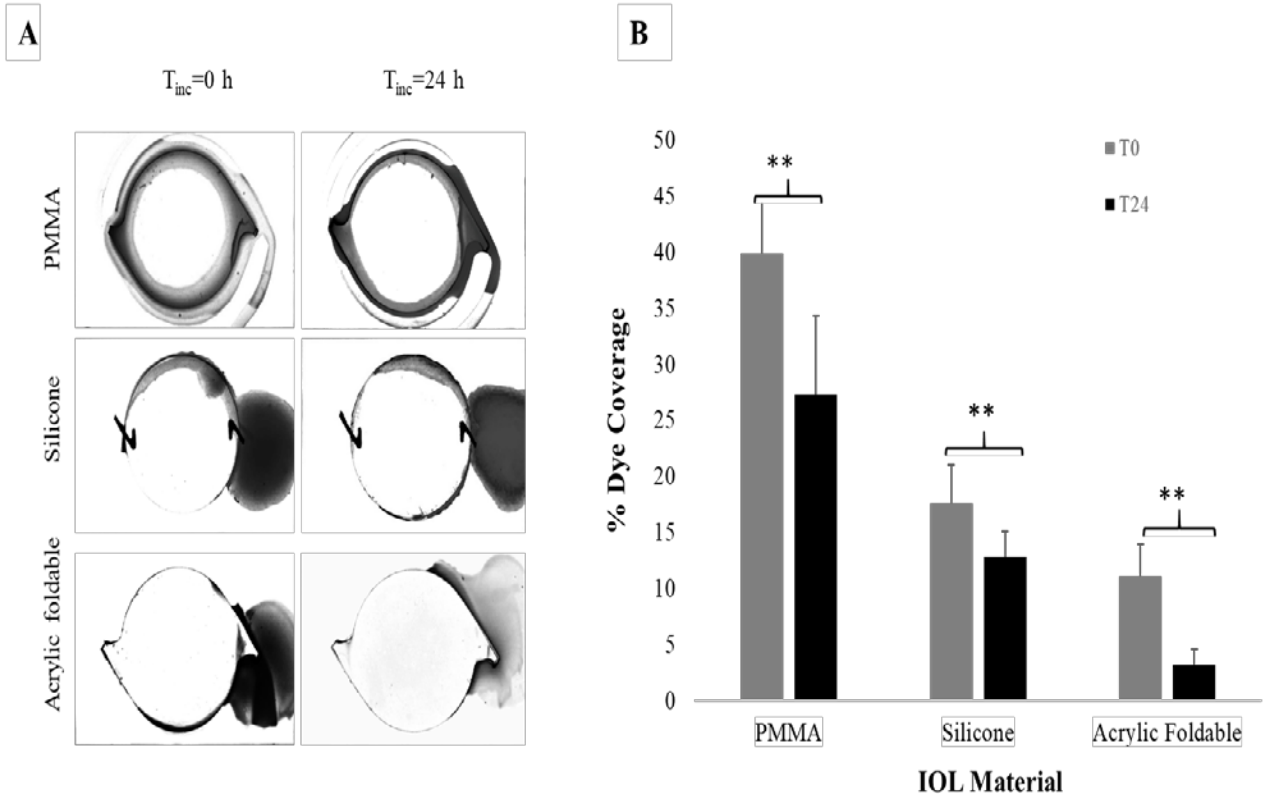

Figure 3.7. Photographs collected using the IOL: LC imaging system depicting visualization of dye penetration at IOL: LC interface at 37°C. (A) Representative images and (B) percentages of dye coverage at IOL: LC interface for for acrylic foldable, PMMA and silicone IOLs (n = 10, significance: **p<0.01).

Results for baseline images indicated as T_{inc}=0 h, show Blue Dextran occupying the inside optic of the different IOL materials. Total average percent of dye penetration was ~ 10.26% for Acrylic foldable IOLs, ~16.53% for Silicone IOLs, and ~ 42.37% for PMMA IOLs (Fig. 7, B). Images captured after gelatin mold was incubated for 24 hours showed a decrease in the total percent of Blue Dextran penetration at the IOL: LC interface for all materials (Fig. 3.7, A). The total percent of dye occupying the IOL: LC interface after 24 hour incubation was observed to be 3.16% for

Acrylic foldable IOLs, 12.85% for Silicone IOLs, and 27.32% for PMMA IOLs (Fig. 3.7, B). The amount of dye occupying the area under optic of the IOL is a quantification of the visual cue used to mimic cell infiltration and confirm the role that adhesion force plays in limiting the space between the IOL and posterior capsule. To further examine how fast the space between different IOL materials and simulated capsules close as a function of time and temperature, dye infusion study was conducted on samples incubated for 4 hours and is included in the supplement materials of this chapter (Supplemental Section 3.S.2, Supplemental Figure 3.1).

3.4. Discussion

Our study has found that the interactions between IOL: LC are significantly enhanced at body temperature – 37 °C in comparison with ambient temperature – 21 °C. The increase of temperature was found to increase the IOL: LC adhesion forces of all IOLs and to reduce the surface hydrophobicity of acrylic foldable IOLs. However, in this study, we found that temperature has insignificant effect on the surface roughness of IOLs. The increase of adhesion force may be associated with the increase of surface hydrophilicity post IOL implantation. Such relationship is supported by several early observations, which have indicated a relationship between IOLs surface hydrophilicity and its adhesion force to ECM (Bertrand et al., 2014; Miyata and Yaguchi, 2004). The mechanism governing temperature- and incubation time- dependent increase of surface hydrophilicity requires further studies and has yet to be determined. However, many previous studies support such observations. For example, a study showed that, under hydration, the surface hydrophobicity of 3 different hydrophobic polymers - Benz R&D's Benz IOL 25 (a copolymer of 2-hydroxyethyl methacrylate (HEMA) and ethoxyethyl methacrylate (EEMA)), Benz R&D's Benz HF1 (A copolymer of EEMA and ethoxyethyl acrylate (EEA) and PhysIOL.s.a's GF (A polymer blend of ethylene glycol phenyl ether acrylate (EGPEA), HEMA and poly(propylene

glycol) dimethaacrylate (PPGDMA) decreased owing to dynamic surface changes resulting from reorganization of the polar hydroxyl groups in the aqueous environment accompanied by likely variation in surface roughness and swelling of material in the aqueous medium (Bertrand et al., 2014). Other studies also suggest that a dynamic surface transformation under hydration and temperature increase may be responsible for the increase in surface hydrophilicity of the acrylic foldable lens (Bertrand et al., 2014; Miyata and Yaguchi, 2004). Finally, a separate study also found that Alcon's MA60BM, a hydrophobic acrylic, increased its equilibrium water content and hydrophilicity at elevated temperatures (Miyata and Yaguchi, 2004). These results suggest that after implantation, an acrylic foldable IOL increases its water uptake and surface hydrophilicity and leads to strong adhesion force with LC. In fact, implanted soft acrylic IOLs such as Alcon's Acrysof are increasing difficult to explant if the procedure is not conducted within a few weeks of surgery owing to their strong adhesion with the lens capsule post cataract surgery (Ursell et al., 1998).

The mean adhesion force for PMMA group lenses was observed to be the lowest with minimal influence by temperature and hydration time among all studied materials. PMMA IOL is reported to have high incidence of PCO in the clinic (Gift et al., 2009; Ram et al., 2014; Rönbeck et al., 2009; Rønbeck and Kugelberg, 2014a, 2014b) and is known to have minimal adhesion to lens capsule post implantation as demonstrated by various *in vitro* and *ex vivo* studies (Oshika et al., 1998a, 1998b; Wejde et al., 2003) . The Silicone IOLs reported higher adhesion forces than the PMMA IOLs which is in agreement with clinical observations for these materials (Wejde et al., 2003). These higher forces for the Silicone IOLs can be attributed to the presence of functional moieties on its surface that possess a high affinity for collagen (a major constituent of the gelatin capsule) (Rønbeck and Kugelberg, 2014a; Vasavada and Praveen, 2014).

Previous studies have shown that PMMA material IOLs have significantly more surface irregularities than silicone and acrylic IOLs (Lombardo et al., 2009; Yang et al., 2017). Further, both acrylic and silicone IOLs have been reported to have smooth surfaces with lowest surface roughness for acrylic IOLs (Mukherjee et al., 2012). In fact, many studies have concluded that higher surface roughness of an IOL biomaterial leads to higher PCO growth as surface irregularities could increase the number of inflammatory cells adhering to the IOL optic surface and result in tissue formation (Katayama et al., 2007; Tanaka et al., 2005). Our results support this conjecture as lowest *Sa* measurements were reported for the acrylic foldable group (best clinical PCO outcomes), followed by silicone and PMMA (worst clinical PCO outcomes) at body temperature. Therefore, the reported consistent increase in adhesion force between the acrylic foldable IOLs and simulated LC may be attributed to its smooth surface, and water uptake characteristics under hydration. On the contrary, the small increase in adhesive forces for silicone material may be due to its relatively smooth surface and the presence of functional moieties on its surface that possess a high affinity for Collagen (Rønbeck and Kugelberg, 2014a; Vasavada and Praveen, 2014). Lastly, PMMA IOLs are reported to have minimal capsule adhesion, a hard brittle surface (Linnola et al., 2003; Oshika et al., 1998b) and high surface irregularities (Lombardo et al., 2006; Mukherjee et al., 2012; Yang et al., 2017). As a result, PMMA IOLs do not bind tightly to the lens capsule resulting in low IOL: LC adhesion forces and thus high PCO incidence.

Our results show that IOL material properties affect their adhesiveness to the simulated LC. Our results agree with previous observations which show that the adhesiveness of an IOL with the lens capsule is inversely proportional to the rate of PCO formation post-implantation in clinic (Linnola, 1997; Linnola et al., 2003; Katayama et al., 2007; Nagata et al., 1998; Oshika et al., 1998a, 1998b; Wejde et al., 2003). It should be noted that, in addition to surface adhesiveness, the geometry of

IOL posterior optic edge has been shown to influence PCO rates (Buehl et al., 2007, 2005; Cheng et al., 2007; Eldred et al., 2014; Haripriya et al., 2017; Maddula et al., 2011; Mylonas et al., 2013; Nishi, 1999a; Nishi et al., 2000, 1998b; Wormstone, 2020; Wormstone and Eldred, 2016b). For example, round-edged IOLs are reported to have higher PCO rates owing to their inability to create a 'barrier effect' to prevent infiltration and proliferation of LECs (Buehl et al., 2005; Cheng et al., 2007; Maddula et al., 2011; Nishi et al., 2001, 2000). Furthermore, by testing the PCO progression of different materials with both round-edged and sharp-edged IOLs in pigmented rabbits, several studies found that there was no significant difference in the observed IOL PCO rates between IOLs with sharp posterior edges, irrespective of the IOL's material composition (Nishi, 1999a, 1999b, Nishi et al., 2004a, 2000, 1998b, 1998a; Nishi and Nishi, 2002). It is believed that the presence of a sharp posterior optic edge creates a capsular bend or angle at the IOL-LC interface leading to firm binding of the lens capsule to the rectangular sharp optic edge thereby inhibiting the migration of LECs, and eventually reducing extent of PCO formation (Nishi, 1999a). On the other hand, round edged lenses fail to form a capsular bend at the IOL-LC interface that leads to firm binding with the lens capsule (Nishi et al., 1998b). Interestingly, in another retrospective and comparative 2-year follow-up study that compared Nd: YAG procedure rates for 3 IOLs with different degree of edge sharpness in following order: Hoya PY60AD > Acrysof SN60WF > HOYA FY60AD showed lowest Nd: YAG rates for the Acrysof SN60WF IOL (Morgan-Warren and Smith, 2013) . It was concluded that while IOL edge sharpness contributes to the reduced PCO rates, the variation in the material constitution of these IOLs can potentially influence their susceptibility to PCO development independent of edge sharpness (Morgan-Warren and Smith, 2013). While surface hydrophilicity and roughness are the focus of this investigation, our results do not exclude the potential influence of IOL edge profile on the adhesion force of IOLs

which will be evaluated in a future study.

Overall, our results support a general hypothesis that time, temperature and hydration of IOL materials, specifically, hydrophobic acrylic foldable IOLs such as Alcon's Acrysof affect the physical and chemical properties of an IOL and the reduction of surface hydrophobocity at body temperature may influence IOL: LC interactions and subsequent PCO formation (Figure 3.8). This assumption is also supported by many previous observations. First, IOL material properties are found to influence the speed of the capsule bending (Nishi et al., 1998b). For instance, using Optical Coherence tomography, studies have found that the capsule-IOL contact was much faster (10 days) for the Acrysof lens as opposed to a Silicone lens (~15 days) (Sacu et al., 2005). Rapid adhesion of IOL materials after IOL implantation can potentially seal off the interfacial space and prevent cell infiltration i.e. 'No space, No cell' (Pearlstein et al., 1988; Ursell et al., 1998). This assumption supports our results that there is an inverse relationship between adhesive force and dye penetration ratios. Specifically, the results of IOL adhesion force were in the following sequence: Acrylic foldable IOL > Silicone IOL > PMMA IOL while the dye penetrations results was in the following sequence: PMMA IOL> Silicone IOL> Acrylic foldable IOL.

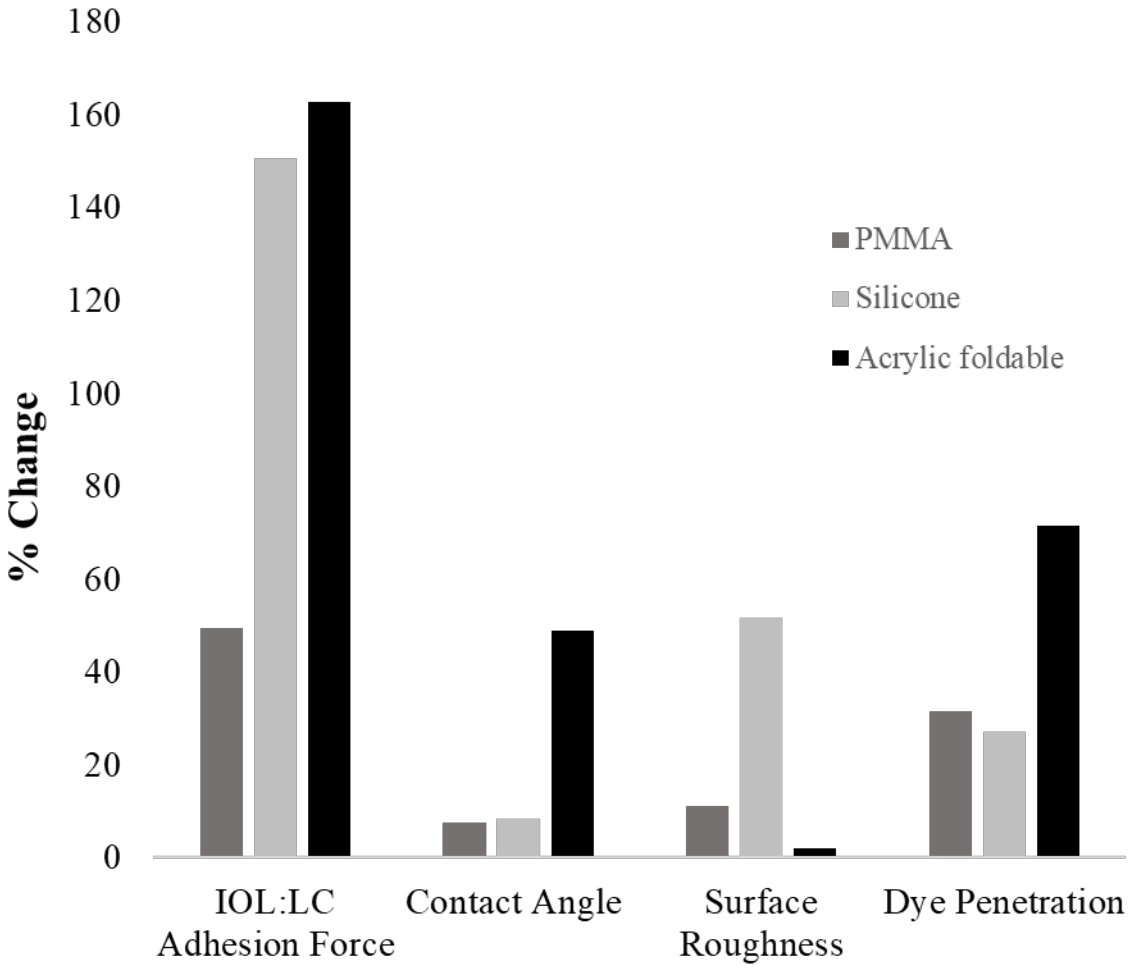

Figure 3.8. Percentage change in average IOL: LC adhesion force, contact angle, surface roughness and dye penetration for PMMA, silicone and acrylic foldable IOLs at 37°C.

It is also worth nothing that while our model initially assumes perfect contact between the IOL and capsule during the fabrication of the simulated capsules, capsule shrink wrapping of the IOL is governed by cell driven events post implantation and can be influenced by the posterior optic edge geometry and haptic design of the IOL (Nishi, 1999a; Nishi et al., 2000, 1998b; Wormstone, 2020; Wormstone and Eldred, 2016b). This is addressed by utilizing specific capsules generated from the test IOL itself. Our adhesion force and dye penetration results have indirectly shown that

different IOL materials bind to the surface of the IOL capsules differently. Further, our results determined by IOL: LC adhesion force and dye penetration are a measure of the IOL: LC surface interactions and gap closure as a function of time. A direct measure of IOL: LC interface using this model for different IOL materials and designs as a function of time should be studied in the future.

The results of this work provide several major substantiations that are essential to the pathogenesis of IOL-mediated PCO formation. Specifically, we showed that body temperature might alter the material properties, such as surface hydrophobicity of some IOLs by dynamic surface transformations. By reducing the hydrophobicity of IOLs similar to material characteristics of an acrylic foldable IOL such as Alcon's Acrysof lens may develop strong adhesion force with LCs. Finally, the tight interaction between IOLs and LCs mediated by IOL material's bioadhesiveness and design would reduce the space available for cell migration or infiltration. Our studies have also lent strong support that future *in vitro* or *ex vivo* studies should be carried at body temperature to better mimic the IOL: LC interactions and to assess their potential influence in PCO formation.

3.5. Conclusions

Here we report a potential effect of temperature-dependent changes in surface properties of IOLs on their influence on IOL: LC adhesion forces using a newly established *in vitro* system. The overall results suggest that, at body temperature, the decrease of surface hydrophobicity may be responsible for the significant increase of adhesive force between acrylic foldable and LC. Such increase of adhesive force significantly reduced the extent of dye penetration in this study and, perhaps, reduces cell infiltration and PCO formation in the clinic. While the influence of IOLs' edge profile on IOL:LC interactions has yet to be determined, our results provide new evidence to support 'No Space, No Cell' hypothesis and the potential role of temperature, hydration time,

surface hydrophobicity and IOL material properties on affecting the incidence of IOL-induced PCO.

Supplemental Materials

3.S.1. Crosslinking of simulated gelatin capsules

In our previous studies (Jaitli et al, 2021), non-crosslinked 10% high strength gelatin solution in deionized water was used to prepare the simulated lens capsules. However, with non-crosslinked gelatin, the adhesion force could only be measured at room temperature because of the thermoreversible nature of gelatin (Kozlov and Burdygina, 1983). With increase in temperature, gelatin solution tends to become more viscous which affects its interaction with the IOL. A non-crosslinked 10% solution of gelatin was observed to remain in its solid gel state up to a temperature of 28 °C but at higher temperatures, the gelatin starts liquefying. To keep the physical properties of gelatin stable at body temperature of 37 °C, a crosslinking agent is required which stops the thermoreversibility of gelatin and allows it to remain in its solid state at a higher temperature (Campiglio et al., 2019). Crosslinking agents are very useful in material sciences as they form chemical links between molecular chains and form a three-dimensional network of connected molecules. Different chemicals have been used to crosslink gelatin, one of the most commonly used chemicals being Glutaraldehyde (Dardelle et al., 2011). Glutaraldehyde is readily available and affordable, and the crosslinking procedure using it is a quick and simple process. Although, it is also known to be toxic, making it less favorable for most *in vivo* studies and some *in vitro* studies which involve live cells (Beauchamp et al., 1992). However, glutaraldehyde was successfully used as a chemical cross linker in this study as the adhesion force instrument setup used in this study did not involve any *in vivo* or cell studies. A series of tests were performed to determine the appropriate concentration of crosslinking. 10% w/v solution of gelatin was cross-linked with different concentrations of glutaraldehyde, ranging from 0.1% w/v to 0.5% w/v. The goal of this experiment was to find the lowest concentration of crosslinking, which could keep the gelatin stable at body temperature. Crosslinking concentration of 0.1% w/v was observed to be very low

and the gelatin could not remain stable at a higher temperature. On the other hand, 0.5% w/v of crosslinking altered the physical properties of gelatin resulting in a stiff, non-adhesive surface. A crosslinking concentration of 0.25% w/v was found to be appropriate for the study. At this concentration, the gelatin could successfully remain stable at 37 °C and had an adhesive surface.

3.S.2. Dye Infusion Results after incubation of IOL: LC for 4 hours at 37 °C

Figure 3.S.1 indicates lowest dye penetration for acrylic foldable IOLs (~8%), followed by silicone (~16%) and PMMA (~26%) after incubation with LC for 4 hours at 37 °C. As indicated by results in the text, the % dye penetration reduces further as a function of time for the acrylic foldable group (~3%), with minimal changes observed for PMMA (~18%) and silicone (~13%) groups.

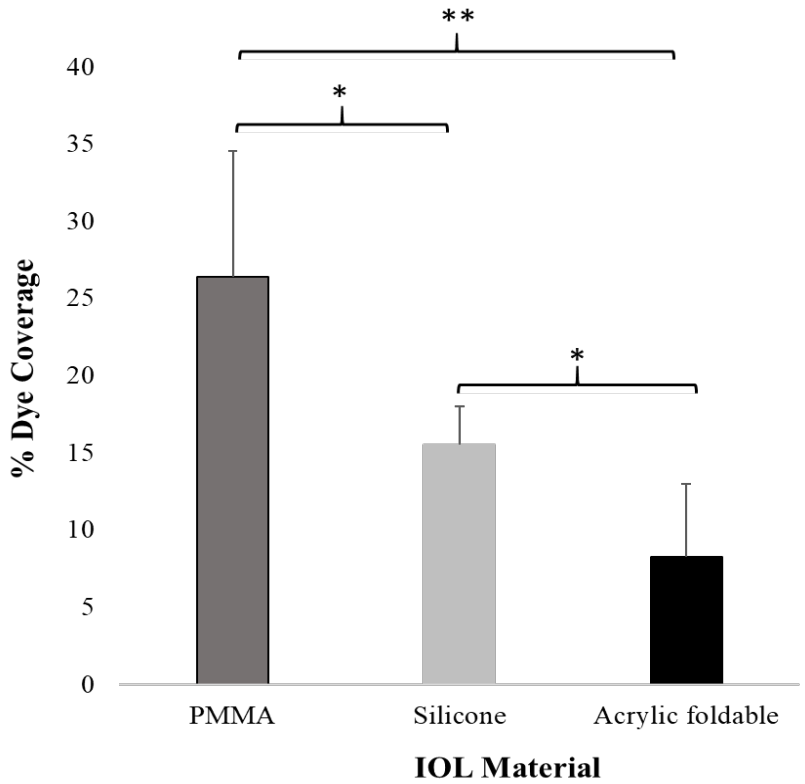

Supplementary Figure 3.1. Dye penetration results before and after incubation for 4 hours @ 37°C for PMMA, silicone and acrylic foldable IOLs

CHAPTER 4

Role of Fibronectin and IOL surface modification in IOL: Lens Capsule Interactions

4.1. Introduction

The role of an IOL material in PCO formation and its interaction with the lens capsule has been extensively studied (Hayashi et al., 1998; Jaitli et al., 2021; Katayama et al., 2007; Linnola et al., 2000a; Nishi et al., 2004b; Oshika et al., 1998b; Pérez-Vives, 2018; Ursell et al., 1998; Versura, 1999). The interaction of an implanted IOL with the lens capsule mediated by ECM proteins, residual lens epithelial cells and growth factors that are released in abundance after the break down of the aqueous-blood barrier after surgical intervention is known to dictate the course of PCO (Eldred et al., 2019; Linnola et al., 2003, 2000a, 2000b; Wormstone et al., 2021). It is generally believed that the adhesiveness of an IOL material can affect the rate of PCO formation (Jaitli et al., 2021). Within hours of cataract surgery, the implanted IOL adsorbs a complex protein biofilm that determines the cellular and tissue reactions to the IOL (Kochounian et al., 1994). Various ECM proteins like fibronectin, vitronectin, fibrinogen, and transferrin have been identified in these biofilms in various animal studies (Kochounian et al., 1994). ECM proteins play an important role in PCO formation and can act as mediators of IOL adhesion and have been observed in the connective tissue that accumulates between the capsule and IOL (S. Saika, 1997; Saika et al., 1993; Shizuya Saika, 1997).

Fibronectin, a major glycoprotein of the extracellular matrix is believed to impact the degree of IOL-induced PCO formation owing to its affinity for collagen, an essential material constituent of the lens capsule (Linnola et al., 2000a). The breakdown of the blood–aqueous barrier after cataract surgery increases the soluble fibronectin available in the aqueous humor that interacts with the implanted IOL's surface and determines cellular responses (Linnola et al., 2003). Fibronectin's several functional domains specifically I6II1-II2-I7-I8-I9 modules (i.e. amino acids Thr^{260} through Pro^{570}) promote its binding to collagen and the cell surface (Shimizu et al., 1997; Sottile et al., 2007). It is believed that this collagen and cell surface binding property of fibronectin enables it to

be a mediator between an IOL and the lens capsule (Linnola et al., 2000b) . Coincidentally, fibronectin is believed to serve as a key mediator of IOL induced PCO that can affect the progression of PCO (Linnola 1997). Specifically, an *ex vivo* study conducted to examine the adhesion of various ECM proteins to explanted IOLs fabricated from different materials (hydrophobic soft acrylate, PMMA and Silicone) showed significant amount of fibronectin and vitronectin on the hydrophobic soft acrylates (Linnola et al., 2000a) that are clinically known to show low rates of PCO (Pérez-Vives, 2018; Rönbeck et al., 2009; Rønbeck and Kugelberg, 2014b; Ursell et al., 1998). This phenomenon was further confirmed in an *in vitro* study that examined the adhesion of various ECM proteins to different IOL materials that showed increased amounts of fibronectin adsorption on the hydrophobic acrylates (Linnola et al., 2003). Thus, differences in fibronectin adsorption to the IOL surface may be responsible for determining the extent of PCO progression for different IOL implants. While many *in vitro* and *ex vivo* studies have examined the interaction of fibronectin with various IOL materials, the potential role of adsorbed fibronectin on influencing PCO progression has yet to be directly investigated. Since fibronectin has been suggested to act as a biological clue between the IOL material and the capsular bag for lens materials that are associated with less PCO (Apple et al., 2001), we assume that adsorbed fibronectin may enhance the interactions and adhesion force between IOLs and LCs.

The significant progress made to prevent IOL-induced PCO has led to improved surgical techniques and development of novel IOL materials and designs. To improve IOL material properties, surface modification of IOL materials to increase their surface hydrophilicity has become increasingly popular. Hydrophilic coatings such as Poly (ethylene glycol) (PEG), Poly (ethylene glycol) methyl acrylate and PEG-like thin coatings such as Di(ethyleneglycol) dimethyl ether (Digylme) are used to modify various biopolymers and are associated with reduced

inflammatory responses (Lee et al., 2007; Ribeiro et al., 2009; Tognetto et al., 2003; Welch et al., 2016; Xu et al., 2016b). Specifically, various IOL materials have been coated with different polymers such as PEG, PEGMA and Heparin to assess their efficacy in controlling and mediating PCO formation (Arthur et al., 2001; Bozukova et al., 2007; Hyeon et al., 2007; Kang et al., 2008; Kim et al., 2001; Lee et al., 2007; Tognetto et al., 2003; Xu et al., 2016b, 2016a). For example, the surface of the Acrysof lens, a soft hydrophobic acrylic IOL modified with both Poly (ethylene glycol) (PEG) and Poly (ethylene glycol) methyl acrylate has been shown to reduce cell attachment in *in vitro* and to retard PCO development in rabbits (Lee et al., 2007). On the other hand, heparin coating has been shown to reduce cell attachment and *in vivo* PCO rates of PMMA IOLs that are known to have high rates of PCO (Tognetto et al., 2003). More recently, PEG, a high molecular weight hydrophilic polymer has gained popularity as a hydrophilic coating. Specifically, PEG can be tethered on the surface of IOLs to provide a surface shield for preventing protein deposition, inflammatory cell accumulation, and, perhaps, PCO formation (Lee et al., 2007). Most recently, surface PEGlylation of silicone and acrylic material IOLs using PEGMA has also been used to reduce PCO rates in rabbits (Xu et al., 2016b, 2016a). While these hydrophilic surface coatings are known to reduce initial cell attachment post implantation, the long-term PCO performance of these coatings has not been fully studied yet. Before clinical testing, it is important to know whether these coatings would influence IOL: LC interactions. Another class of surface coatings that has gained popularity is the 'low fouling' thin film 'PEG-like' coatings that can resist or inhibit protein adsorption within the body. Specifically, Di(ethyleneglycol) dimethyl ether, commonly known as 'Digylme' has been used to coat the surface of various biomaterials to improve their biocompatibility (Deng and Lahann, 2014; Menzies et al., 2012; Ribeiro et al., 2009; Welch et al., 2016). It is believed that plasma polymer films produced with monomers consisting of two or more

ethylene oxide units can exhibit low-fouling properties and are easier to implement in manufacturing processes than conventional graft-polymerization techniques (Menzies et al., 2012). Further, by controlling the parameters of the plasma deposition process, it is possible to modfiy the surface chemistry of these coatings and customize their properties for specific applications (Johnston et al., 2005). However, Digylme coatings have not been utilized thusfar on IOL materials and further studies are needed to evaluate the possibility of implementing these to improve their surface properties and potentially reduce PCO.

To test the hypotheses mentioned above using a recently established model (Jaitli et al., 2021), we will first assess the effect of fibronectin on IOL surface properties and IOL: LC interactions using commercially available IOLs, including acrylic foldable, PMMA and silicone IOLs. To study the influence of surface coatings on IOL: LC interactions, acrylic foldable IOLs will be coated with PEG via graft polymerization (Lee et al., 2007) and Digylme (DG) by modifying previously established vapor plasma deposition techniques (Johnston et. al., 2005; Menizes et al., 2012). The influence of surface coating(s) on IOL surface properties and IOL: LC interactions in the presence and absence of fibronectin will also be studied. Lastly, using an established dye infusion model to simulate cell infiltration, we will determine the influence of fibronectin and surface coatings on potential cell infiltration and PCO formation at IOL: LC interface.

4.2. Materials and Methods

4.2.1. Intraocular Lenses

This study comprised of IOLs from five different groups – Hydrophobic acrylic foldable (hereafter referred to as 'acrylic foldable'), PMMA, silicone, PEG-treated acrylic foldable and Diglyme-treated acrylic foldable. The acrylic foldable IOLs had a 6.0 mm biconvex optic, a sharp rectangular posterior edge and planar haptics with an overall length of 13.0 mm (Alcon's

SN60WF, Alcon Research, Fort Worth, Texas) with a dioptric power of 21.0D. The PMMA group were single piece IOLs with a 5.5 mm PMMA optic, round posterior edge and multiflex haptics with an overall length of 13.0 mm (Alcon's MTA4U0, Alcon Research, Fort Worth, Texas) with a dioptric power of 23.5D. The Silicone group comprised of three-piece posterior chamber biconvex silicone 6.0 mm optics that had a round edged profile and blue PMMA mod C haptics with an overall length of 13.0 mm (Allergan's AMO Array SA40N, Allergan Inc, Irvine, California) with dioptric powers between 10.0 D and 26.0 D.

4.2.2. Surface modification of acrylic foldable IOLs

Some of the acrylic foldable IOLs were used for surface modification with either Polyethylene glycol (PEG) or Diethylene glycol dimethyl ether (Diglyme) hereafter referred to as acrylic foldable-PEG and acrylic foldable-DG, respectively. Diglyme deposition was achieved by a plasma deposition process utilizing a vapor deposition plasma chamber (Nordson March PD-1000; Nordson Electronics Solutions, CA, USA) using a modified procedure (Menzies et al., 2012). Briefly, the surface of the IOLs was first treated with oxygen plasma under low pressure (200 mTorr) at 200 W for 5 min, followed by treatment with Argon gas at 250 mTorr at 100W for 1 min. Finally, digylme deposition was achieved by treating the functionalized IOLs under a pressure of 250 mTorr at 40W for 20 min. Graft polymerization of PEG was performed using previously established procedures (Lee et al, 2007, Xu et al, 2016). The surface of the IOLs was first treated with oxygen plasma under low pressure (200 mTorr) at 200 W for 5 min. The IOLs were then incubated in PEG solutions at 60°C for 24 hours immediately after removal from plasma chamber. After incubation, the IOLs were rinsed with purified water 3X for a minimum of 60 seconds to wash away any non-covalently bond monomers from the lens surfaces. Immediately after the rinsing step, the IOLs were dried in a vacuum oven at 80°C for 12 hours prior to the study.

4.2.3. Preparation of Simulated Capsules

Simulated LCs were created to possess a spherical cup shaped structure that closely mimics the morphology, structure and mechanical integrity of the human capsular bag using previously established procedures (Jaitli et al, 2021). All simulated LCs were gently cross-linked with glutaraldehyde using previously published crosslinking method (Dardelle et al., 2011; Jaitli et al., 2021 (in review)). The prepared solution was poured into acrylic petri-dishes immediately prior to the placement of IOLs. Next, IOLs with haptics intact were taped onto small thin circular lightweight support materials to ensure the IOL stayed afloat through the solidification process at 4°C for 1 hour. IOLs were then gently peeled from the gelatin surfaces with the help of thin forceps to create a capsule as described recently (Jaitli et al., 2021).

4.2.4. Surface Coating and Fibronectin Adsorption on IOL: LC force and cell penetration

All test IOLs and LC assemblies were incubated in a temperature controlled chamber at 37±1°C for 24 hours prior to the study. In some groups, 2 µL of human fibronectin solution (with 0, 1, 10, 100, and 1000 µg/mL, Sigma-Aldrich, Lot # SLCG9672) was added onto the surface of the simulated capsule for the test IOLs. Simulated capsules were then covered with corresponding test IOLs and then incubated in a 37 °C incubator for 24 hours prior to adhesion force measurement. The adhesion force measurement was carried out using a microforce tester as described previously (Jaitli et al., 2021). Further studies were carried out to assess the influence of fibronectin adsorption and surface coating on cell penetrations at the IOL: LC interface using an established dye penetration model as described recently (Jaitli et al, 2021 (in review)). Briefly, after IOL:LC incubation for 24 hours, blue dextran dye solution (10µL at 5 mg/mL, Sigma-Aldrich D575) was then injected at the edge of IOL-filled molds and the molds were then imaged to visualize and quantify the extent of dye penetration in the space between IOL and LC.

4.2.6. Surface characterization of various treated IOLs

The influence of various coatings and adsorbed fibronectin on the surface properties of all test IOLs was characterized by measuring their surface contact angle. For fibronectin coated samples, IOLs were incubated with 500 µL of human fibronectin solution (0.2 mg/mL) for 24 hours at 37 °C prior to the surface characterization. Contact Angle measurements of all IOLs were made using the Video Contact Angle (VCA) Optima system (AST Product Inc., Billerica, MA) by following manufacturer's instruction. The contact angle was calculated using the Sessile Drop method with an accuracy of ± 0.5° as described earlier (Cunanan et al., 1998; Jung et al., 2017).

4.2.7. Statistical analyses

All statistical data analysis was conducted utilizing the Minitab 19 Statistical Software Package. Two- samples t-tests @ 95% Confidence Interval (CI) were conducted to determine statistically significant differences between various groups.

4.3. Results

4.3.1. Effect of Fibronectin on IOL: LC adhesion force for acrylic foldable IOLs

We first evaluated the influence of fibronectin on IOL: LC adhesion force using acrylic foldable IOLs (Alcon's Acrysof SN60WF). For that, different concentrations of fibronectin were added in simulated LC prior to the IOL placement. After incubation for 24 hours, we found that there was a significant increase of adhesion force (2.580 ± 0.138 mN) in 1000 µg/mL (or 2 µg / capsule) treated group when compared with control group (fibronectin free, 1.506 ± 0.102) (Figure 4.1). On the other hand, there was no statistically significant difference between 1 µg/mL (1.368 ± 0.076 mN), 10 µg/mL (1.295 ± 0.207 mN), and 100 µg/mL (1.274 ± 0.134 mN) and control. These results indicate that to simulate clinical phenomenon, the amount of fibronectin present between the acrylic foldable IOL and LC is critical in truly effecting IOL: LC adhesion force. Thus, to

further assess the role of fibronectin in mediating IOL: LC adhesion, subsequent studies were conducted at a fibronectin concentration of 1000 µg/mL i.e. 1 mg/mL.

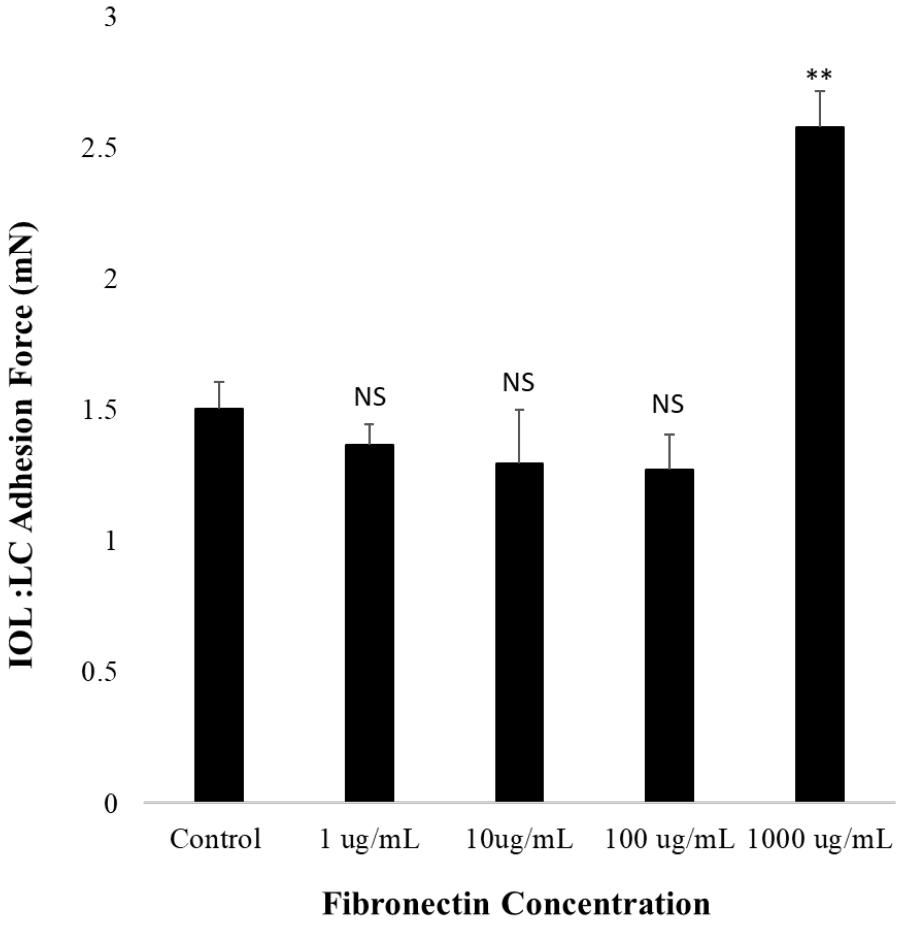

Figure 4. 1. IOL: LC adhesion force as a function of fibronectin concentration after incubation @ 37°C for 24 hours (n=5, Significance vs Control group, NS: $p > 0.05$, **$p<0.01$)

4.3.2. Effect of Fibronectin on IOL: LC adhesion for different materials

We then investigated whether fibronectin would increase the adhesion force of LCs to IOLs made of other materials, such as PMMA IOLs and silicone IOLs. To find the answer, PMMA and silicone IOLs with simulated capsules were injected with 2µL of 0 (as control) or 1 mg/ml fibronectin solution and then incubated for 24 hours @ 37°C prior to adhesion force measurement.

As expected, we found that fibronectin adsorption significantly increased the adhesion force of acrylic foldable IOLs (without vs. with fibronectin adsorption = 1.506 ± 0.102 vs 2.580 ± 0.138 mN). Rather surprisingly, we found that the presence of fibronectin had no influence on the adhesion force of PMMA IOLs (without vs. with fibronectin adsorption = 0.422 ± 0.026 mN vs 0.420 ± 0.034 mN) and silicone IOLs (without vs. with fibronectin adsorption = 1.444 ± 0.147 mN vs 1.375 ± 0.117 mN) (Fig. 4.2).

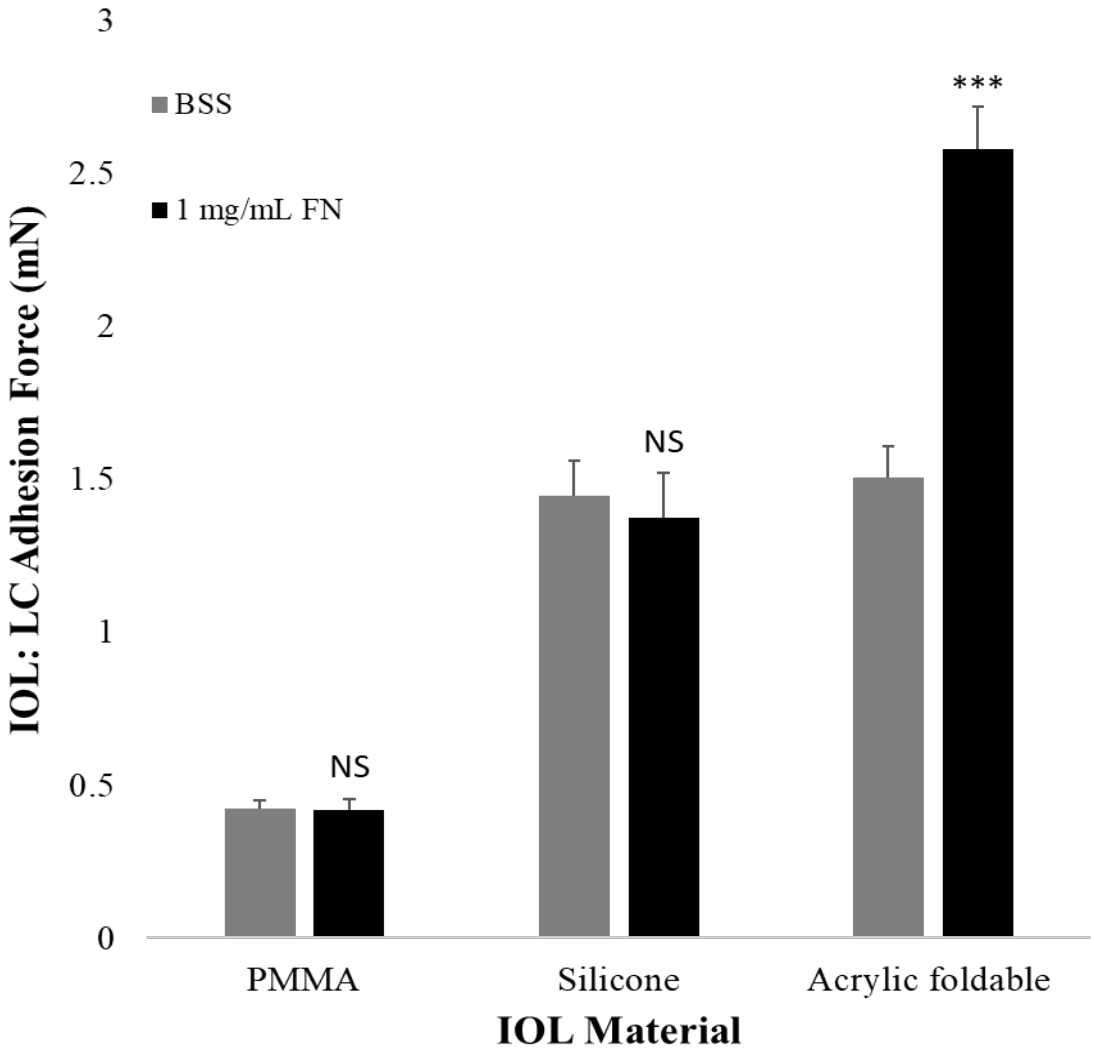

Figure 4. 2. IOL: LC adhesion force after injecting 2 uL of 1 mg/mL FN solution at IOL: LC interface for different IOL materials – Acrylic foldable, PMMA and Silicone (n=5, significance vs Control of same group, NS: $p > 0.05$, ***$p<0.001$)

4.3.3. Dye infusion for different IOL materials in presence of Fibronectin

The influence of fibronectin on cell infiltration at IOL: LC interface was evaluated using a dye penetration model. As shown in the representative images, we found that the presence of fibronectin does not influence dye penetrations in both PMMA (with vs. without fibronectin = 32.14% vs 27.32%) and silicone IOLs (with vs. without fibronectin = 13.84% vs 12.85%) (Fig. 4.3). However, the presence of fibronectin was found to significantly reduce dye penetrations in acrylic foldable IOLs (with vs. without fibronectin = 3.66% vs 1.01%). These results support our overall hypothesis that the adsorption of fibronectin may increase the IOL: LC adhesive force and reduce cell infiltration at the interface.

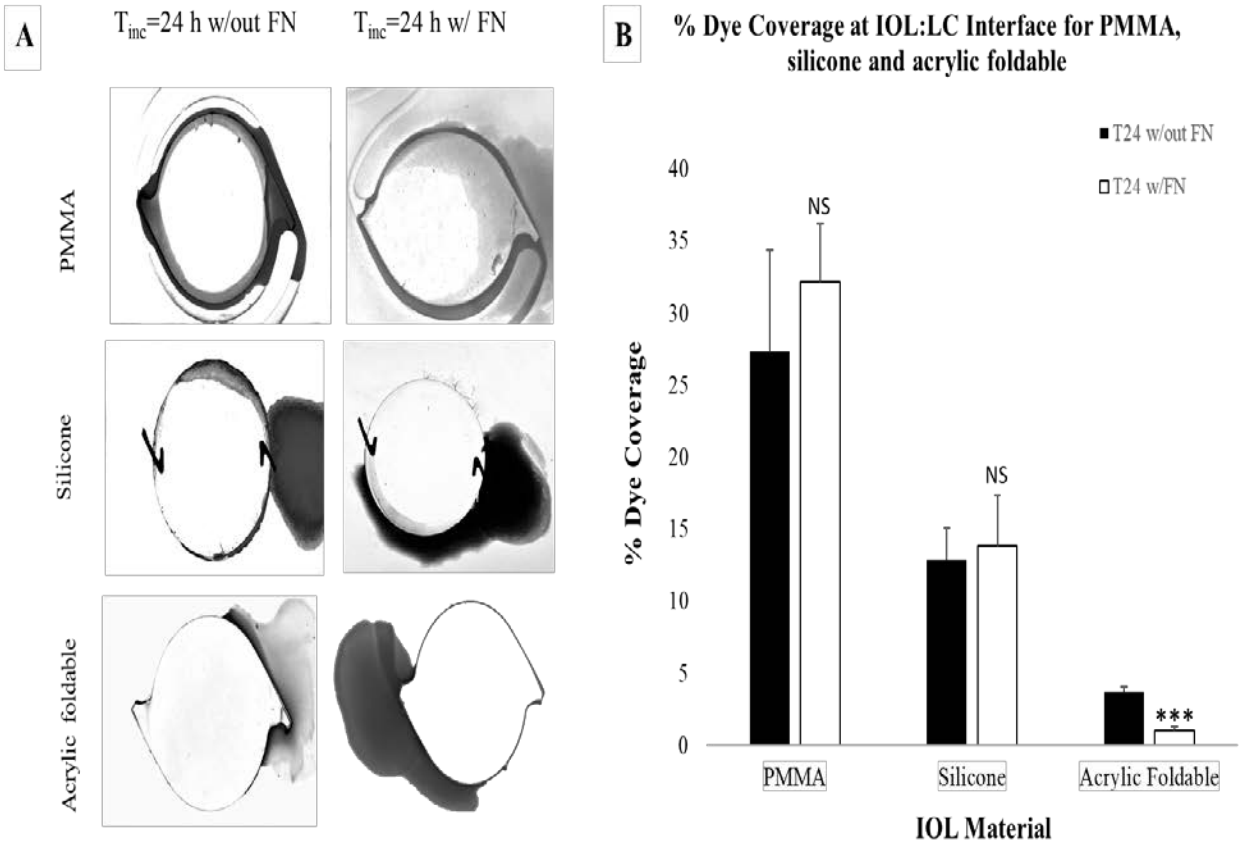

Figure 4. 3. Photographs collected using the IOL: LC imaging system depicting visualization of dye penetration at IOL: LC interface at 37°C. (A) Representative images and (B) percentages of dye coverage at IOL: LC interface for for acrylic foldable, PMMA and silicone IOLs (n=3, significance vs control of same group, NS: $p>0.05$, ***$p<0.001$)

4.3.4. Influence of surface coatings and fibronectin on surface hydrophilicity

Surface coatings have been shown to influence protein and, perhaps, fibronectin adsorption (Johnston et al., 2005; Lee et al., 2007; Menzies et al., 2012; Tognetto et al., 2003; Xu et al., 2016b, 2016a) and surface hydrophobicity/hydrophilicity of an IOL material is known to influence IOL: LC interactions (Li et al., 2013; Zhao et al., 2017). Thus, subsequent studies were carried out to understand the role of surface coatings and fibronectin surface adsorption on the surface properties of IOLs. To find the answer, we first measured the surface hydrophobicity of acrylic foldable IOLs modified with Digylme (acrylic foldable-DG), IOLs modified with PEG (acrylic foldable-PEG IOLs), and acrylic foldable controls. The hydrophobicity of all test IOLs was in the following order: acrylic foldable control = acrylic foldable –DG > acrylic foldable-PEG (Fig. 4.4.). These results indicate that the PEG coating created a hydrophilic surface on the acrylic foldable IOLs. However, Diglyme coating had insignificant influence on the surface hydrophilicity of the IOLs. On the other hand, the presence of fibronectin had a different effect on the surface hydrophilicity of IOLs. While the presence of fibronectin significantly decreased (~43%) the surface hydrophobicity of the untreated IOLs, fibronectin incubation increased (~32%) the hydrophobicity of acrylic foldable-PEG. On the other hand, the presence of fibronectin had no significant influence on the hydrophobicity of acrylic foldable-DG (Fig. 4.4.). These results further confirm that surface coating and surface: fibronectin interaction may influence surface properties, such as hydrophobicity.

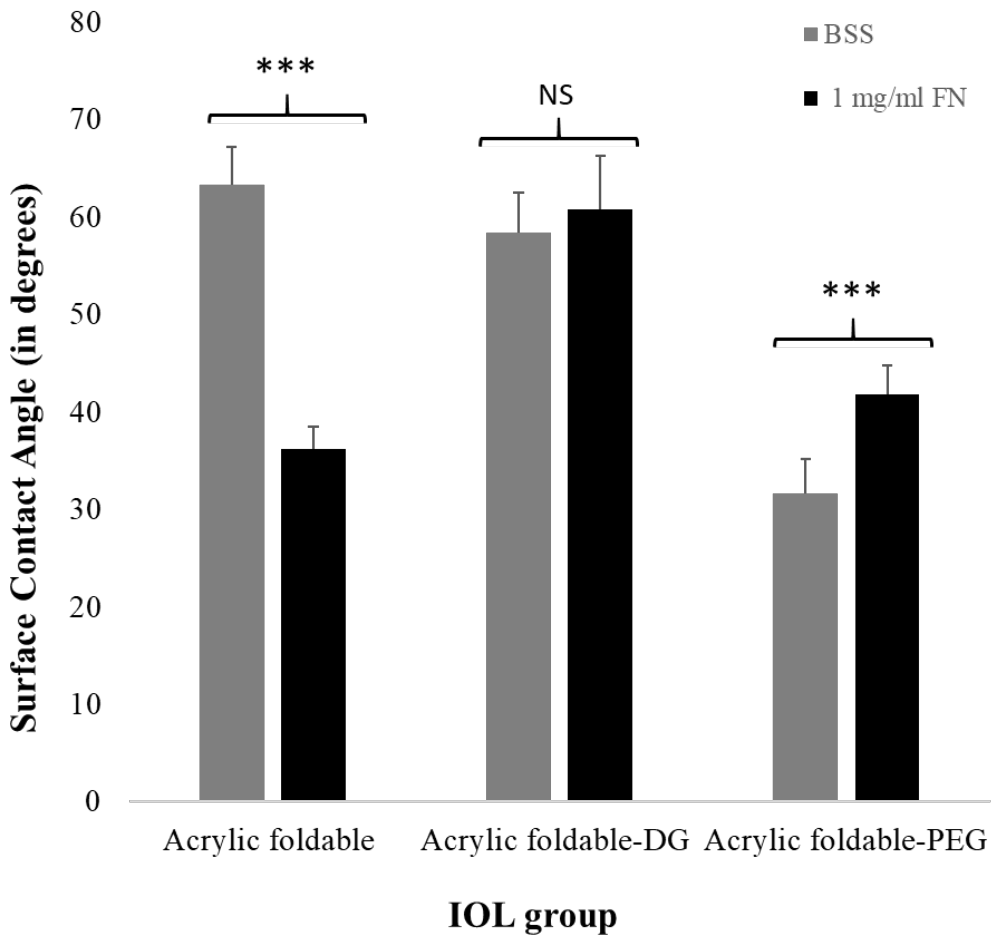

Figure 4. 4. Surface contact angle of acrylic foldable, acrylic foldable-DG and acrylic foldable-PEG) with and without Fibronectin. All test samples were coated with either 0 (labeled as "BSS") or 1 mg/mL FN injection for 24 hours @ 37°C. (n=5, NS: $p > 0.05$, ***$p<0.001$)

4.3.5. Effect of Surface Coatings on IOL: LC adhesion force

Since surface coatings have been shown to influence surface hydrophobicity and protein (including fibronectin) adsorption, it is possible that surface coatings affect the IOL: LC adhesion force. To test that, we measured the adhesion force of acrylic foldable IOLs modified with Digylme (acrylic foldable-DG), IOLs modified with PEG (acrylic foldable-PEG IOLs), and acrylic foldable control IOLs. Initially, we found that surface coatings have no statistically significant influence on the adhesion force (acrylic foldable control, 0.737 ± 0.111 mN; acrylic foldable-DG, 0.893 ± 0.065

mN; acrylic foldable-PEG IOLs, 0.745 ± 0.170 mN) (Fig. 4.5). After incubation for 24 hours @ 37°C, the adhesion force for the acrylic foldable IOLs: LCs increased significantly from 0.737 ± 0.111 mN to 1.934 ± 0.185 mN. However, in comparison to control, both Digylme and PEG coatings showed significant reduction in adhesion force ~ 54% for acrylic foldable-DG (0.894 ± 0.065 mN) and ~22.3% for acrylic foldable-PEG (1.503 ± 0.047 mN) (Fig. 4.5). These results indicate that the presence of different coatings on acrylic foldable IOLs can affect the adhesion of these IOLs with the lens capsule.

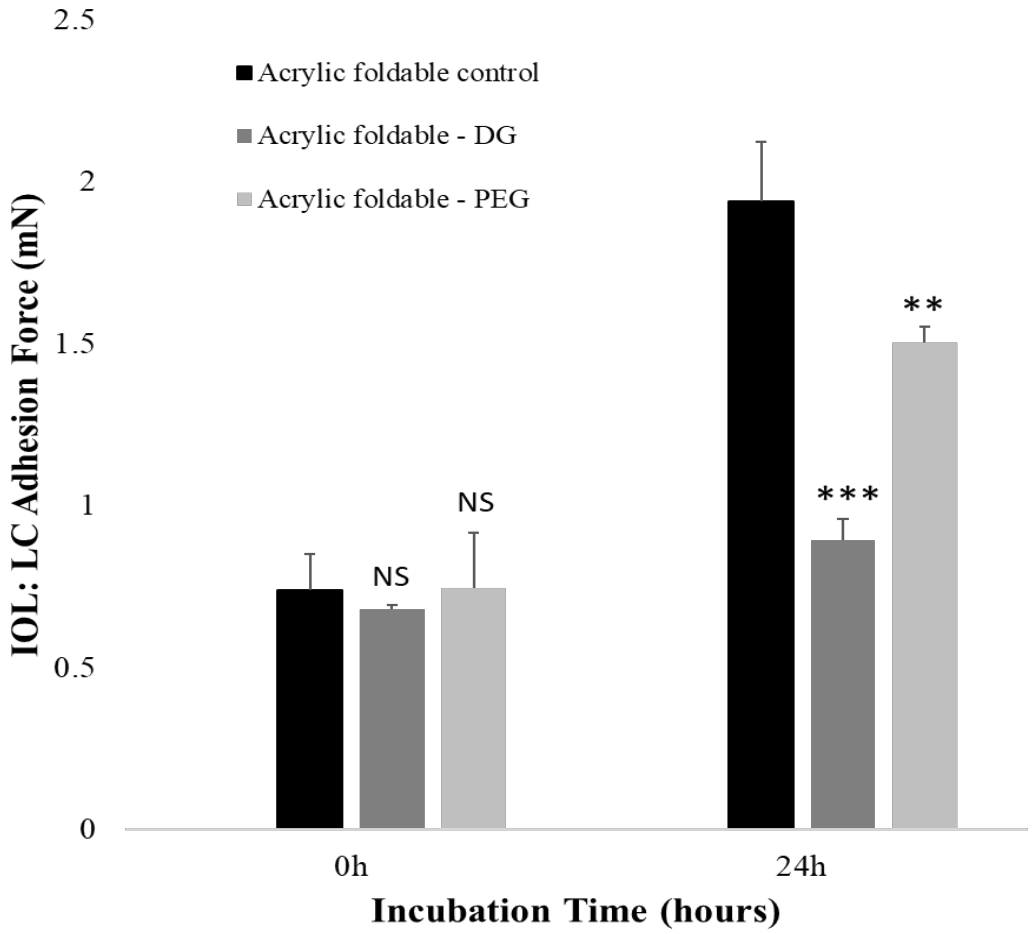

Figure 4. 5. IOL:LC adhesion force for acrylic foldable control, acrylic foldable – DG and acrylic foldable-PEG lenses at different incubation time (0 and 24 hours) @ 37 °C (n=5, Significance vs acrylic foldable control, NS: $p>0.05$, **$p<0.01$, ***$p < 0.001$)

Since fibronectin was found to affect the adhesion of acrylic foldable IOLs and LCs, further adhesion force measurements were conducted on the surface coated IOLs in the presence of fibronectin (2 μL of 1 mg/mL) at 37°C for 24 hours. Similar to acrylic foldable's response, the presence of fibronectin significantly increased the adhesion force between acrylic foldable-PEG and LCs. (without vs. with fibronectin = 1.429 ± 0.087 mN vs. 2.337 ± 0.149 mN) (Fig. 4.6.). On the other hand, the presence of fibronectin was found to slightly but statistically significantly reduce the adhesion force between acrylic foldable-DG IOLs and LCs (without vs. with fibronectin = 0.872 ± 0.071 mN vs. 0.720 ± 0.076 mN) (Fig. 4.6.). Thus, these results indicate that surface modification of acrylic foldable IOLs with PEG does not affect the fibronectin-binding properties of these IOLs. However, coating of these IOLs with Diglyme may reduce the IOL: LC adhesion force by interfering with its interaction with fibronectin.

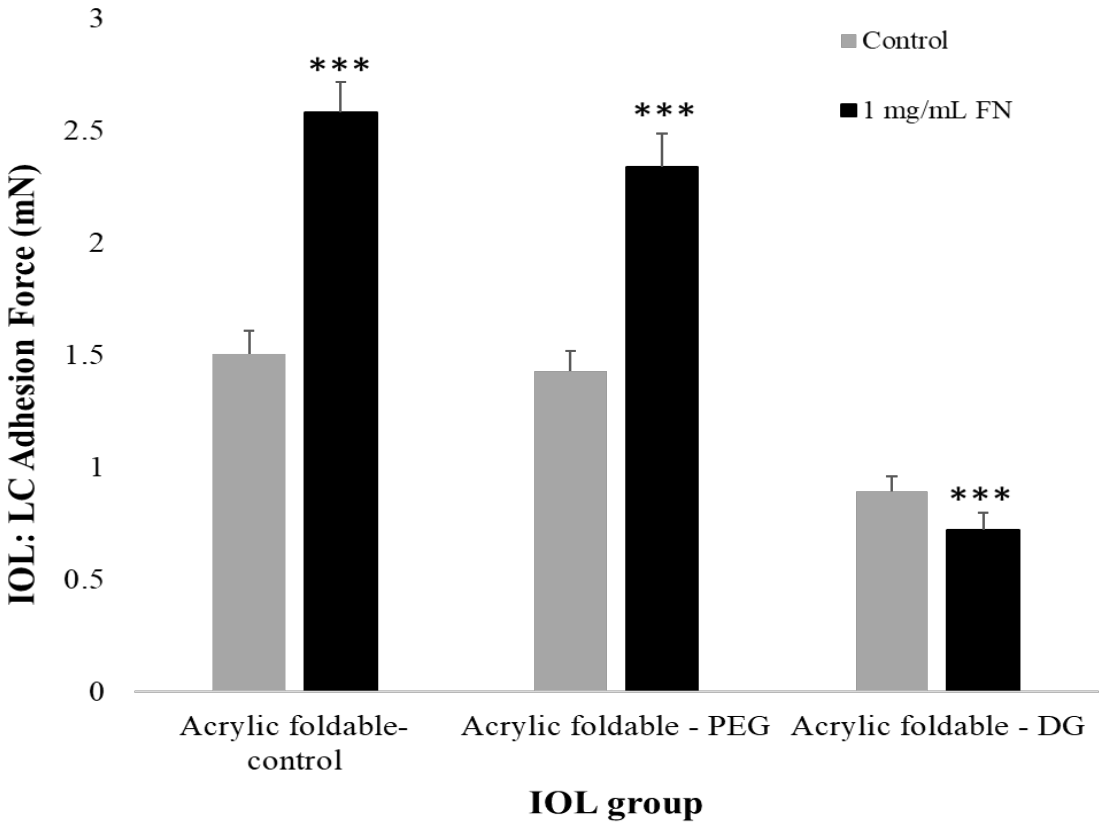

Figure 4. 6. IOL:LC adhesion force for coated acrylic foldable lenses after injecting 2 uL of 1 mg/mL FN solution for acrylic foldable – PEG and acrylic foldable – DG lenses (n=3, significance vs control of same group, ***p < 0.001)

4.3.6. Dye Infusion for Acrylic foldable-PEG and acrylic foldable-DG IOLs

Subsequent studies were carried out to assess the influence of surface coating: fibronectin interactions on cell infiltration using a dye penetration model. As expected, the presence of fibronectin significantly reduced the dye penetrations at acrylic foldable-PEG IOL: LC assemblies (with vs. without fibronectin = 6.11% vs. 12.87%) similar to acrylic foldable IOL: LC (control) assemblies (with vs. without fibronectin = 1.01% vs. 3.66%) (Fig. 4.7). On the other hand, the presence of fibronectin had no statistically significant influence on the dye penetration at acrylic foldable-DG IOL: LC assemblies (with vs. without fibronectin = 59.63% vs. 68.00%) (Fig. 4.7.).

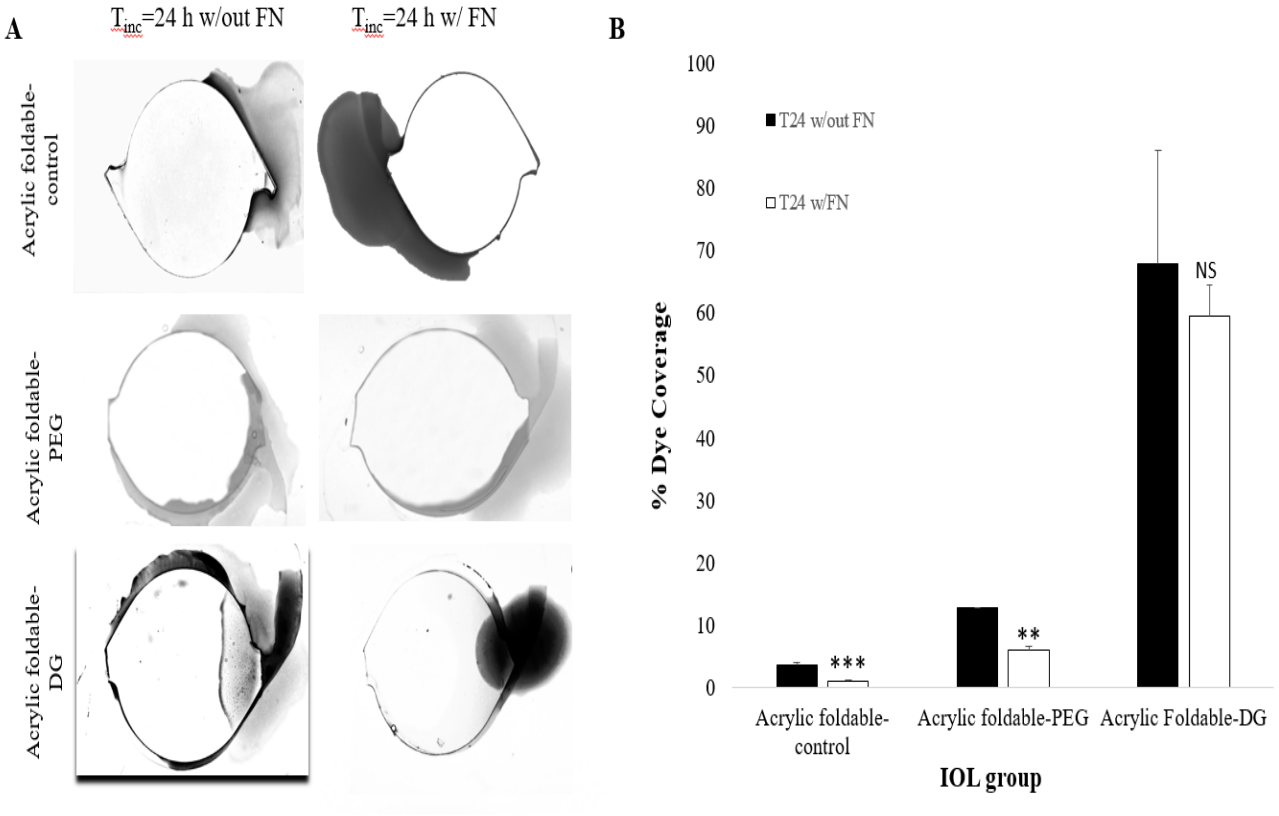

Figure 4. 7. Photographs collected using the IOL: LC imaging system depicting visualization of dye penetration at IOL: LC interface at 37°C. (A) Representative images and (B) percentages of dye coverage at IOL: LC interface for for acrylic foldable-control, acrylic foldable-PEG and acrylic foldable-DG IOLs (n=3, Significance vs control group (without FN), NS: $p > 0.05$, **$p<0.01$, ***$p<0.001$)

4.4. Discussion

Our study has shown that fibronectin can significantly influence the IOL: LC adhesion force in at least one group of commercial IOLs, such as the acrylic foldable IOLs. In that case, fibronectin adsorption made the acrylic foldable IOL surface more hydrophilic than the control lenses. It is possible that the increase in hydrophilicity of the IOL surface resulting from fibronectin may increase its binding force with lens capsule via hydrophilic interactions (Schroeder et al., 2009; Yang et al., 2017) and fibronectin: collagen binding (Shimizu et al., 1997; Sottile et al., 2007). Such increased binding between acrylic foldable IOLs and LCs is thought to result in lowest rates

of PCO in the clinic (Linnola, 1997; Linnola et al., 2003, 2000a; Oshika et al., 1998b, 1996; Rönbeck et al., 2009b; Rønbeck and Kugelberg, 2014b; Ursell et al., 1998).

The potential influence of fibronectin and IOL material properties on IOL-induced PCO in the clinical setting is not totally understood. However, vast research evidences support such hypothesis. For example, it is well established that the acrylic foldable IOLs is hydrophobic in dry condition (Cunanan et al., 1998; Jung et al., 2017). After incubation with BSS at 37°C for 24 hours to simulate human physiological environment, acrylic foldable IOLs were found to undergo dynamic surface changes leading to a more hydrophilic surface (Jaitli et al., 2021, in review). Further, the breakdown of the aqueous blood barrier during IOL implantation procedure, may lead to an influx of complex proteins including fibronectin in the vitreous fluid (Linnola et al., 2000b). The interaction between the hydrated acrylic foldable IOLs with fibronectin makes their surface more hydrophilic, which allows the IOLs to adhere tightly and uniformly to the capsule leading to higher adhesive force. Further studies support that the tighter adhesive force may prevent cell infiltration. These observations further support the hypothesis that fibronectin-mediated strong binding of the acrylic foldable IOLs to LCs passively prevents the infiltration of LECs, thereby reducing their PCO rates.

Our results indicated that the adhesive force between acrylic foldable IOLs and LCs was increased by the presence of fibronectin at concentrations higher than 1 mg/mL (or 2 µg/capsule). While an *in vitro* study that specifically tests the role of fibronectin concentration in IOL: LC adhesion force has not been conducted before, several predicate studies support these observations. For example, the amount of fibronectin adsorption is reported to be the highest for acrylic foldable lenses such as the Acrysof lens (Linnola et al., 2003), which is reported to have high degree of capsule adhesion and abundance of fibronectin in the IOL: LC interface (Linnola, 1997; Linnola et al., 2000a,

2000b). Further, IOLs with different degree of fibronectin adsorption are associated with different rates of PCO in the clinic (Linnola et al., 2000a, 2000b). Thus, the amount of fibronectin present in the IOL: LC capsule interface available could play a critical role in determining the adhesion of an implanted IOL with the capsule and subsequent PCO formation.

Our studies have also found that IOL: LC adhesion force for both PMMA and silicone IOLs did not change in the presence of fibronectin. These observations confirm Linnola's findings of reduced fibronectin adsorption on both of these IOLs *in vitro* (Linnola et al., 2003) combined with *ex vivo* histological findings (Linnola et al., 2000a, 2000b) of insignificant amounts of fibronectin present in the region on both the IOL and the lens capsule for these IOLs. Our dye infusion study further confirmed that the adhesion of both PMMA and silicone IOLs with lens capsule is in fact unaffected by the presence of fibronectin by reporting insignificant changes in average dye penetration when compared with control groups that contained no fibronectin.

The influence of surface modified acrylic foldable IOLs, including acrylic foldable-PEG IOLs and acrylic foldable-DG IOLs was examined on fibronectin adsorption and IOL: LC interactions. The increase in adhesion force of the PEG group (in acrylic foldable-PEG IOLs) after incubation with the simulated capsule in the presence of fibronectin increased by ~ 50%, a behavior that was observed for the acrylic foldable control groups. In other words, PEG coating does not change the PCO potential of acrylic foldable IOLs. It is worth noting that while the direct interaction of a PEG coated acrylic foldable IOL with fibronectin has not been directly investigated, there is evidence in literature that suggests that despite their anti-inflammatory and cell attachment repelling properties, PEG coatings do not alter a biomaterial's response to fibronectin. For instance, a study conducted to assess the impact of different concentrations of PEG on fibronectin adsorption showed that bioactivity of fibronectin was unperturbed irrespective of PEG concentrations

(Tziampazis et al., 2000). Further, another study aimed at studying the cell attachment of a biomaterial coated with different molecular weight PEGs actually showed better biocompatibility and reduced cell attachment when used on surface containing pre-adsorbed fibronectin (Altankov et al., 2001). On the other hand, the supplement of fibronectin showed no influence on the adhesion force of acrylic foldable-DG IOLs and LCs. While the causes for the low adhesion forces of the diglyme group are yet to be determined, the low hydrophilicity and low cell affinity of Diglyme group (Ribeiro et al., 2009; Welch et al., 2016) may be reducing fibronectin adsorption and LC interactions resulting in low adhesion forces. The low protein affinity properties of Diglyme group is indirectly supported by our observations that the surface contact angles of acrylic-foldable-DG IOLs was not altered by the presence of fibronectin.

4.5.Conclusions

Here we report a potential effect of fibronectin protein and hydrophilic coatings in altering surface properties of IOLs and their influence on IOL: LC adhesion forces using a newly established *in vitro* system. The overall results suggest that, fibronectin is a key mediator in altering acrylic foldable IOL: LC interactions by reducing the surface hydrophobicity of acrylic foldable lenses thereby preventing hydrophobic inflammatory, cell and bacterial interactions and increases the adhesion of its surface with the lens capsule thereby preventing further cell infiltration and subsequent PCO formation. Fibronectin, on the other hand, plays no significant role on the IOL: LC interactions of other commercial IOLs, such as PMMA IOLs and silicone IOLs. Surface modification of acrylic foldable IOLs with PEG showed no influence on fibronectin adsorption, adhesion force, and cell infiltration at the IOL: LC interface. However, surface modification of acrylic foldable IOLs with DG reduced fibronectin adsorption and adhesive force and resulted in increased cell infiltration at IOL: LC assembly. The overall results, at least in the case of acrylic

foldable IOLs and acrylic foldable-PEG IOLs, provide major substantiations to support Linnola's sandwich theory that deems fibronectin to be a key mediator in increasing IOL: LC adhesiveness, reducing cell infiltration and, thus, reducing PCO incidence in the clinical setting.

CHAPTER 5

Conclusions and Future Direction

5.1. Conclusions

This research effort focused on the development of *in vitro* model that can study IOL: Lens Capsule interactions and study their role in IOL-induced PCO development.

Chapter 2 led to the creation of a new *in vitro* 3D model that was shown to be an effective tool for measuring the adhesion force between an IOL material with a synthetic gelatin-based capsule. Model development included establishing a process for creating 3D optimized gelatin molds with a curvature resembling the human capsule-bag like structure. With the help of a custom micro-force tester mechanical apparatus, the adhesion force of different IOL materials was measured and showed correlation with clinical PCO outcomes. This new system addresses current gaps in existing PCO models, is inexpensive to build, enables rapid quantitative data collection and can be utilized as an effective tool to simulate clinical PCO phenomena.

In Chapter 3, the potential effect of temperature-dependent changes in surface properties of IOLs on IOL: LC adhesion forces for different materials was examined using our newly established *in vitro* system. Further, a novel macromolecular dye infusion system was developed to simulate cell infiltration. The results acquired from these studies suggested that, at body temperature, the decrease of surface hydrophobicity may be responsible for the significant increase of adhesive force between acrylic foldable lenses and the LC. The tight binding between the IOL surface and lens capsule leads to a high adhesion force. In line with clinical observations, the extent of dye penetration i.e. simulated cell infiltration was found to be the lowest for acrylic foldable IOLs followed by silicone and PMMA. These results provided new evidence to support the potential role of temperature, hydration time, surface hydrophobicity and IOL material properties on affecting the incidence of IOL-induced PCO.

Lastly, in Chapter 4, the effect of fibronectin and surface coatings on IOL: LC adhesion force was studied. Our results suggested that the absorption of fibronectin on the acrylic foldable IOLs

leads to a more hydrophilic surface that could be responsible for high adhesion forces observed for these lenses with the simulated capsules. Surface modification of IOLs with hydrophilic coatings such as PEG further increases the hydrophilicity of acrylic foldable IOLs in a dry state, without affecting their adhesion to the lens capsule and interaction with fibronectin, factors that are known to reduce PCO rates of acrylic foldable IOLs such as Acrysof.

5.2. Future Direction

The *in vitro* model established in this effort was instrumental in deciphering key mechanisms that influence IOL: LC interactions and subsequent PCO formation. While these studies provide major substantiations to the current understanding of PCO development, future studies are required for a more in-depth assessment of mechanisms contributing to PCO.

First, studies conducted in this research effort focused on the role of IOL material in pathogenesis of PCO. The role of the IOL design, specifically the posterior edge of the IOL optic will need to be investigated using this model. Studies that test the difference in IOL: LC adhesion and simulated cell infiltration for IOLs fabricated from the same materials and different optic edge profiles should be conducted in the future.

Second, the synthetic capsules utilized in this effort were fabricated from gelatin, which is denatured collagen. However, human capsule consists of other ECM components like collagen (type IV), laminin, nidogen/entactin, heparan sulfate proteoglycans, perlecan, collagen XVIII, fibronectin and SPARC (osteonectin). Thus, more studies are required to incorporate these ECM components in the gelatin capsules to better mimic the mechanical strength and material composition of the human capsule. Further, the gelatin capsules used in our studies were cross-linked with glutaraldehyde to improve their stability at body temperature. However, glutaraldehyde is a highly toxic substance that will not allow any cell studies. Therefore, more

studies need to be conducted to optimize the formulation of the mold and to identify a suitable biocompatible cross-linker to enable cell studies and to truly simulate clinical phenomenon.

Third, the concentration of fibronectin utilized in adhesion force studies will need to be optimized further and compared with physiologically relevant concentrations of fibronectin in aqueous humor to further prove the clinical relevance of this system. Other biological cues such as collagen, laminin, vitronectin, growth factors etc. need to be implemented in the IOL: LC interface to better simulate physiological environments.

Last, long-term incubation studies (~ 4-6 weeks) in the presence of various ECM components and lens epithelial cells is required to simulate in vitro tissue formation and PCO growth for different IOL materials and designs to further improve the clinical relevance of this model.

REFERENCES

Aliancy, J., Werner, L., Ludlow, J., Nguyen, J., Masino, B., Ha, L., Mamalis, N., 2018. Long-term capsule clarity with a disk-shaped intraocular lens. J. Cataract Refract. Surg. 44, 504–509. https://doi.org/10.1016/j.jcrs.2017.12.029

Alió, J.L., Simonov, A.N., Romero, D., Angelov, A., Angelov, Y., Van Lawick, W., Rombach, M.C., 2018. Analysis of Accommodative Performance of a New Accommodative Intraocular Lens. J. Refract. Surg. 34, 78–83. https://doi.org/10.3928/1081597X-20171205-01

Altankov, G., Vladkova, T., Krasteva, N., Kostadinova, A., 2001. Fibroblasts and fibronectin on PEG-coated surfaces. Eur. Cells Mater. 1, 33.

Apple, D.J., Peng, Q., Visessook, N., Werner, L., Pandey, S.K., Escobar-Gomez, M., Ram, J., Auffarth, G.U., 2001. Eradication of posterior capsule opacification: Documentation of a marked decrease in Nd:YAG laser posterior capsulotomy rates noted in an analysis of 5416 pseudophakic human eyes obtained postmortem. Ophthalmology. https://doi.org/10.1016/S0161-6420(00)00589-3

Apple, D.J., Solomon, K.D., Tetz, M.R., Assia, E.I., Holland, E.Y., Legler, U.F.C., Tsai, J.C., Castaneda, V.E., Hoggatt, J.P., Kostick, A.M.P., 1992. Posterior capsule opacification. Surv. Ophthalmol. 37, 73–116. https://doi.org/10.1016/0039-6257(92)90073-3

Artaria, L.G., Ziliotti, F., Ziliotti-Mandelli, A., 1994. [Long-term follow-up of implantation of foldable silicon posterior lenses]. Klin. Monatsbl{ä}tter f{ü}r Augenheilkd. https://doi.org/10.1055/s-2008-1035532

Báez, J., Olsen, D., Polarek, J.W., 2005. Recombinant microbial systems for the production of human collagen and gelatin. Appl. Microbiol. Biotechnol. https://doi.org/10.1007/s00253-005-0180-x

Beauchamp, R.O., St Clair, M.B.G., Fennell, T.R., Clarke, D.O., Morgan, K.T., Karl, F.W., 1992. A critical review of the toxicology of glutaraldehyde. Crit. Rev. Toxicol. 22, 143–174. https://doi.org/10.3109/10408449209145322

Beer, F.P., Johnston Jr, E.R., DeWolf, J.T., 2005. Mechanics of Materials 4th Edition. Paperback. 8-19

Bertrand, V., Bozukova, D., Svaldo Lanero, T., Huang, Y.S., Schol, D., Rosière, N., Grauwels, M., Duwez, A.S., Jérôme, C., Pagnoulle, C., De Pauw, E., De Pauw-Gillet, M.C., 2014. Biointerface multiparametric study of intraocular lens acrylic materials. J. Cataract Refract. Surg. 40, 1536–1544. https://doi.org/10.1016/j.jcrs.2014.01.035

Boulton, M., Saxby, L., 1998. Adhesion of IOLs to the posterior capsule. Br. J. Ophthalmol. https://doi.org/10.1136/bjo.82.5.468

Bozukova, D., Pagnoulle, C., De Pauw-Gillet, M.C., Desbief, S., Lazzaroni, R., Ruth, N., Jérôme, R., Jérôme, C., 2007. Improved performances of intraocular lenses by poly(ethylene glycol) chemical coatings. Biomacromolecules 8, 2379–2387. https://doi.org/10.1021/bm0701649

Brown, M.M., 2002. Extracapsular cataract extraction compared with small incision surgery by

phacoemulsification: A randomized trial. Evidence-Based Eye Care 3, 100–101. https://doi.org/10.1097/00132578-200204000-00019

Buehl, W., Findl, O., Menapace, R., Sacu, S., Kriechbaum, K., Koeppl, C., Wirtitsch, M., 2005. Long-term effect of optic edge design in an acrylic intraocular lens on posterior capsule opacification. J. Cataract Refract. Surg. 31, 954-961. https://doi.org/10.1016/j.jcrs.2004.09.053

Buehl, W., Menapace, R., Findl, O., Neumayer, T., Bolz, M., Prinz, A., 2007. Long-term Effect of Optic Edge Design in a Silicone Intraocular Lens on Posterior Capsule Opacification. Am. J. Ophthalmol. 143, 913-919. https://doi.org/10.1016/j.ajo.2007.02.017

Byju, A.G., Kulkarni, A., Gundiah, N., 2013. Mechanics of gelatin and elastin based hydrogels as tissue engineered constructs. 13th Int. Conf. Fract. 2013, ICF 2013 6, 4406–4415.

Campiglio, C.E., Negrini, N.C., Farè, S., Draghi, L., 2019. Cross-linking strategies for electrospun gelatin scaffolds. Materials (Basel). 12, 1–19. https://doi.org/10.3390/ma12152476

Cheng, J.W., Wei, R.L., Cai, J.P., Xi, G.L., Zhu, H., Li, Y., Ma, X.Y., 2007. Efficacy of Different Intraocular Lens Materials and Optic Edge Designs in Preventing Posterior Capsular Opacification: A Meta-Analysis. Am. J. Ophthalmol. 143, 428-426. https://doi.org/10.1016/j.ajo.2006.11.045

Chien, J.C.W., Chang, E.P., 1972. Dynamic mechanical and rheo-optical studies of collagen and gelatin. Biopolymers. https://doi.org/10.1002/bip.1972.360111003

Cunanan, C.M., Ghazizadeh, M., Buchen, S.Y., Knight, P.M., 1998. Contact-angle analysis of intraocular lenses. J. Cataract Refract. Surg. 24, 341–351. https://doi.org/10.1016/S0886-3350(98)80322-2

Danysh, B.P., Duncan, M.K., 2009. The lens capsule. Exp. Eye Res. https://doi.org/10.1016/j.exer.2008.08.002

Dardelle, G., Subramaniam, A., Normand, V., 2011. Determination of covalent cross-linker efficacy of gelatin strands using calorimetric analyses of the gel state. Soft Matter. https://doi.org/10.1039/c0sm01374a

Davidenko, N., Schuster, C.F., Bax, D. V., Farndale, R.W., Hamaia, S., Best, S.M., Cameron, R.E., 2016. Evaluation of cell binding to collagen and gelatin: a study of the effect of 2D and 3D architecture and surface chemistry. J. Mater. Sci. Mater. Med. https://doi.org/10.1007/s10856-016-5763-9

Davidson, M.G., Harned, J., Grimes, A.M., Duncan, G., Wormstone, I.M., McGahan, M.C., 1998. Transferrin in after-cataract and as a survival factor for lens epithelium. Exp. Eye Res. https://doi.org/10.1006/exer.1997.0413

Dawes, L.J., Illingworth, C.D., Michael Wormstone, I., 2012. A fully human in vitro capsular bag model to permit intraocular lens evaluation. Investig. Ophthalmol. Vis. Sci. 53, 23–29. https://doi.org/10.1167/iovs.11-8851

Eldred, J.A., Spalton, D.J., Wormstone, I.M., 2014. An in vitro evaluation of the Anew Zephyr open-bag IOL in the prevention of posterior capsule opacification using a human capsular bag model. Investig. Ophthalmol. Vis. Sci. 55, 7057–7064. https://doi.org/10.1167/iovs.14-

15302

Eldred, J.A., Zheng, J., Chen, S., Wormstone, I.M., 2019. An in vitro human lens capsular bag model adopting a graded culture regime to assess putative impact of iols on pco formation. Investig. Ophthalmol. Vis. Sci. 60, 113–122. https://doi.org/10.1167/iovs.18-25930

Eysturskard, J., Haug, I.J., Ulset, A.S., Draget, K.I., 2009. Mechanical properties of mammalian and fish gelatins based on their weight average molecular weight and molecular weight distribution. Food Hydrocoll. https://doi.org/10.1016/j.foodhyd.2009.06.007

Farrer, A.I., Odéen, H., de Bever, J., Coats, B., Parker, D.L., Payne, A., Christensen, D.A., 2015. Characterization and evaluation of tissue-mimicking gelatin phantoms for use with MRgFUS. J. Ther. Ultrasound. https://doi.org/10.1186/s40349-015-0030-y

Findl, O., Menapace, R., Sacu, S., Buehl, W., Rainer, G., 2005. Effect of optic material on posterior capsule opacification in intraocular lenses with sharp-edge optics: Randomized clinical trial. Ophthalmology. https://doi.org/10.1016/j.ophtha.2004.07.032

Gift, B.W., English, R. V., Nadelstein, B., Weigt, A.K., Gilger, B.C., 2009. Comparison of capsular opacification and refractive status after placement of three different intraocular lens implants following phacoemulsification and aspiration of cataracts in dogs. Vet. Ophthalmol. 35, 1935–1940. https://doi.org/10.1111/j.1463-5224.2009.00667.x

GMIA, 2012. Gelatin Handbook 1–25.

Haripriya, A., Chang, D.F., Vijayakumar, B., Niraj, A., Shekhar, M., Tanpreet, S., Aravind, S., 2017. Long-term Posterior Capsule Opacification Reduction with Square-Edge Polymethylmethacrylate Intraocular Lens: Randomized Controlled Study. Ophthalmology. 124, 295-302. https://doi.org/10.1016/j.ophtha.2016.11.010

Hayashi, H., Hayashi, K., Nakao, F., Hayashi, F., 1998. Quantitative comparison of posterior capsule opacification after polymethylmethacrylate, silicone, and soft acrylic intraocular lens implantation. Arch. Ophthalmol. 116, 1579–1582. https://doi.org/10.1001/archopht.116.12.1579

Huang, X.D., Yao, K., Zhang, Z., Zhang, Y., Wang, Y., 2010. Uveal and capsular biocompatibility of an intraocular lens with a hydrophilic anterior surface and a hydrophobic posterior surface. J. Cataract Refract. Surg. 36, 290–298. https://doi.org/10.1016/j.jcrs.2009.09.027

Hyeon, I.L., Mee, K.K., Jung, H.K., Hyun, J.L., Won, R.W., Jin, H.L., 2007. The efficacy of an acrylic intraocular lens surface modified with polyethylene glycol in posterior capsular opacification. J. Korean Med. Sci. 22, 502–507.

Jaitli, A., Roy, J., Mcmahan, S., Liao, J., Tang, L., 2021. An in vitro system to investigate IOL: Lens capsule interaction. Exp. Eye Res. https://doi.org/10.1016/j.exer.2020.108430

Jaitli, A., Roy J., Liao J.m Tang, L., 2021 (in review). Effect of Time and Temperature Dependent Changes of IOL Material Properties on IOL: Lens Capsule Interactions. Exp. Eye Res

Javitt, J.C., 1996. Blindness Due to Cataract: Epidemiology and Prevention. Annu. Rev. Public Health 17, 159–177. https://doi.org/10.1146/annurev.publhealth.17.1.159

Johnston, E.E., Bryers, J.D., Ratner, B.D., 2005. Plasma deposition and surface characterization of oligoglyme, dioxane, and crown ether nonfouling films. Langmuir 21, 870–881. https://doi.org/10.1021/la036274s

Jordan-Lloyd, D., 1931. CLXXI. The absorption of water by gelatin. VI. The influence of the thickness and original concentration of the gel. Laboratoties of the British Leather Manufacturers' Research Association.

Jung, G.B., Jin, K.H., Park, H.K., 2017. Physicochemical and surface properties of acrylic intraocular lenses and their clinical significance. J. Pharm. Investig. 47, 453–460. https://doi.org/10.1007/s40005-017-0323-y

Kang, S., Kim, M.J., Park, S.H., Joo, C.K., 2008. Comparison of clinical results between heparin surface modified hydrophilic acrylic and hydrophobic acrylic intraocular lens. Eur. J. Ophthalmol. 18, 377–383. https://doi.org/10.1177/112067210801800311

Katayama, Y., Kobayakawa, S., Yanagawa, H., Tochikubo, T., 2007. The relationship between the adhesion characteristics of acrylic intraocular lens materials and posterior capsule opacification. Ophthalmic Res. 39, 276–281. https://doi.org/10.1159/000108121

Kim, M.K., Park, I.S., Park, H.D., Wee, W.R., Lee, J.H., Park, K.D., Kim, S.H., Kim, Y.H., 2001. Effect of poly(ethylene glycol) graft polymerization of poly(methyl methacrylate) on cell adhesion: In vitro and in vivo study. J. Cataract Refract. Surg. 27, 766–774. https://doi.org/10.1016/S0886-3350(00)00701-X

Kochounian, H.H., Kovacs, S.A., Sy, J., Grubbs, D.E., Maxwell, W.A., 1994. Identification of Intraocular Lens-Adsorbed Proteins in Mammalian In Vitro and In Vivo Systems. Arch. Ophthalmol. https://doi.org/10.1001/archopht.1994.01090150125034

Kozlov, P. V., Burdygina, G.I., 1983. The structure and properties of solid gelatin and the principles of their modification. Polymer (Guildf). 24, 651–666. https://doi.org/10.1016/0032-3861(83)90001-0

Lai, J.Y., 2009. The role of bloom index of gelatin on the interaction with retinal pigment epithelial cells. Int. J. Mol. Sci. 10, 3442–3456. https://doi.org/10.3390/ijms10083442

Lai, J.Y., Lin, P.K., Hsiue, G.H., Cheng, H.Y., Huang, S.J., Li, Y.T., 2009. Low bloom strength gelatin as a carrier for potential use in retinal sheet encapsulation and transplantation. Biomacromolecules 10, 310–319. https://doi.org/10.1021/bm801039n

Lee, H. Il, Kim, M.K., Ko, J.H., Lee, H.J., Wee, W.R., Lee, J.H., 2007. The Efficacy of an Acrylic Intraocular Lens Surface Modified with Polyethylene Glycol in Posterior Capsular Opacification. J. Korean Med. Sci. https://doi.org/10.3346/jkms.2007.22.3.502

Leibinger, A., Forte, A.E., Tan, Z., Oldfield, M.J., Beyrau, F., Dini, D., Rodriguez y Baena, F., 2016. Soft Tissue Phantoms for Realistic Needle Insertion: A Comparative Study. Ann. Biomed. Eng. https://doi.org/10.1007/s10439-015-1523-0

Li, Y., Wang, J., Chen, Z., Tang, X., 2013. Effect of hydrophobic acrylic versus hydrophilic acrylic intraocular lens on posterior capsule opacification: Meta-analysis. PLoS One. 8, e77864. https://doi.org/10.1371/journal.pone.0077864

Linnola, R.J., 1997. Sandwich theory: Bioactivity-based explanation for posterior capsule opacification. J. Cataract Refract. Surg. https://doi.org/10.1016/S0886-3350(97)80026-0

Linnola, R.J., Sund, M., Ylönen, R., Pihlajaniemi, T., 2003. Adhesion of soluble fibronectin, vitronectin, and collagen type IV to intraocular lens materials. J. Cataract Refract. Surg. 29, 146–152. https://doi.org/10.1016/S0886-3350(02)01422-0

Linnola, R.J., Werner, L., Pandey, S.K., Escobar-Gomez, M., Znoiko, S.L., Apple, D.J., 2000a. Adhesion of fibronectin, vitronectin, laminin, and collagen type IV to intraocular lens materials in pseudophakic human autopsy eyes. Part 2: Exploited intraocular lenses. J. Cataract Refract. Surg. 26, 1807–1818. https://doi.org/10.1016/S0886-3350(00)00747-1

Linnola, R.J., Werner, L., Pandey, S.K., Escobar-Gomez, M., Znoiko, S.L., Apple, D.J., 2000b. Adhesion of fibronectin, vitronectin, laminin, and collagen type IV to intraocular lens materials in pseudophakic human autopsy eyes. Part 1: Histological sections. J. Cataract Refract. Surg. https://doi.org/10.1016/S0886-3350(00)00748-3

Liu, D., Nikoo, M., Boran, G., Zhou, P., Regenstein, J.M., 2015. Collagen and gelatin. Annu. Rev. Food Sci. Technol. https://doi.org/10.1146/annurev-food-031414-111800

Lois, N., Dawson, R., McKinnon, A.D., Forrester, J. V., 2003. A new model of posterior capsule opacification in rodents. Investig. Ophthalmol. Vis. Sci. 44, 3450–3457. https://doi.org/10.1167/iovs.02-1293

Lombardo, M., Carbone, G., Lombardo, G., De Santo, M.P., Barberi, R., 2009. Analysis of intraocular lens surface adhesiveness by atomic force microscopy. J. Cataract Refract. Surg. 35, 1266–1272. https://doi.org/10.1016/j.jcrs.2009.02.029

Lombardo, M., De Santo, M.P., Lombardo, G., Barberi, R., Serrao, S., 2006. Analysis of intraocular lens surface properties with atomic force microscopy. J. Cataract Refract. Surg. 32, 1378–1384. https://doi.org/10.1016/j.jcrs.2006.02.068

Maddula, S., Werner, L., Ness, P.J., Davis, D., Zaugg, B., Stringham, J., Burrow, M., Yeh, O., 2011. Pathology of 157 human cadaver eyes with round-edged or modern square-edged silicone intraocular lenses: Analyses of capsule bag opacification. J. Cataract Refract. Surg. 37, 740–748. https://doi.org/10.1016/j.jcrs.2010.10.058

Meacock, W.R., Spalton, D.J., Stanford, M.R., 2000. Role of cytokines in the pathogenesis of posterior capsule opacification. Br. J. Ophthalmol. https://doi.org/10.1136/bjo.84.3.332

Menzies, D.J., Nelson, A., Shen, H.H., McLean, K.M., Forsythe, J.S., Gengenbach, T., Fong, C., Muir, B.W., 2012. An X-ray and neutron reflectometry study of "PEG-like" plasma polymer films. J. R. Soc. Interface 9, 1008–1019. https://doi.org/10.1098/rsif.2011.0509

Mester, U., Fabian, E., Gerl, R., Hunold, W., Hütz, W., Strobel, J., Hoyer, H., Kohnen, T., 2004. Posterior capsule opacification after implantation of CeeOn Edge 911A, PhacoFlex SI-40NB, and AcrySof MA60BM lenses: One-year results of an intraindividual comparison multicenter study. J. Cataract Refract. Surg. https://doi.org/10.1016/j.jcrs.2003.09.052

Miyata, A., Yaguchi, S., 2004. Equilibrium water content and glistenings in acrylic intraocular lenses. J. Cataract Refract. Surg. 30, 1768–1772. https://doi.org/10.1016/j.jcrs.2003.12.038

Morgan-Warren, P.J., Smith, J. m. A., 2013. Intraocular lens-edge design and material factors contributing to posterior-capsulotomy rates: Comparing Hoya FY60AD, PY60AD, and AcrySof SN60WF. Clin. Ophthalmol. 7, 1661–1667 https://doi.org/10.2147/OPTH.S48824

Mukherjee, R., Chaudhury, K., Das, S., Sengupta, S., Biswas, P., 2012. Posterior capsular

opacification and intraocular lens surface micro-roughness characteristics: An atomic force microscopy study. Micron 43, 937–947. https://doi.org/10.1016/j.micron.2012.03.015

Mylonas, G., Prskavec, M., Baradaran-Dilmaghani, R., Karnik, N., Buehl, W., Wirtitsch, M., 2013. Effect of a single-piece and a three-piece acrylic sharp-edged IOL on posterior capsule opacification. Curr. Eye Res. 38, 86–90. https://doi.org/10.3109/02713683.2012.717242

Nagata, T., Minakata, A., Watanabe, I., 1998. Adhesiveness of AcrySof to a collagen film. J. Cataract Refract. Surg. 24, 367-370. https://doi.org/10.1016/S0886-3350(98)80325-8

Nibourg, L.M., Gelens, E., Kuijer, R., Hooymans, J.M.M., van Kooten, T.G., Koopmans, S.A., 2015. Prevention of posterior capsular opacification. Exp. Eye Res. 136, 100–115. https://doi.org/10.1016/j.exer.2015.03.011

Nishi, O., 1999a. Posterior capsule opacification. Part 1: Experimental investigations. J. Cataract Refract. Surg. 25, 106–117. https://doi.org/10.1016/S0886-3350(99)80020-0

Nishi, O., 1999b. Preventing posterior capsule opacification by creating a discontinuous sharp bend in the capsule. J. Cataract Refract. Surg. 25, 521-526. https://doi.org/10.1016/S0886-3350(99)80049-2

Nishi, O., Nishi, K., 2002. Preventive effect of a second-generation silicone intraocular lens on posterior capsule opacification. J. Cataract Refract. Surg. 28, 1236–1240. https://doi.org/10.1016/S0886-3350(02)01430-X

Nishi, O., Nishi, K., Akura, J., Nagata, T., 2001. Effect of round-edged acrylic intraocular lenses on preventing posterior capsule opacification. J. Cataract Refract. Surg. 27, 608-613. https://doi.org/10.1016/S0886-3350(00)00644-1

Nishi, O., Nishi, K., Mano, C., Ichihara, M., Honda, T., 1998a. The inhibition of lens epithelial cell migration by a discontinuous capsular bend created by a band-shaped circular loop or a capsule-bending ring. Ophthalmic Surg. Lasers. 29, 119-125 https://doi.org/10.3928/1542-8877-19980201-07

Nishi, O., Nishi, K., Osakabe, Y., 2004. Effect of intraocular lenses on preventing posterior capsule opacification: Design versus material. J. Cataract Refract. Surg. 30, 2170–2176. https://doi.org/10.1016/j.jcrs.2004.05.022

Nishi, O., Nishi, K., Sakanishi, K., 1998b. Inhibition of migrating lens epithelial cells at the capsular bend created by the rectangular optic edge of a posterior chamber intraocular lens. Ophthalmic Surg. Lasers. 29, 587–594. https://doi.org/10.3928/1542-8877-19980701-10

Nishi, O., Nishi, K., Wickström, K., 2000. Preventing lens epithelial cell migration using intraocular lenses with sharp rectangular edges. J. Cataract Refract. Surg. 26, 1543-1546. https://doi.org/10.1016/S0886-3350(00)00426-0

Oshika, T., Nagata, T., Ishii, Y., 1998a. Adhesion of lens capsule to intraocular lenses of polymethylmethacrylate, silicone, and acrylic foldable materials: An experimental study. Br. J. Ophthalmol. 82, 549–553. https://doi.org/10.1136/bjo.82.5.549

Oshika, T., Nagata, T., Ishii, Y., 1998b. Adhesion of lens capsule to intraocular lenses of polymethylmethacrylate, silicone, and acrylic foldable materials: An experimental study. Br. J. Ophthalmol. 82, 549–553. https://doi.org/10.1136/bjo.82.5.549

Oshika, T., Suzuki, Y., Kizaki, H., Yaguchi, S., 1996. Two year clinical study of a soft acrylic intraocular lens. J. Cataract Refract. Surg. 22, 104-109. https://doi.org/10.1016/S0886-3350(96)80278-1

Pearlstein, C.S., Lane, S.S., Lindstrom, R.L., 1988. The Incidence of Secondary Posterior Capsulotomy in Convex-Posterior vs. Contex-Anterior Posterior Chamber Intraocular Lenses. J. Cataract Refract. Surg. https://doi.org/10.1016/S0886-3350(88)80020-8

Pérez-Vives, C., 2018. Biomaterial influence on intraocular lens performance: An overview. J. Ophthalmol. 2018, 1-17. https://doi.org/10.1155/2018/2687385

Pogue, B.W., Patterson, M.S., 2006. Review of tissue simulating phantoms for optical spectroscopy, imaging and dosimetry. J. Biomed. Opt. https://doi.org/10.1117/1.2335429

Prajna, N.V., Chandrakanth, K.S., Kim, R., Narendran, V., Selvakumar, S., Rohini, G., Manoharan, N., Bangdiwala, S.I., Ellwein, L.B., Kupfer, C., 1998. The Madurai intraocular lens study II: Clinical outcomes. Am. J. Ophthalmol. https://doi.org/10.1016/S0002-9394(99)80230-X

Raj, S.M., Vasavada, A.R., Johar, S.R.K., Vasavada, V.A., Vasavada, V.A., 2007. Post-operative capsular opacification: a review. Int. J. Biomed. Sci. 3, 237–50.

Ram, J., Jain, V.K., Agarwal, A., Kumar, J., 2014. Hydrophobic acrylic versus polymethyl methacrylate intraocular lens implantation following cataract surgery in the first year of life. Graefe's Arch. Clin. Exp. Ophthalmol. 252, 1443–1449. https://doi.org/10.1007/s00417-014-2689-0

Ribeiro, M.A., Ramos, A.S., Manfredini, M.I., Alves, H.A., Honda, R.Y., Kostov, K.G., Lucena, E.F., Ramos, E.C.T., Mota, R.P., Algatti, M.A., Kayama, M.E., 2009. Polyurethane coating with thin polymer films produced by plasma polymerization of diglyme. J. Phys. Conf. Ser. 167. https://doi.org/10.1088/1742-6596/167/1/012056

Riaz, Y., Js, M., Wormald, R., Jr, E., Foster, A., Ravilla, T., Snellingen, T., 2006. Surgical interventions for age-related cataract (Review). https://doi.org/10.1002/14651858.CD001323.pub2.www.cochranelibrary.com

Rønbeck, M., Kugelberg, M., 2014a. Posterior capsule opacification with 3 intraocular lenses: 12-year prospective study. J. Cataract Refract. Surg. https://doi.org/10.1016/j.jcrs.2013.07.039

Rønbeck, M., Kugelberg, M., 2014b. Posterior capsule opacification with 3 intraocular lenses: 12-year prospective study. J. Cataract Refract. Surg. https://doi.org/10.1016/j.jcrs.2013.07.039

Rönbeck, M., Zetterström, C., Wejde, G., Kugelberg, M., 2009a. Comparison of posterior capsule opacification development with 3 intraocular lens types. Five-year prospective study. J. Cataract Refract. Surg. https://doi.org/10.1016/j.jcrs.2009.05.048

Rönbeck, M., Zetterström, C., Wejde, G., Kugelberg, M., 2009b. Comparison of posterior capsule opacification development with 3 intraocular lens types. Five-year prospective study. J. Cataract Refract. Surg. 35, 1935–1940. https://doi.org/10.1016/j.jcrs.2009.05.048

Sacu, S., Findl, O., Linnola, R.J., 2005. Optical coherence tomography assessment of capsule closure after cataract surgery. J. Cataract Refract. Surg. 31, 330–336.

https://doi.org/10.1016/j.jcrs.2004.04.057

Saika, S., 1997. Deposition of extracellular matrix on silicone intraocular lens implants in rabbits. Graefe's Arch. Clin. Exp. Ophthalmol. 235, 517–522. https://doi.org/10.1007/BF00947010

Saika, S., 1997. Deposition of extracellular matrix on intraocular lenses in rabbits: An immunohistochemical and transmission electron microscopic study. Graefe's Arch. Clin. Exp. Ophthalmol. 235, 241–247. https://doi.org/10.1007/BF00941766

Saika, S., Kawashima, Y., Miyamoto, T., Okada, Y., Tanaka, S.I., Ohmi, S., Minamide, A., Yamanaka, O., Ohnishi, Y., Ooshima, A., Yamanaka, A., 1998. Immunolocalization of prolyl 4-hydroxylase subunits, α-smooth muscle actin, and extracellular matrix components in human lens capsules with lens implants. Exp. Eye Res. https://doi.org/10.1006/exer.1997.0434

Saika, S., Kobata, S., Yamanaka, O., Yamanaka, A., Okubo, K., Oka, T., Hosomi, M., Kano, Y., Ohmi, S., Uenoyama, S., Tamura, M., Kanagawa, R., Uenoyama, K., 1993. Cellular fibronectin on intraocular lenses explanted from patients. Graefe's Arch. Clin. Exp. Ophthalmol. 231, 718–721. https://doi.org/10.1007/BF00919287

Shepherd, J.R., 1989. Capsular opacification associated with silicone implants. J. Cataract Refract. Surg. https://doi.org/10.1016/S0886-3350(89)80069-0

Sheppard, A.L., Bashir, A., Wolffsohn, J.S., Davies, L.N., 2010. Accommodating intraocular lenses: A review of design concepts, usage and assessment methods. Clin. Exp. Optom. 93, 441–452. https://doi.org/10.1111/j.1444-0938.2010.00532.x

Shimizu, M., Minakuchi, K., Moon, M., Koga, J., 1997. Difference in interaction of fibronectin with type I collagen and type IV collagen. Biochim. Biophys. Acta - Protein Struct. Mol. Enzymol. 1339, 53–61. https://doi.org/10.1016/S0167-4838(96)00214-2

Slade, L., Levine, H., 1987. Polymer-Chemical Properties of Gelatin in Foods, in Advances in Meat Research: Collagen as Food.

Sottile, J., Shi, F., Rublyevska, I., Chiang, H.Y., Lust, J., Chandler, J., 2007. Fibronectin-dependent collagen I deposition modulates the cell response to fibronectin. Am. J. Physiol. - Cell Physiol. 293, 1934–1946. https://doi.org/10.1152/ajpcell.00130.2007

Su, K., Wang, C., 2015. Recent advances in the use of gelatin in biomedical research. Biotechnol. Lett. 37, 2139–2145. https://doi.org/10.1007/s10529-015-1907-0

Tanaka, T., Shigeta, M., Yamakawa, N., Usui, M., 2005. Cell adhesion to acrylic intraocular lens associated with lens surface properties. J. Cataract Refract. Surg. 31, 1648-1651. https://doi.org/10.1016/j.jcrs.2004.11.050

Thylefors, B., Negrel, A.D., Pararajasegaram, R., Dadzie, K.Y., 1995. Global data on blindness. Bull. World Health Organ. 73, 115–121.

Tognetto, D., Toto, L., Minutola, D., Ballone, E., di Nicola, M., Di Mascio, R., Ravalico, G., 2003. Hydrophobic acrylic versus heparin surface-modified polymethylmethacrylate intraocular lens: A biocompatibility study. Graefe's Arch. Clin. Exp. Ophthalmol. 241, 625–630. https://doi.org/10.1007/s00417-003-0711-z

Tziampazis, E., Kohn, J., Moghe, P. V., 2000. PEG-variant biomaterials as selectively adhesive protein templates: Model surfaces for controlled cell adhesion and migration. Biomaterials 21, 511–520. https://doi.org/10.1016/S0142-9612(99)00212-4

Ursell, P.G., Spalton, D.J., Pande, M. V., Hollick, E.J., Barman, S., Boyce, J., Tilling, K., 1998. Relationship between intraocular lens biomaterials and posterior capsule opacification. J. Cataract Refract. Surg. 24, 352–360. https://doi.org/10.1016/S0886-3350(98)80323-4

Usta, M., Piech, D.L., MacCrone, R.K., Hillig, W.B., 2003. Behavior and properties of neat and filled gelatins. Biomaterials. https://doi.org/10.1016/S0142-9612(02)00274-0

Van Tenten, Y., Schuitmaker, J.J., De Groot, V., Willekens, B., Vrensen, G.F., Tassignon, M.J., 2000. Cell biological mechanisms underlying posterior capsule opacification: search for a therapy. Bull. Soc. Belge Ophtalmol.

Vasavada, A.R., Praveen, M.R., 2014. Posterior Capsule Opacification After Phacoemulsification. Asia-Pacific J. Ophthalmol. https://doi.org/10.1097/apo.0000000000000080

Versura, P., 1999. Adhesion mechanisms of human lens epithelial cells on 4 intraocular lens materials. J. Cataract Refract. Surg. 25, 527–533. https://doi.org/10.1016/s0886-3350(99)80050-9

Wang, H., Boerman, O.C., Sariibrahimoglu, K., Li, Y., Jansen, J.A., Leeuwenburgh, S.C.G., 2012. Comparison of micro- vs. nanostructured colloidal gelatin gels for sustained delivery of osteogenic proteins: Bone morphogenetic protein-2 and alkaline phosphatase. Biomaterials. https://doi.org/10.1016/j.biomaterials.2012.08.024

Weed, B.C., Borazjani, A., Patnaik, S.S., Prabhu, R., Horstemeyer, M.F., Ryan, P.L., Franz, T., Williams, L.N., Liao, J., 2012. Stress state and strain rate dependence of the human placenta. Ann. Biomed. Eng. 40, 2255–2265. https://doi.org/10.1007/s10439-012-0588-2

Wejde, G., Kugelberg, M., Zetterström, C., 2003. Posterior capsule opacification: Comparison of 3 intraocular lenses of different materials and design. J. Cataract Refract. Surg. 29, 1556–1559. https://doi.org/10.1016/S0886-3350(03)00342-0

Welch, N.G., Madiona, R.M.T., Easton, C.D., Scoble, J.A., Jones, R.T., Muir, B.W., Pigram, P.J., 2016. Chromium functionalized diglyme plasma polymer coating enhances enzyme-linked immunosorbent assay performance. Biointerphases 11, 041004. https://doi.org/10.1116/1.4967442

Wolffsohn, J.S., Hunt, O.A., Naroo, S., Gilmartin, B., Shah, S., Cunliffe, I.A., Benson, M.T., Mantry, S., 2006. Objective accommodative amplitude and dynamics with the 1CU accommodative intraocular lens. Investig. Ophthalmol. Vis. Sci. 47, 1230–1235. https://doi.org/10.1167/iovs.05-0939

Wormstone, I.M., 2020. The human capsular bag model of posterior capsule opacification. Eye 34, 225–231. https://doi.org/10.1038/s41433-019-0680-z

Wormstone, I.M., Damm, N.B., Kelp, M., Eldred, J.A., 2021. Assessment of intraocular lens/capsular bag biomechanical interactions following cataract surgery in a human in vitro graded culture capsular bag model. Exp. Eye Res. 205, 108487. https://doi.org/10.1016/j.exer.2021.108487

Wormstone, I.M., Eldred, J.A., 2016a. Experimental models for posterior capsule opacification research. Exp. Eye Res. 142, 2–12. https://doi.org/10.1016/j.exer.2015.04.021

Wormstone, I.M., Eldred, J.A., 2016b. Experimental models for posterior capsule opacification research. Exp. Eye Res. 142, 2–12. https://doi.org/10.1016/j.exer.2015.04.021

Xing, Q., Yates, K., Vogt, C., Qian, Z., Frost, M.C., Zhao, F., 2014. Increasing mechanical strength of gelatin hydrogels by divalent metal ion removal. Sci. Rep. 4, 1–10. https://doi.org/10.1038/srep04706

Xu, X., Tang, J.M., Han, Y.M., Wang, W., Chen, H., Lin, Q.K., 2016a. Surface PEGylation of intraocular lens for PCO prevention: An in vivo evaluation. J. Biomater. Appl. 31, 68–76. https://doi.org/10.1177/0885328216638547

Xu, X., Tang, J.M., Han, Y.M., Wang, W., Chen, H., Lin, Q.K., 2016b. Surface PEGylation of intraocular lens for PCO prevention: An in vivo evaluation. J. Biomater. Appl. https://doi.org/10.1177/0885328216638547

Yang, N., Zhang, D.D., Li, X.D., Lu, Y.Y., Qiu, X.H., Zhang, J.S., Kong, J., 2017. Topography, Wettability, and Electrostatic Charge Consist Major Surface Properties of Intraocular Lenses. Curr. Eye Res. 42, 201–210. https://doi.org/10.3109/02713683.2016.1164187

Zhao, Y., Yang, K., Li, J., Huang, Y., Zhu, S., 2017. Comparison of hydrophobic and hydrophilic intraocular lens in preventing posterior capsule opacification after cataract surgery An updated meta-analysis. Med. (United States). 96 , e.8301. https://doi.org/10.1097/MD.0000000000008301

Ziebarth, N.M., Arrieta, E., Feuer, W.J., Moy, V.T., Manns, F., Parel, J.M., 2011. Primate lens capsule elasticity assessed using Atomic Force Microscopy. Exp. Eye Res. https://doi.org/10.1016/j.exer.2011.03.008

BIOGRAPHICAL INFORMATION

Arjun is a biomedical engineer and works as a Process Integration & Automation Engineer at Alcon Research LLC in Fort Worth, TX. Arjun grew up in New Delhi, India and moved to the Unties States at the age of 17 to pursue his Bachelors of Science in Biomedical Engineering at Purdue University, West Lafayette, IN.

As a Purdue undergrad, Arjun was selected to pursue the combined 5-year BS/MS program, which put him on an accelerated path to complete his Masters within a year of completing his bachelor's degree. During his junior year at Purdue, Arjun secured the summer undergraduate research fellowship and went on to create algorithms to distinguish between sleep spindles and electrographic seizures to reduce the rate of false positives for different seizure detection algorithms. In the later years of his academic career at Purdue, Arjun worked on the development of an *in vivo* model to assess the efficacy of an event-based seizure detection algorithm in detecting spontaneous seizures in epileptic rats.

In 2012, Arjun began his journey with Alcon as an Optical Test Engineer. Over the years, Arjun has held several roles of increasing responsibilities from being a test method Validation Engineer to managing IOL R&D Production & Operations. Arjun is now leading efforts to automate the production and assembly processes of different Class II and Class III ophthalmic devices. In 2017, Arjun accepted a doctoral position under Dr. Liping Tang and for the last 3+ years, Arjun has enjoyed working on several projects focused on studying mechanisms of IOL-induced Posterior Capsule Opacification. Under Dr. Tang's mentorship and through strong collaboration with other doctoral candidates, Arjun was able to develop an *in vitro* model to study IOL: LC interactions. Arjun feels extremely fortunate that he was able to work with a great group of scientists and engineers during his time as a doctoral student at UT Arlington and is excited to utilize his new

skills and experience in his personal and professional life.

Arjun loves traveling and experiencing different places and cultures with his wife, Palak. Arjun is an amateur cook, enjoys working out and is always ready for an adventure!